Kinetics and Effects of H_2 Partial Pressure on Hydrotreating of Heavy Gas Oil

A Thesis Submitted to the College of Graduate Studies and Research

in Partial Fulfillment of the Requirements for the

Degree of Master of Science

in the Department of Chemical Engineering

University of Saskatchewan

Saskatoon

By

Majak Mapiour

Oct2009

COPYRIGHT

ABSTRACT

The impact of H_2 partial pressure (H_2 pp) during the hydrotreating of heavy gas oil, derived from Athabasca bitumen, over commercial NiMo/γ-Al_2O_3 catalyst was studied in a micro-trickle bed reactor. The experimental conditions were varied as follows: temperature: 360 to 400ºC, pressure: 7 to 11 MPa, gas/oil ratio: 400 to 1270 mL/mL, H_2 purity range of 0 to 100 vol. % (with the rest either CH_4 or He), and LHSV range of 0.65 to 2 h^{-1}. The two main objectives of the project were to study the nature of the dependence of H_2 pp on temperature, pressure, gas/oil ratio, LHSV (Liquid Hourly Space Velocity), and H_2 purity. The project was divided into three phases: in phase one the effect of H_2 purity on hydrotreating of heavy gas oil (HGO) was studied, in phase two the nature of H_2 pp dependency and the effect of H_2 pp on hydrotreating of HGO was investigated, and in phase three kinetic studies were carried out using different kinetic models.

The objective of phase one was to study the effect of hydrogen purity on hydrotreating of HGO was studied in a trickle bed reactor over a commercial Ni−Mo/γ-alumina catalyst. Methane was used as a diluent for the hydrogen stream, and its effect on the catalyst performance was compared to that of helium, which is inert toward the catalyst. Furthermore, a deactivation study was conducted over a period of 66 days, during which the catalyst was subjected to H_2 purities ranging from 75 to 95% (with the rest methane); no significant deterioration in the hydroprocessing activities of the catalyst was observed. Therefore, it was concluded that methane was inert toward a

commercial Ni−Mo/γ-alumina catalyst. However, its presence resulted in hydrogen partial pressure reduction, which in turn led to a decrease in hydrodesulphurization (HDS), hydrodenitrogenation (HDN), hydrodearomatization (HDA) conversions. This reduction can be offset by increasing the total pressure of the system. HDS, HDN, HDA, and mild hydrocracking (MHC) conversions were studied. Also determined were cetane index, density, aniline point, diesel index, and fractional distribution of the products.

The main objective of phase two was to study the effects of H_2 pp on hydrotreating conversions, feed vaporization, H_2 dissolution, and H_2 consumption were studied. The results show that HDN and HDA are significantly more affected by H_2 partial pressure than HDS; with the HDN being the most affected. For instance as the inlet H_2 partial pressure was increased from 4.6 to 8.9 MPa HDS, HDN, and HDA conversions increased for 94.9%, 55.1%, and 46.0% to 96.7%, 83.9%, and 58.0% , respectively. Moreover, it was observed that H_2 dissolution and H_2 consumption increased with increasing H_2 pp. No clear trend was observed for the effect of H_2 pp on feed vaporization.

In phase three the kinetics of HDS, HDN, and HDA were studied. The power law, multi-parameter, and Langmuir - Hinshelwood type models were used to fit the data. The prediction capacities of the resulting models were tested. It was determined that, while multi-parameter model yielded better prediction, L-H had an advantage in that it took a lesser number of experimental data to determine its parameters. Kinetic fitting of the data to a pseudo-first-order power law model suggested that conclusions on the effect of H_2 pp on hydrotreating activities could be equally drawn from either inlet or

outlet hydrogen partial pressure. However, from the catalyst deactivation standpoint, it is recommended that such conclusions are drawn from the outlet H_2 partial pressure, since it is the reactor point with the lowest hydrogen partial pressure.

ACKNOWLEDGEMENT

I would like to acknowledge the input and contribution of a number of persons who helped in this endeavor:

My supervisors Drs A. K. Dalai and J. Adjaye for every second that they invested in supporting and guiding me in every step of the project.

Dr. V. Sundaramurthy for being a source of encouragement and inspiration when the "going got tough".

Drs. Dr. Richard W. Evitts and Hui Wang for their time, contribution, and guidance.

Mr. Ted Wallenting for being funny and extremely patient and for turning experimental difficulties into laughter.

Mr. Richard Blondin for always "going the extra mile".

Mr. Dragan Celkic for always being helpful and punctual.

My friends Philip, Chiryu, and Cristina for their constant support. They spent countless hours proof-reading my works.

I would like to thank all members of Catalysis and Chemical Reaction Engineering Laboratories (Department of Chemical Engineering, U of S) for being so cooperative and understanding.

Financial assistance from NSERC IPS is gratefully acknowledged.

Above all, I wholeheartedly thank God for placing such wonderful individuals on my path, and may He continue to bless every single one of them abundantly.

DEDICATION

This thesis is dedicated to:

My parents, Loi and Grace, for all the sacrifices they made so that I could get an education

My brothers and sisters for being my role models

My friends and lab-mates for making this a fun journey

TABLES OF CONTENTS

LIST OF TABLES

LIST OF FIGURES

NOMENCLATURE and ABBREVIATIONS

NOMENCLATURE

C	sulfur, nitrogen, or aromatics content (wt. %)
C_A	aromatic carbon content (wt. %)
C_f	concentration of the feed
C_i	concentration of species 'i"
C_p	concentration of the product
C_{So}	sulfur concentration in the feed
C_{Sp}	sulfur concentration in the product
ºC	Degree Celsius
D	Density
E	activation energy (kJ/mol)
G/O	gas/oil ratio (mL/mL)
H_2pp	hydrogen partial pressure (MPa)
H'_{H_2S}	amount of H_2 necessary to form hydrocarbon during HDS (scf/bbl)
H_{H_2S}	H_2 content of H_2S in the product gas (scf/bbl)
H'_{NH_3}	amount of H_2 necessary to form hydrocarbon during HDN (scf/bbl)

H_{NH_3}	H_2 content of NH_3 in the product gas (scf/bbl)
K	Kelvin
k_f	rate constant for the forward reaction
K_{H2}	adsorption constant of hydrogen
K_{H2S}	adsorption constant fro hydrogen sulphide
K_i	adsorption constant of species "i"
k_i	rate constant for species "i"
k_o	Arrhenius constant
k_r	rate constant for the reverse reaction
LHSV	liquid hourly superficial velocity
m, q, and c	empirical regression factors
N	nitrogen contents (wt.%)
n, m	reaction orders
P_H	hydrogen partial pressure (MPa)
P_{H2S}	hydrogen sulphide partial pressure (MPa)
R	gas constant; kJ/mol.K
R^2	The fraction of the variance in the data that is explained by a regression

r_i	reaction rate of species "i"
S	sulfur content (wt. %)
t	residence time
T	Temperature
T_{10N}	Temperature at 10% recovery point. It is obtained from Simulated distillation data
T_{50N}	Temperature at 50% recovery point. It is obtained from Simulated distillation data
T_{90N}	Temperature at 90% recovery point. It is obtained from Simulated distillation data

ABBREVIATIONS

AP	Aniline Point
CCC	Central Composite Circumscribed
CCD	Central Composite Design
CCI	Central Composite Inscribed
CI	Cetane Index
DEA	Diethanolamine

G	Gasoline
HGO	Heavy Gas Oil
HT	Hydrotreatment
K	Kerosene
L-H	Langmuir-Hinshelwood kinetic model
LGO	Light Gas Oil
MEA	Monoethanolamine
MHC	Mild Hydrocracking
M-P	Multi-Parameter kinetic model
NMR	Nuclear Magnetic Resonance
RSM	Response Surface Method
P-L	Power Law kinetic model
TMS	Tetra-methylsilane
VGO	Vacuum Gas Oil
VLE	Vapor-Liquid Equilibrium

Definitions and Terminologies

Conventional crude oil: is oil produced by the traditional oil well method. It is less viscous oil and generally better in quality than unconventional crude oil (Gautier, 2008).

Unconventional crude oil: is generally thicker and contains higher levels of sulfur, nitrogen, heavy metals contaminants; therefore requires more vigorous refining than conventional crude oil. Its types are: heavy oils, tar sands, oil shale (Gautier, 2008).

Hydrotreating: is a catalytic process that uses H_2 to stabilize petroleum product by hydrogenating unsaturated hydrocarbon or remove contaminants such as sulfur and nitrogen (Gray H. et al. 2007).

Hydrogenation: is a chemical reaction resulting from H_2 addition to unsaturated hydrocarbon molecules (Leffler, 2000).

Catalytic reforming: is a catalytic process in which hydrocarbon molecules are rearranged and re-structured to produce higher-octane aromatics and significant amounts of by-product H_2 (Gray H. et al. 2007).

Hydrocracking: is a catalytic petroleum refining process that uses H_2 to convert heavier feedstock into desirable lighter products (Speight, 1981).

Hydrorefining: is a catalytic process for the improvement of the product quality by reacting it with H_2.

HYSYS: is a powerful engineering simulation tool with a strong thermodynamic foundation. It can be used for vapor/liquid equilibrium calculations among other things.

CCD(Central Composite Design): is a statistical experimental design widely used for estimating second order response surfaces. It is popular because it is flexible, very

efficient, providing much information on experiment variable effects and overall experimental error in a minimum number of required runs.

1.0 INTRODUCTION

The global oil demand is on a constant climb. According to World Energy Outlook (WEO), the demand for oil is expected to increase from 85 million bbl/day in 2008 to 106 million bbl/day by 2030. With the expected decline in conventional oil production, unconventional oil such as oil sands will be major players on meeting this future global oil demand.

Canada's oil sands deposits are second only to Saudi Arabia reserves. The output of marketable oil sands production was 1.126 million bbl/day in 2006, and was expected to rise to 3 million bbl/day by 2020 and 5 million bbl/day by 2030 (Government of Alberta). The expected increase in oil sands production will bring forth an increase in hydrogen demand; hydrogen is used to refine crude oil.

1.1 Research background

Conventional and non-conventional crude oil must be refined before they are made available for public consumption. The refining processes involve consumption of hydrogen (H_2) which is a valuable commodity. It is predicted that refining H_2 consumption will be increasing for two main reasons. First, the quality of the crude oil is on a steady decline; meaning that higher levels of contaminants such as sulfur and nitrogen are becoming present in the crude. A major reason for this is that unconventional oil is increasingly relied upon as a fuel source, and it is

relatively lower in quality than conventional oil. This trend is expected to continue as the deposit of unconventional oil far surpasses that of conventional oil. There has been a significant progress in unconventional oil extraction and refining technology. Second, the environmental regulations against the levels of contaminants in the fuel are becoming increasingly stringent by the day (Peramanu et al., 1999). For these two reasons, careful study of H_2 management options is important.

To get an appreciation for the importance of H_2 to refiners a brief historical background must be reviewed. In 1897, hydrotreating (one of the refinery's processes which use H_2 to upgrade petroleum stocks) had its origin when Sabatier and Senderens reported that hydrogenation of unsaturated hydrocarbons could be carried out in the vapor phase over nickel catalyst (Gruia, 2006). The first industrial plant however was not built until 1927 in Leuna, Germany. In 1944, during the WWII, Germany used hydrogenation to produce 3.5 million tons of gasoline, which by today's standards is just a minute production. Though hydrotreating and hydrogenation were of particular interest to the petroleum industry, very little commercialization had taken place prior to the 1950s due to the lack of low cost H_2. However, in the early 1950s, the advent of the catalytic reforming process made by-product H_2 readily available. Therefore, an enormous growth in hydrotreating and other H_2-consuming processes occurred. By 2001, there were more than 1,600 hydrotreaters operating worldwide with total capacity exceeding 39 million B/D (4.8 million MT/D) (Gruia, 2006).The increasing utilization of H_2 in petroleum calls for better H_2 utilization for optimal economics. One approach to better H_2 management is to fully understand the H_2 cycle in each of the H_2-consuming processes such as hydrotreating, hydrocracking, and hydrorefining. A H_2-consuming process of particular interest is hydrotreating. A popular example demonstrating the

importance of hydrotreating was a set of data cited by Radler (Speight and Ozum, 2002). The data showed that of the total worldwide refinery capacity of approximately 81.5 million bbl/d of oil, approximately 4 million bbl/d was dedicated to catalytic hydrocracking, 8.5 million bbl/d was dedicated to catalytic hydrorefining, and approximately 28.1 million bbl/d was dedicated to catalytic hydrotreating. For this reason, this research work focuses on understanding the H_2 cycle in a hydrotreater unit.

1.2 Knowledge gaps

After careful review of the literature (Chapter 2) regarding the effect of H_2 partial pressure on the hydrotreating activities, the following knowledge gaps were arrived at:

- Even though H_2 purity is an important hydrotreating variable, its effect has not been examined in a vast majority of the studies available in the open literature.
- The fact that H_2 partial pressure a dependent variable is not adequately studied. As a result there is limited information in the open literature on the effects of the independent variables (temperature, pressure, gas/oil ratio, H_2 purity, and LHSV (Liquid Hourly Space Velocity)) on H_2 partial pressure.
- There are limited studies on the effects of the independent variables on important factors such as feed vaporization, H_2 dissolution, and H_2 consumption, which greatly influence H_2 partial pressure.

1.3 Hypothesis

The following hypothesis has been outlined for this research work:

- Within the hydrotreatment conditions, methane will not inhibit the catalyst; however, its presence may result in minor decreases in HDS, HDN, and HDA activities as it reduces the H_2 partial pressure.
- Increasing reactor pressure, H_2 purity, and gas/oil ratio will enhance both the inlet and the outlet H_2 partial pressure.
- Langmuir-Hinshelwood model, in comparison to power law model or multi-parameter model, will better represent the kinetic data since it accounts for the inhibition of HDS, HDN, and HDA reactions caused by H_2S.

1.4 Research objectives

The main objectives of this work were 1): to study the effects of independent variables (temperature, pressure, gas/oil ratio, H_2 purity, and LHSV) on inlet and outlet H_2 partial pressure. 2): to correlate H_2 partial pressure and hydrotreating activities, and H_2 consumption.

Scope:

Phase I: The focus was on the effect of H_2 purity on hydrotreating activities and product quality. Hydrotreating experiments were performed in which methane was used to adjust H_2 purity, and the effects of H_2 purity on HDS, HDN, HDA, and MHC, and on cetane index, density, viscosity, aniline point, diesel index and fractional distribution of the products were determined.

Phase II: The activities that were carried out in this section include the following:

- To determine the impact of the interaction of pressure, H_2 purity, and gas/oil ratio on inlet and outlet H_2 partial pressure, feed vaporization, H_2 dissolution, H_2 consumption. CCD (Composite Central Design) statistical experimental design approach was followed, hydrotreating experiments were carried out, and samples were collected and analyzed. Inlet and outlet H_2 partial pressure, feed vaporization, H_2 dissolution, and H_2 consumption were determined using HYSYS, and Expert-Design 6.0.1 was used for the regression analysis of the data.

- Inlet and outlet H_2 partial pressure were correlated to hydrotreating activities and to feed vaporization, H_2 dissolution, and H_2 consumption.

- Effects of Temperature and LHSV on hydrotreating activities, inlet and outlet H_2 partial pressure, feed vaporization, H_2 dissolution, and H_2 consumption were determined following a simple factorial experimental design.

Phase III: Kinetics of HDS, HDN, and HDA using different models were developed and compared.

2.0 LITERATURE REVIEW

This chapter presents a review on hydrotreating of heavy gas oil. Emphasis is placed on the introduction and explanation of concepts which aid the understanding of H_2 partial pressure dependency. Concepts pertaining to the kinetic modeling of hydrotreating reactions are also discussed.

2.1 Hydrotreating

Hydrotreating is a catalytic process in which petroleum products are stabilized by hydrogenation of unsaturated hydrocarbons and/or removal of contaminants such as sulfur, nitrogen, oxygen, and metals (Ni, V) from feedstocks by reacting them with hydrogen under relatively high temperatures and pressures (Gary et al. 2007). The sulfur and nitrogen are converted into H_2S and NH_3, respectively. Hydrotreating is especially essential in meeting the progressing stringent emissions and environmental regulations, and also for pre-treating petroleum stocks for downstream processes such as catalytic cracking and reforming whose catalysts are poisoned by the aforementioned contaminants if not removed (Leffler, 2000). The important factors that constitute and determine the nature of a hydrotreating process are highlighted in Figure 2.1. In brief these factors include: feed properties, catalyst, and process.

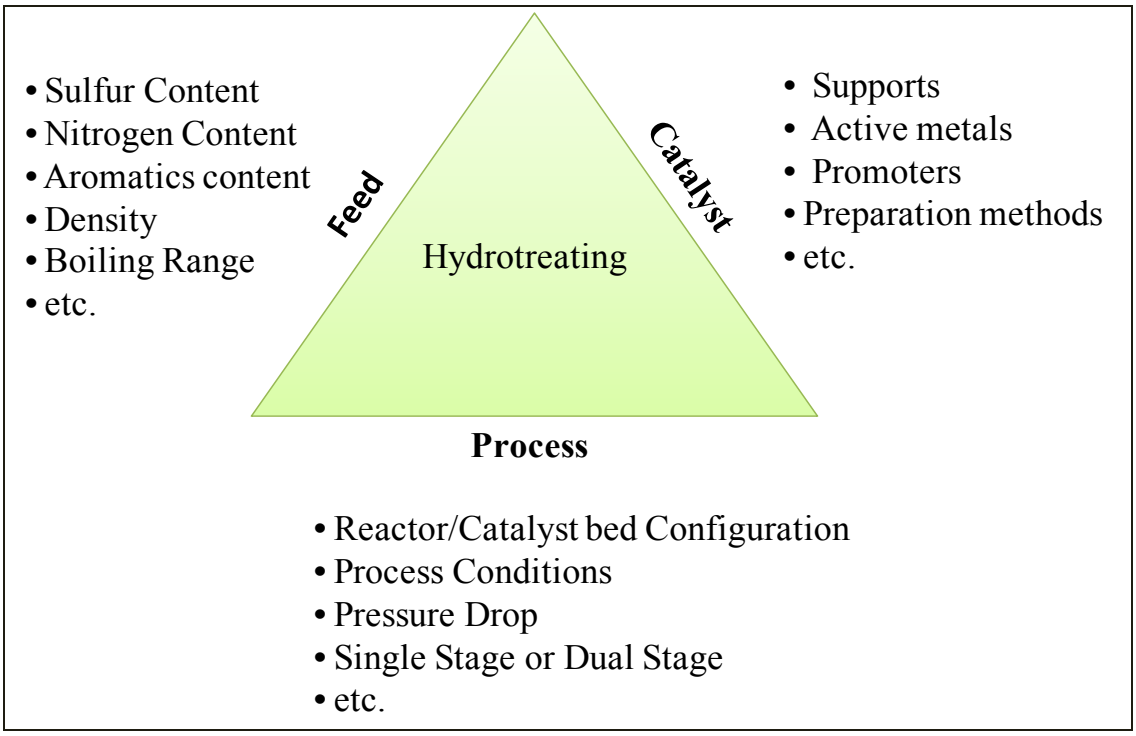

Figure 2.1: Key factors affecting hydrotreating activities.

There are approximately 30 hydrotreating processes available for licensing (Gary et al. 2007). However, most of these have basically the same process flow (see Figure 2.2). A mixture of hydrocarbon feedstock and H_2 is heated to a desired inlet temperature and then introduced into a fixed bed reactor loaded with the catalyst. In the presence of the catalyst, H_2 reacts with the oil to produce mainly saturated hydrocarbons, hydrogen sulfide (H_2S), and ammonia (NH_3). The reactor effluent enters high and low pressure separators where the liquid and gaseous products are separated. The liquid product is sent to the fractionation unit for further separation. Un-reacted H_2 is recovered from the gaseous product and recycled to the reactor (Leffler, 2000; Gary et al. 2007).

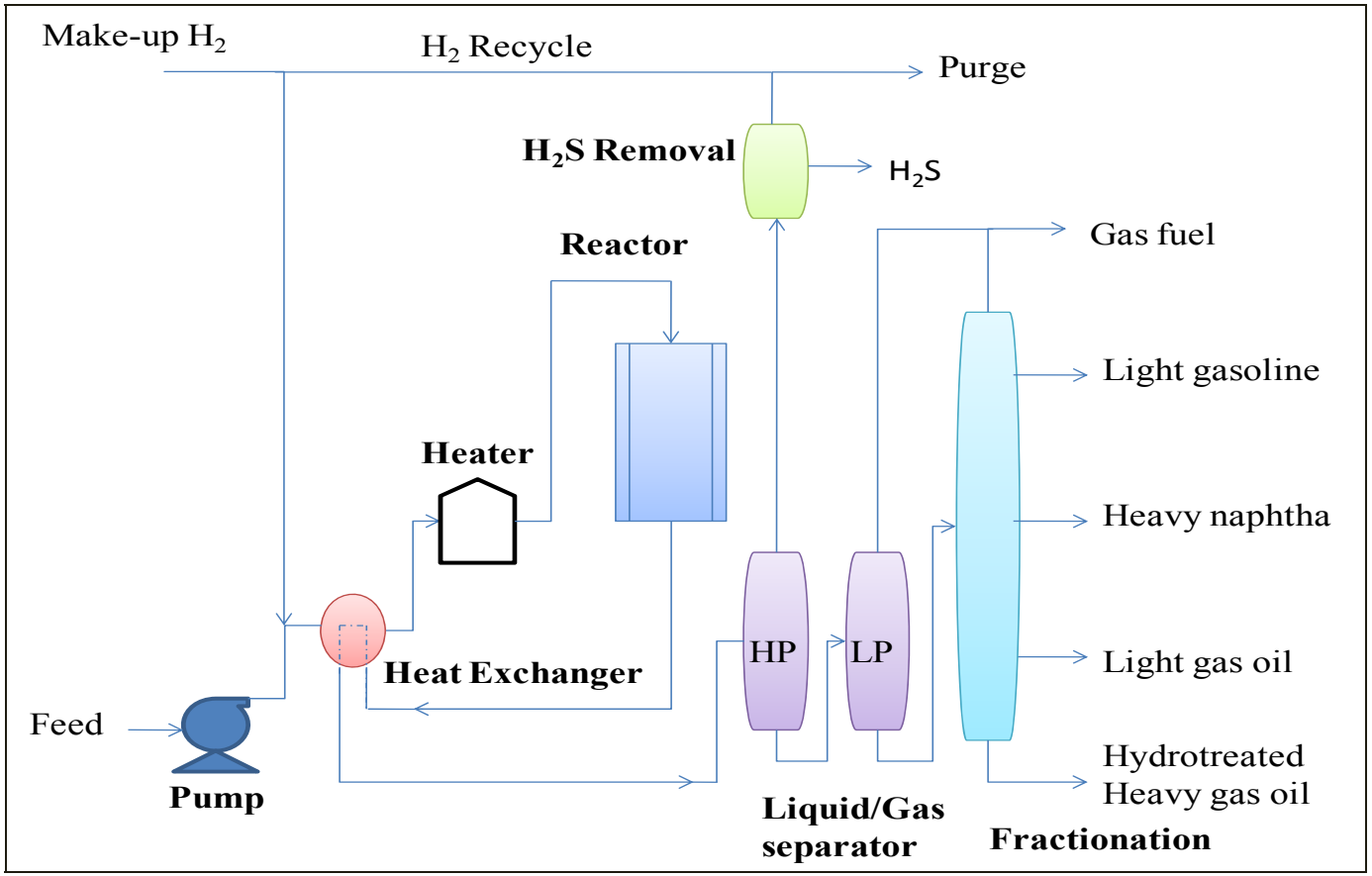

Figure 2.2: A simplified schematic of a typical trickle-bed hydrotreating process. (HP= high pressure; LP = low pressure).

2.1.1 Hydrotreating reactions

Even though the main hydrotreating reaction is hydrodesulphurization (HDS), other reactions simultaneously occur to a degree proportional to the severity of the operation conditions (Mochida, 2004). These reactions include: hydrodenitrogenation (HDN), hydrodearomatization (HDA), hydrodemetallization (HDM), hydrodeoxygenation (HDO), and olefin saturation. It must be noted that most crudes contain low levels of oxygen; therefore HDO is of a lesser concern. As an example, for hydrodesulphurization, the prefix "hydro-de" the "hydro" refers to the use of hydrogen and the "de" means "removal of", and suffix sulphurization refers to sulfur. HDS is the main reaction because the sulfur content along with the API gravity are the two greatest properties that influence the value of a heavy oil and residuum (Speight, 1981). HDS, HDN, and HDA are discussed in greater details in section 2.2, 2.3, and 2.3, respectively.

2.1.2 Hydrotreating operating variables

Hydrotreating operating variables include: temperature, pressure, H_2 partial pressure, gas/oil ratio, and LHSV (Liquid Hourly Space Velocity). The values of these operating variables depend on the quality of the feedstock and the desired product specifications. For example, for low-boiling petroleum feedstock such as naphtha, reactor's pressure and temperature in the ranges of 1.4-3.4 MPa, and 260-343ºC, respectively, are sufficient for hydrotreating. However, for high-boiling petroleum feedstock such as residua more severe conditions are required. Pressure and temperature ranges for hydrotreating of such feedstock can be as high as 6.9-13.8 MPa and 343-427ºC, respectively (McKetta, 1992; Botchwey, 2003).

In the research works that dealt with hydrotreating of heavy gas oil (HGO), these operating variables had the following ranges: temperature: 340-450ºC, pressure: 4.5-12.5 MPa, gas/oil ratio: 400-1200 mL/mL, and LHSV: 0.5-4 h^{-1}(Mann et al., 1987 and 1988; Ferdous et al., 2006; Botchwey et al., 2003; Bej et al., 2001). The trends of the effects of these operating variables on hydrotreating of HGO are summarized in Table 2.1. Moreover a more elaborate summary of the effects of these operating variables is present in Table 2.2. Other operating variables not yet mentioned that are rarely discussed in the open literature include H_2 purity and H_2 partial pressure, with H_2 purity being the least examined.

Table 2.1: The Effects of increasing operating variables on hydrotreating activities.

Variables	**Temperature**	**Pressure**	**Gas/oil ratio**	**LHSV**
Ranges	300-450°C	4.5-12.5 MPa	400-1200 mL/mL	0.5-4 h^{-1}
HDS	Increase	Increase	Plateaus at higher Gas/oil ratio	Decrease
HDN	Increase	Increase	Plateaus at higher Gas/oil ratio	Decrease
HDA	Maximum (375-385°C)	Increase	Plateaus at higher Gas/oil ratio	Decrease

Table 2.2: Summary of the effect of the operating variables on the hydrotreating activities

Process variables	**Feed, catalysts, reactor type**	**Operating Conditions**	**Significant results**	**Comments**	**References**
Temperature Pressure LHSV	Heavy gas oil (Athabasca bitumen) -Co-Mo/γAl_2O_3 Trickle bed	300-450°C 4.25-12.51 MPa 0.67-3.8 hr^{-1}	-Both HDS and HDN improved with increasing temperature and pressure, and decreasing LHSV. -HDA did not improve substantially with increasing temperature. However, increasing pressure and decreasing LHSV had a positive effect on HDA	This is the general trend that is seen in the literature for HDS and HDN. For HDA, it is often reported (Girgis and Gates, 1991) that it passes through a maximum (between 375 and 385°C) with increasing temperature	Sambi Inderjit S., et. al. (1982)
Temperature Pressure LHSV	Heavy gas oil (Athabasca bitumen) Co-Mo/γAl_2O_3 Ni-Mo/γAl_2O_3 Ni-W/γAl_2O_3	300-450°C 4.25-12.51 MPa 0.5-4 hr^{-1}	-Both HDS and HDN improved with increasing pressure, however, HDN improvement was more significant than HDS, The latter being more sensitive to temperature -While Ni-W/γAl_2O_3 was best for cracking, hydrogenation,	Even though, Ni-W/γAl_2O_3 is better than Ni-Mo/γAl_2O_3 in many ways, Ni-Mo/γAl_2O_3 is more economical; thus, usually is industrially used (Gary, H., et. al. 2007)	Ranveer S. Mann, et. al. (1987)

	Trickle bed		Hydrodesulfurization, Ni-Mo/γAl_2O_3 was best for HDN		
Temperature Pressure LHSV Gas/oil	Gas oil fractions Pt-Pd/USY Trickle bed reactor	260-360 °C 3.5-6.0 MPa 1.0-4.0 hr^{-1} 600 ml/ml	HDA increased with temperature at lower temperature range until the optimum point (320 °C). At this point the thermodynamic equilibrium of aromatics hydrogenation is established. Further temperature increase retarded the equilibrated hydrogenation	Here the HDS and HDN was carried out first on a different catalysts (Co-Mo/γAl_2O_3 or Ni-Mo/γAl_2O_3) and then Pt-Pd/USY was used for HDA; Pt-Pd/USY is poisoned by sulfur and/or nitrogen compounds	Gabor Nagy et. al. (2007)
Temperature Pressure LHSV Gas/oil	Heavy gas oil Ni-Mo/γAl_2O_3 Trickle bed reactor	365-415 °C 6.5-8.8 MPa 0.5-2 hr^{-1} 400-1000 ml/ml	-The rate of removal of non-basic nitrogen compounds is much lower than that of basic nitrogen -HDN increased with increase in gas/oil from 400-800 ml/ml beyond which there was no beneficial effect of increasing the gas oil on conversion	Non basic nitrogen compounds have to undergo hydrogenation to become basic before the C-N Bond scission	Shyamal et. al. (2000)

Hydrogen partial pressure Temperature Space time (LHSV)	Pyridine, aniline, and quinoline Ni-Mo-P/γAl_2O_3 Trickle bed reactor	300°C 2.3-9.4 MPa 470-2500 g-cat h/gmol	-The greater the adsorption strength of the nitrogen compounds on the catalyst surface, the lesser the effect of partial pressure of hydrogen. Aniline had lower adsorption strength than pyridine; thus, was affected more by the partial pressure of hydrogen	Aniline is non-basic (pka = 4.87) whereas pyridine is basic (pka = 5.21). Non-basic compounds undergo hydrogenation to become basic, and possibly, this is the reason why they are affected more by the hydrogen partial pressure in comparison to basic compounds	M. Machida et. al. (1999)
Hydrogen partial pressure Temperature	Quinoline Ni-Mo/γAl_2O_3 Stirred tank reactor	350 °C 1.05-15.16 MPa	-hydrogen partial pressure affected the reaction path and kinetics -At larger hydrogen partial pressures the HDN was faster than at lower hydrogen partial pressures, but the reaction proceeded via a "high hydrogen consumption" path way.	Hydrogen consumption increased with increasing hydrogen partial pressure because of the increase in the degree of hydrogenation of the ring (s) before the nitrogen removal	F.Gioia and V. Lee, (1986)

2.1.2.1 Temperature

Generally, increasing temperature leads to increase in HDS and HDN activities. However, HDA activity passes through a maximum. This maximum HDA activity is achieved between 375 and 385ºC (Gray et al. 2007). Hydrotreating operating temperature must be minimized while desired product quality is maintained (i.e. temperature must be high enough so that the desired hydrotreating conversion is achieved but not excessively high). Higher temperature operations results in accelerated catalyst deactivation; and therefore shortened operating cycle (Gruia, 2006). Nonetheless, operating temperature is gradually increased if the desired product quality is to be maintained. This is because as the hydrotreating operation proceeds the catalyst gradually loses some of its activity.

2.1.2.2 Liquid Hourly Space velocity (LHSV)

The Liquid Hourly Space velocity (LHSV) is defined as the ratio of the volumetric flow rate (hourly) of the liquid feedstock to the volume of the catalyst. LHSV is the inverse of the residence time. Decreasing LHSV usually results in an improvement of hydrotreating activities. However, an extreme reduction of LHSV may cause the unit operation to become difficult due to hydraulic considerations (Gruia, 2006). Severe reduction of LHSV may cause channeling which leads to poor liquid distribution and under-utilization of the catalyst. Operation at too high of LHSV does not only reduce the feedstock-catalyst contact time but it also increase the reactor pressure drop and may present some hydraulic challenges.

2.1.2.3 Gas/oil ratio

Gas/oil ratio is the ratio of total gas fed into the reactor to the amount of feedstock. This variable is of great importance and if kept too low, will result in rapid catalyst deactivation. In general, the minimum gas/oil ratio should be at least 4 times the amount of hydrogen consumption (Gruia, 2006). Bej et al. 2001 reported that for HDS and HDN there is an optimal value for gas/oil ratio which depends on the nature of the feedstock and the values of other operating variables.

2.1.2.4 H_2 purity

Un-reacted H_2 are recovered from the reactor effluent, mixed with make-up H_2 to increase the purity, and then recycled into the hydrotreater. If the H_2 is not recovered from the reactor gaseous effluent and recycled, the hydrotreating process economics are unfavorable (Gray et al., 2007). Minimum H_2 purity is usually in the range of 70 to 80 mol% (Gruia, 2006). To achieve the desired product quality lower, H_2 purity must be offset with a higher operating temperature which results in faster catalyst deactivation rates. "H_2 purity" is discussed in greater details in future sections (section 2.7)

2.1.3 Hydrotreating catalysts

Hydrotreating catalysts are solid with three main constituents: an active component, a promoter, and a support. The support constituent is usually, gamma alumina (γ-Al_2O_3). The acidity of the support is enhanced by the addition of a small amount of phosphorus or silica (Gruia, 2006). The active component is normally molybdenum, however, tungsten is occasionally used. Molybdenum catalysts are promoted with cobalt or nickel; a promoter is a second metal, aside from the active

metal, which role is to stabilize the catalyst and as a result enhances the overall catalytic activity. CoMo is the most economic catalyst for sulfur removal. However, if considerable nitrogen removal and/or aromatic content reduction are desired, then NiMo is more efficient (Girgis and Gates, 1991; Gray et al., 2007). In fact, NiW is the most efficient catalyst for nitrogen removal and/or aromatic content reduction (Gray et al., 2007). However, it is much more expensive than NiMo thus is seldom used.

2.1.3.1 Hydrotreating catalyst structure

Hydrotreating catalysts are synthesized in oxide form and must be activated by turning them into sulfide form through a sulfidation process (discussed in detail in Chapter 3) (Gruia, 2006). The active phase for the hydrotreating catalyst is believed to be CoMoS (or NiMoS for Nickel promoted catalyst) (Topsøe et al. 1981). Other species such as Co_9S_8 (Ni_xS_Y) and Co/Al_2O_3 (Ni/Al_2O_3) also exist but are much less active than CoMoS (NiMoS).

The MoS_2 phase consists of layers of Mo alternating with layers of S, where the overall structure is a hexagonal close packed (HCP) (Sun, 2005). Mo exists as MoS_2 in the sulfides Mo catalyst In a promoted MoS_2 catalyst, the promoters replace some of the Mo atoms either on the S-edge or the Mo-edge of the MoS_2 HCP layers (Topsøe, 2007). Nickel tends to prefer the Mo-edge while cobalt prefers the S-edge (Sun, 2005). The Co-Mo-S structure is shown schematically in Figure 2.3.

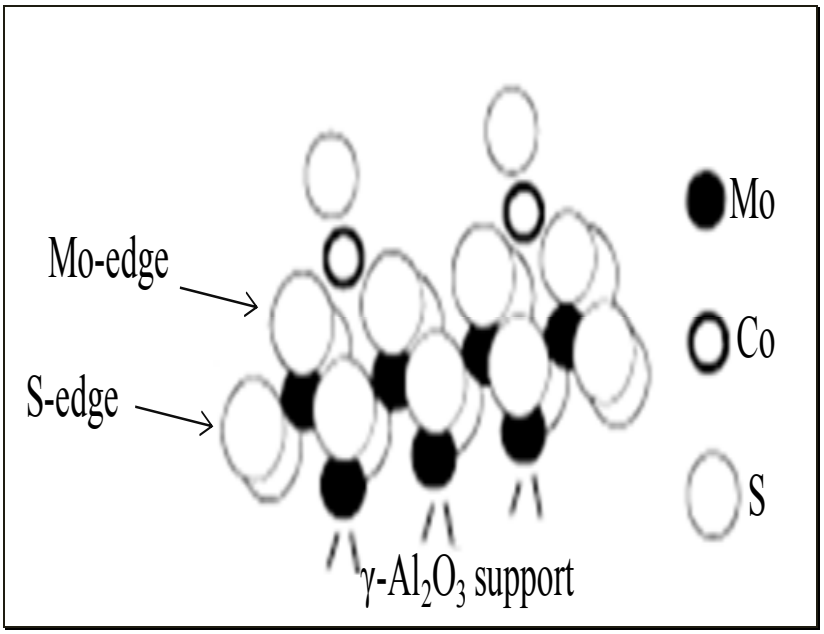

Figure 2.3: A representation of Co-Mo-S structure (Adopted from, Leliveld et al., 1997

Regarding to how the catalyst works, the key element for the catalyst's hydrotreating activity is the concept of vacancies (Mochida and Choi, 2004). After sulfidation of the catalyst, it is speculated that these vacancies form as hydrogen reacts with a surface sulfide group resulting in the release of H_2S and the creation of an S-vacancy. Since, the original site (non-vacant site) was thermodynamically favorable there would be a tendency for its re-creation. This tendency acts as a driving force for organosulfur and organonitrogen compounds to occupy the site and undergo HT. This process is known as sulfur breathing, and is shown schematically in Figure 2.4. In CoMoS species, a strong Co-Mo interaction results in a weaker metal-sulfur bond than in MoS_2, thus leading to an enhanced sulfur breathing and ultimately improved HT activity (Topsøe, 1996). This explains the promoting effects of the promoters (Co and Ni).

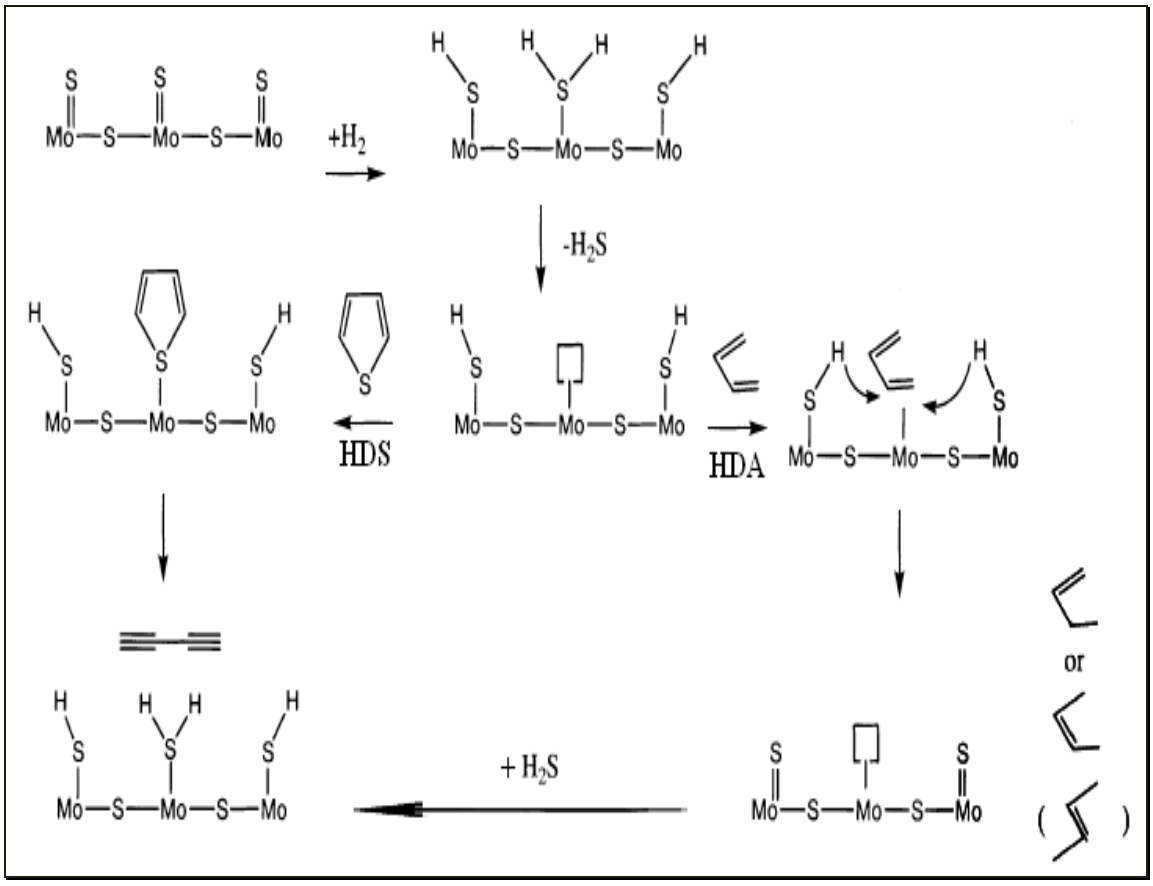

Figure 2.4: An illustration of the sulfur breathing mechanism (adopted from Mochida and Choi, 2004).

2.1.3.2 Hydrotreating catalyst deactivation

Over time the activity of the catalyst decreases mainly for reasons such as coke deposition, metal deposition, and support sintering. Coke is formed as hydrocarbons undergo dehydrogenation followed by thermal condensation or polymerization. Coke is a hydrogen-deficient carbonaceous material which when deposited on the catalyst surface blocks the pore openings and consequently reduces the accessibility of the active sites inside the pores (Gruia, 2006). At higher H_2 partial pressure, hydrogenation of the

coke precursors reduces coke formation. Catalyst deactivation due to coke formation is reversible in that the catalyst can be regenerated by burning off the coke.

Petroleum feedstocks contain metals such as Nickel and Vanadium. These metals can cause catalyst deactivation by blocking the pore entrances, resulting in a reduction in the accessibility of the active sites inside the pores (Speight, 1981; Gruia, 2006). Excessively high temperatures along with high water partial pressures can result in catalyst deactivation due to sintering. The collapse of the pores leads to a decrease in surface area and thus activity (Gruia, 2006). Catalyst deactivation due to metal deposition and support sintering are irreversible.

2.1.4 Corrosion concerns

Organosulfur components present in the crude oil are generally not acidic, except for mercaptans, and thus are not directly a major corrosion threats (Abdel-Aal et al., 1992). However, these compounds are thermally unstable and produce H_2S which is responsible for sulfide corrosion (see Equation 2.2) in the crude processing. Therefore, hydrotreating of petroleum fractions is necessary to reduce the risk of corrosion in other refining units.

The main corrosion problem in the petroleum industry is naphthenic acids (NA) corrosion (Zeinalov et al., 2009). NAs are present in petroleum fractions and hydrotreating can help reduce their contents. A noteworthy point that is found in the literature is that corrosive effect of NAs decrease with increasing sulfur-content of the crude. Yepez (2005) showed that H_2S presence leads to formation of FeS protective

layer, thus further naphthenic acids corrosion is stopped. The reactions of the formation of the protective layer are as follows (Slavcheva et al., 1999; Zeinalov et al, 2009):

$$Fe + RCOOH \longrightarrow Fe(RCOO)_2 + H_2 \quad (2.1)$$

$$Fe + H_2S \longrightarrow FeS + H_2 \quad (2.2)$$

$$Fe(RCOO)_2 + H_2S \longrightarrow FeS + 2RCOOH \quad (2.3)$$

2.1.5 Environmental concerns

Hydrotreating is absolutely necessary to remove or reduce the contaminants concentrations present in the petroleum feedstock such as sulfur, nitrogen, and aromatics. If these contaminants are not removed prior to the releasing of the petroleum products for public use, they may eventually form pollutants such as SO_x, NO_x, and particulate matter. These pollutants have severely detrimental environmental and health effects (Environment Canada, 2004a & 2004b). The harmful environmental effects include: acid rain, smog, vegetation damage, lack of biodiversity, water and soil contamination, acidification of aquatic and terrestrial ecosystems, and even ozone layer depletion. The damaging health effects include cancer and respiratory system problems which may lead to premature death.

Due to the aforementioned potentially detrimental effects of the contaminants present in petroleum crude, countries have stringent regulations for fuel specifications, and these regulations are growing even more stringent. For instance, Environment Canada regulations for the sulfur content of on road diesel fuel vehicles became increasing stricter. The limit was 500 ppm sulfur prior to 2006, and was 15 ppm by October 2006 (Environment Canada, 2005). Such a trend is expected to continue as more nations are pushing towards zero-sulfur content fuels.

2.2 Hydrodesulphurization reactivity and mechanism

Hydrodesulphurization of organosulfur compounds is exothermic and irreversible under typical industrial conditions (Temperature: 340-425°C and Pressure: 55-170 atm) (Girgis and Gates, 1991). The organosulfur compounds in the petroleum crude range from thiols to thiophene and its derivatives (see Figure 2.5). Organosulfur compounds such as thiols, disulfide, and six- membered ring structures are highly active in comparison to compounds where sulfur is present in a five membered ring structure (thiophenes). For thiophenes, the reactivity increases with the increase in the number of rings (one rings <two rings > three rings) (Whitehurst et al. 1998). However, this trend reverses for thiophenes with four or more rings (i.e. thiophenes with four rings are less active than those with five rings etc.). This change in the trend is due to the fact that HDS has two possible reaction pathways (see Figure, 2.6), and the preferred pathway depends on the structure of the organosulfur compound (Mochdia and Choi, 2004, Girgis and Gates, 1991). The first is direction hydrogenolysis or direct removal of sulfur. In this pathway the sulfur is replaced by hydrogen in the organosulfur compound without hydrogenation of any of C=C bonds. In the second pathway, ring hydrogenation is carried out prior to sulfur removal, thus, leading to higher hydrogen consumption than the first pathway. The presence of two possible reaction pathways makes HDS less dependent on hydrogen partial pressure in comparison to HDN and HDA.

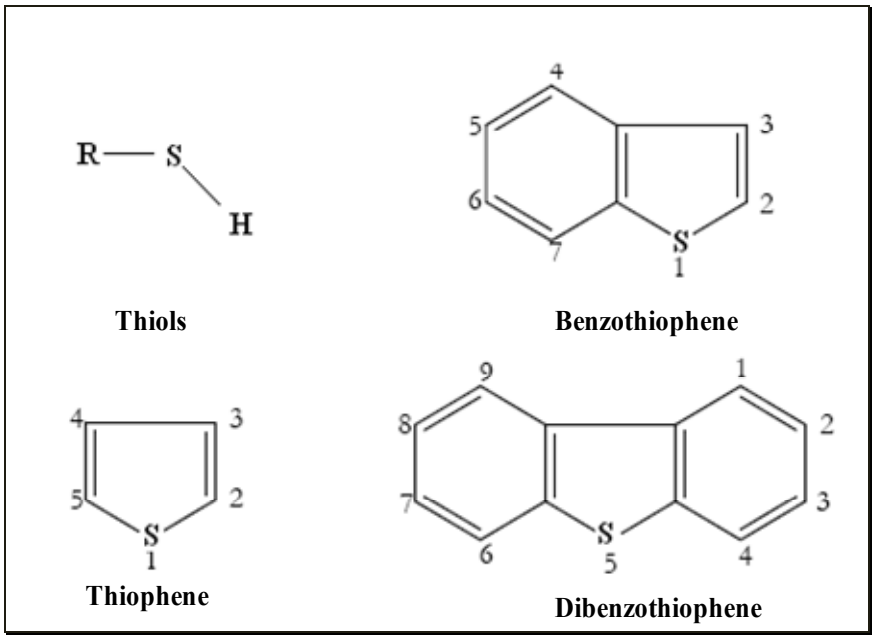

Figure 2.5: Examples of organosulfur compounds in petroleum (Girgis and Gates, 1991).

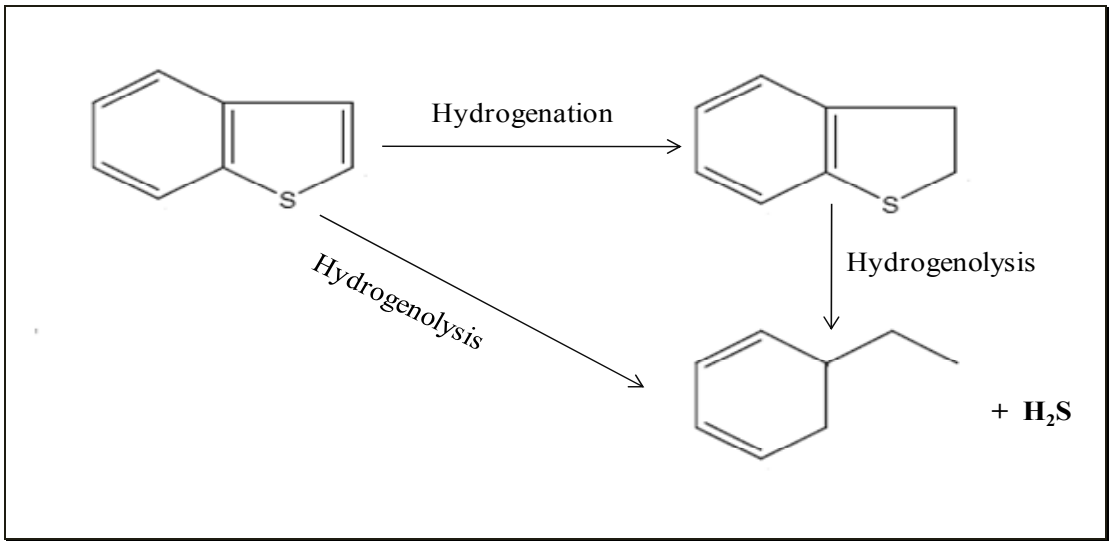

Figure 2.6: HDS reaction pathways (Girgis and Gates, 1991).

2.3 Hydrodenitrogenation reactivity and mechanism

Organonitrogen compounds in the petroleum crude are mainly in heterocyclic aromatic compounds form (see Figure 2.7). Amines and nitriles are also present in the

petroleum crude, but are of less concern because they are easily processed (Girgis and Gates, 1991). Heterocyclic organonitrogen compounds can be divided into basic (e.g. quinoline, acridine) and non-basic (e.g. carbazole, indole) compounds. In the basic nitrogen compounds the lone pair of electrons on the nitrogen atom is not part of the aromatic system, whereas in the non-basic compounds, this lone pair of electrons is delocalized over the aromatic ring and is unavailable for donation to a Lewis acid, see Figure 2.8. This makes the non-basic compounds less reactive than the basic compounds (Girgis and Gates, 1991; Bej et al., 2001). In the non-basic compounds, the nitrogen is part of a five membered ring, however, in the basic compounds it is part of a six membered ring.

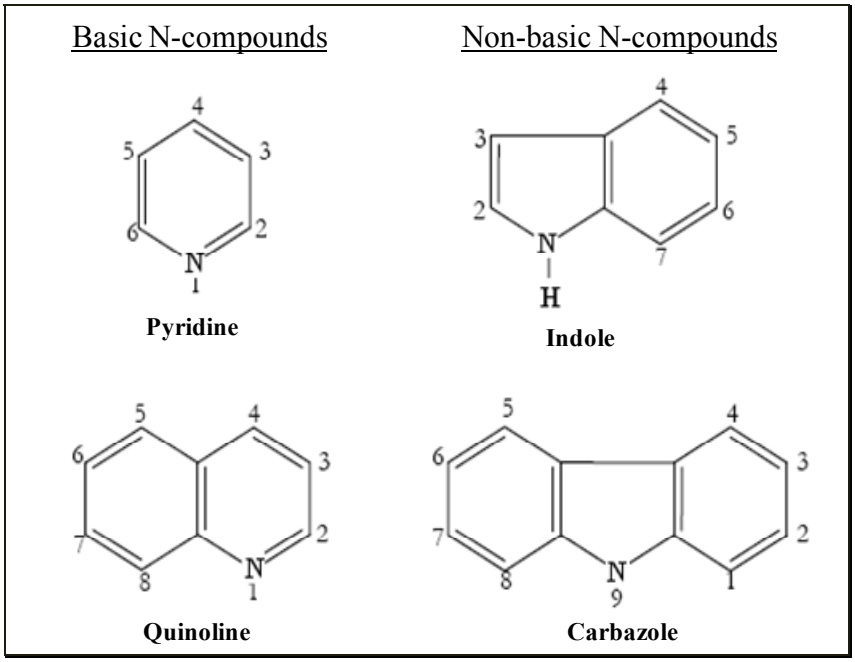

Figure 2.7: Examples of organonitrogen compounds in petroleum (Girgis and Gates, 1991)

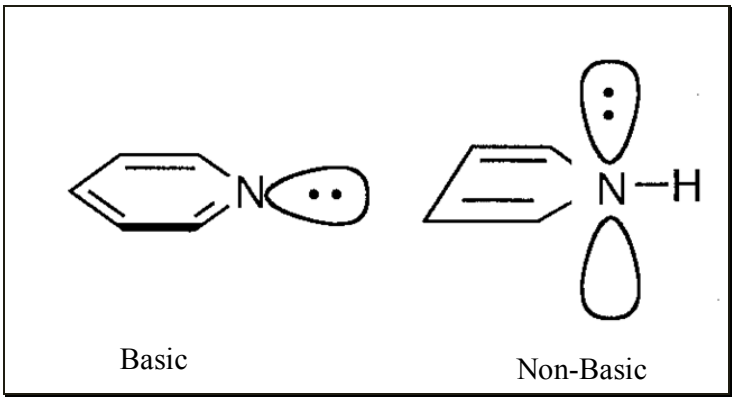

Figure 2.8: Illustration of electronic structure differences between basic and non-basic nitrogen compounds

Unlike HDS, HDN has only one reaction pathway (see Figure 2.9), and that is hydrogenation of organonitrogen compound prior to hydrogenolysis or removal of nitrogen. Hydrogenation of the nitrogen-containing ring is required to reduce the relatively high bond energy of C=N bond (615 kJ/mole) prior to C-N bond (389 kJ/mole) scission (Landau, 1997)**.** For comparison purposes C=S and C-S bond energies are equal at 536 kJ/mol therefore hydrogenation of the sulfur containing ring is not thermodynamically advantageous. On a percent weight basis nitrogen removal consumes more hydrogen than sulfur removal. Hydrogen consumption is about 300-350 scf/bbl per percentage nitrogen, and 70-100 scf/bbl per percentage sulfur (Gray et al., 2007; Ancheyta and Speight, 2007).

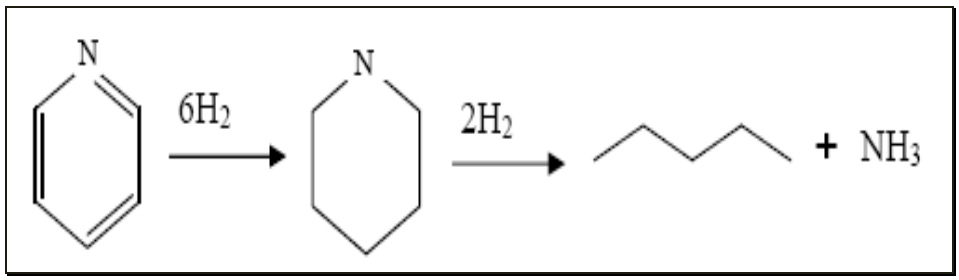

Figure 2.9: HDN reaction pathways (Girgis and Gates, 1991).

2.4 Hydrodearomatization reactivity and mechanism

Like HDS and HDN, HDA of aromatics in the petroleum crude is an exothermic reaction, however it is reversible under industrial conditions (Girgis and Gates, 1991, Gray et al. 2007), and maximum aromatics reduction is realized between 370ºC and 385ºC (Gray et al. 2007). As a result, higher hydrogen partial pressures are necessary to force the equilibrium to the product side and achieve the desired products. Reactivity of aromatic compounds increases with increasing ring numbers (poly- > di- > mono-); hydrogenation of a mono-aromatic ring is difficult because of its resonance stability (Girgis and Gates, 1991). The pathway for HDA is hydrogenation; and the hydrogen consumption for HDA is ~27 scf/bbl per one vol. % of aromatic content (Ancheyta and Speight, 2007). Examples of aromatic compound are presented in Figure 2.10.

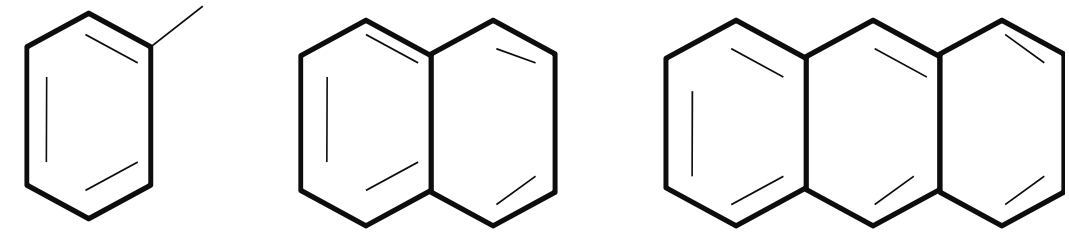

Figure 2.10: Examples of aromatic compounds in petroleum (Girgis and Gates, 1991).

2.5 Hydrotreating reactor

The most widely used hydrotreating reactor is the trickle-bed reactor (TBR) (Al-Dahhan et al., 1997). In TBR, the fixed catalyst bed is contacted by a downward concurrent flow of gas and liquid. When the gas-liquid flow is upward then the reactor is termed flooded bed reactor (FBR). TBR is superior to other three-phase reactors such as

slurried or fluidized bed reactors in that, due to the motionless of the catalyst bed which results in lower Reynolds number, the system can be operated near the plug flow pattern. The industrial TBR operation can be either single-stage or two-stage. In the two-stage approach, H_2S (and some cases NH_3) is removed from the effluent from the first stage prior to the effluent introduction to the next stage (Owusu-Boakye et al., 2006).

2.6 H_2 cycle in hydrotreating

A typical gaseous effluent of a hydrotreating operation is made up of unreacted hydrogen, H_2S, light hydrocarbons (C_1-C_3) and other impurities (Turner and Reisdorf, 2004). The hydrogen content in this stream is 70 – 85% (Peramanu et al., 1999). After reduction of the concentration of the non-hydrogen species, this stream is combined with make-up hydrogen, which is ultra-pure, to bring the purity up to 94 – 96%, and then it is recycled to the hydrotreater. Most of the H_2S is removed in the amine unit, and the light hydrocarbons are separated from the hydrogen in the Hydrogen Recovery Unit (HRU). The H_2 recovery process is shown schematically in Figure 2.11.

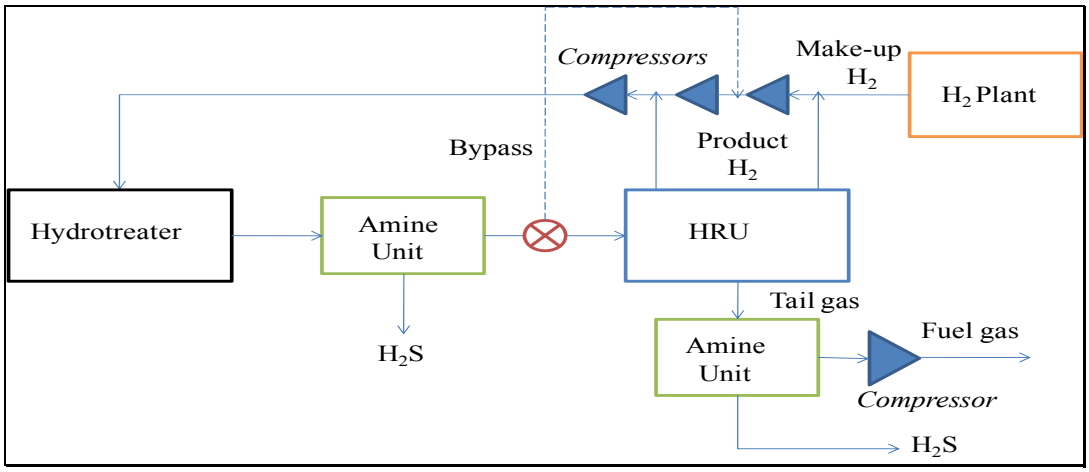

Figure 2.11: H_2 recovery schematic (Peramanu et al., 1999)

2.7 H_2 purity in hydrotreating

2.7.1 Importance of H_2 purity

One way of increasing H_2 partial pressure in a hydrotreater is by increasing the amount of hydrogen in the vapor phase. However, this increase must be relative to the other non-hydrogen species present in the hydrotreater. Therefore, it is necessary to remove the non-hydrogen species from the recycle hydrogen stream, and consequently increase the hydrogen purity. If these non-hydrogen species are not removed and only the recycle hydrogen rate is increased, then the amount of hydrogen in the reactor will increase. However, this will not translate into higher hydrogen partial pressure since the hydrogen mole fraction in the vapor phase remains almost the same (Turner and Reisdorf, 2004). Lower hydrogen purities are unfavorable since a higher temperature is required to maintain the product quality (Gruia, 2006); higher temperature accelerates the catalyst deactivation.

2.7.2 Major impurity in the recycle H_2 stream

Methane is the most abundant impurity in the influent of a HRU. It often builds up to high concentrations in the recycle gas because it is difficult to remove (Turner and Reisdorf, 2004). The effect of methane on the catalyst's performance in the hydrotreating area has not been reported. However, in the area of steam reforming, which uses nickel-based catalysts, it has been reported that methane dissociatively chemisorbs on the nickel surface (Jiang and Goodman, 1990). This may lead to catalyst deactivation via carbon deposition (Yongloi and Hengyong, 2002**)**. Thus, its presence at high concentration in the inlet hydrogen stream into a hydrotreater may interfere with the function of a nickel-molybdenum catalyst. Traditionally, the concentrations of

methane and other light ends are reduced in the recycle stream to boost the hydrogen purity. Consequently, the hydrogen partial pressure is increased inside the hydrotreater, resulting in higher hydrotreating activities (Speight, 1981).

2.7.3 H_2 recovery process

As mentioned in section 2.6.2, the gaseous effluent of a hydrotreater is made up mainly of unreacted hydrogen, H_2S, and light hydrocarbons (C_1-C_3). Also, NH_3 is present in the gaseous effluent, however, at a minute concentration as compared to H_2S and light hydrocarbons (Ferdous et al., 2006). Most of the NH_3 is removed in the water scrubber (refer to section 3.3). H_2S is generated during hydrotreating as a product of HDS reactions. Most studies reported that H_2S inhibits hydrotreating activities (Herbert et al., 2005; Girgis and Gates, 1991; Hanlon, 1987; Sie, 1999; Ancheyta et al., 1999, Bej et al., 2001), yet it is required to maintain the active chemical state of the catalyst (Bej et al., 2001) because the catalyst must be maintained in the sulfided form. H_2S inhibition results when it competes against organosulfur and organonitrogen for the same active sites on the catalyst. H_2S generated inside a hydrotreater can have an equilibrium value as high as 5 mol.% in the recycle gas (Gruia, 2006). This concentration of H_2S not only inhibits hydrotreating activities, it also reduces H_2 partial pressure in the hydrotreater. Therefore, H_2S must be removed from the effluent gaseous stream prior to its recycling. The H_2S is removed in a scrubber by contacting the gas with an amine solution (generally MEA or DEA) (Gruia, 2006). Subsequently, the effluent of the amine unit (see Figure 2.10) is sent to the HRU for the removal of methane and other light ends.

In the industry, reduction in methane and other light ends concentration is achieved using three major processes: cryogenic phase separation, pressure swing adsorption (PSA), and diffusion (Gray et al., 2007). PSA is a mature separation tool widely employed in the industry to purify hydrogen in different process streams (Ruthven et al., 1994). PSA is capable of producing high purity hydrogen; as high as, 99 %+ (Peramanu et al., 1999), however, this is achieved at the expense of recovery. In a study by Huang et al. (2008), a mixture of 50 % methane and 50 % hydrogen was separated using a Laboratory-scale PSA unit. They reported that, in order to increase the product hydrogen purity from 88.7 % to 99.8 %, the operating pressure was to be increased from 4.5 to 5.8 bar. Hydrogen recovery, however, dropped from 47.7 to 39.6 % as a result. If the hydrotreating process can tolerate lower inlet hydrogen purity without affecting the catalyst performance, then higher recovery advantage can be exploited.

2.8 H_2 partial pressure

2.8.1 Importance of H_2 partial pressure

In gas-liquid-solid reactors such as trickle bed reactor, the gaseous reactant dissolves into the liquid prior to its diffusion into the solid (catalyst). The overall reaction rate with respect to the gaseous reactant is a direct function of the efficiency of the gaseous reactant transfer into the catalyst pellet through the liquid phase (Fogler, 1999). Henry's Law states that a gas dissolution is proportional to its partial pressure above the liquid. Thus, increasing H_2 partial pressure will increase the concentration of H_2 in the liquid phase and thereby enhance hydrotreating activities. A reduction in H_2 partial pressure below the design level results in catalyst deactivation due to coke

formation (Gruia, 2006). H_2 partial pressure design level is an economic optimum that balances capital cost and operating costs against catalyst life. Excessively high H_2 partial pressure may merely saturate the catalyst's surface, which is a plus from a catalyst deactivation standpoint, without significantly improving hydrotreating activity (Speight, 1981).

2.8.2 Dependent nature of H_2 partial pressure

Unlike temperature, pressure, LHSV, and gas/oil ratio, H_2 partial pressure is not an independent variable. H_2 partial pressure is a direct function of reactor pressure and vapor phase composition. The vapor phase composition is a function of temperature, pressure, LHSV, and gas/oil ratio because these variables affect hydrogen consumption and vapor-liquid equilibrium. Limited studies have been carried out on the dependent nature of H_2 partial pressure. The most detailed study found was by McCulloch and Roeder (1976).

McCulloch and Roeder (1976) examined the effects of pressure, temperature, and gas/oil ratio on inlet and outlet H_2 partial pressure. The pressure, temperature, and gas/oil ratio ranges were 500-545 psi, 343-380ºC, and 600-1200 scf/bbl. The feed used in the study had a density of 0.87 g/cm^3, a molecular weight of 224 g/mole, and a volumetric average boiling point of 296ºC. The authors made two important conclusions: 1) higher temperature drastically decreased inlet and outlet H_2 partial pressure due to an increase in feed vaporization, and 2) increasing gas/oil ratio did not affect inlet H_2 partial pressure but resulted in an increase in outlet H_2 partial pressure. Perhaps, the purpose of the authors' study was merely to illustrate a method for calculating inlet and outlet H_2 partial pressure, thus they did not provide scientific

explanations for the observed results. Avenues to be explored as an extension of this study are: 1) observation of the effects of the change of feedstock and experimental conditions on feed vaporization, H_2 consumption, H_2 dissolution, and H_2 pp; 2) an attempt to provide scientific explanations for the results observed by the authors.

2.9 Inlet versus outlet H_2 partial pressure

H_2 partial pressure at the hydrotreater's outlet can vary greatly than at its inlet if the hydrogen consumption is significant (McCulloch and Roeder, 1976). H_2 partial pressure at the hydrotreater's outlet condition is more important than its inlet because: 1) Outlet conditions are the catalyst's last chance to cause change in the feedstock, 2) Outlet conditions approximate average conditions throughout the catalyst bed. Moreover, from the catalyst standpoint, the knowledge of H_2 partial pressure at the hydrotreater outlet is essential since it is the point with the lowest H_2 partial pressure.

2.9.1 H_2 consumption

Information about H_2 consumption is important for the determination of the amount of the required make-up H_2 and also for outlet H_2 partial pressure calculation (Ancheyta and Speight, 2007; McCulloch and Roeder, 1976). In the industrial hydrotreater, H_2 consumption is summation of (Gruia, 2006; Hisamitsu et al., 1976):

(a) Chemical hydrogen consumption; The H_2 consumed during the hydrotreating reactions such as HDS, HDN, and HDA

(b) Solution losses; H_2 dissolved in the liquid product

(c) Mechanical losses; H_2 lost in the compressors

(d) Venting losses; H_2 lost in the purge stream

For a laboratory-scale hydrotreater, only chemical H_2 consumption and dissolved H_2 losses are of concern. Dissolved H_2 losses are determined from vapor-liquid equilibrium (VLE) calculations (McCulloch and Roeder, 1976), and for this HYSYS may be used (Mun˜oz et al., 2007).

2.9.1.1 Chemical H_2 consumption

Chemical H_2 consumption is the amount of hydrogen used to carry out hydrotreating activities. There are four procedures generally found in literature for determining the amount of chemical H_2 consumption (Ancheyta and Speight, 2007):

Procedure 1: This is an experimental approach. Here, H_2 consumption is determined by means of H_2 balance in the gas streams (i.e. based on the difference between the amount of H_2 in the inlet gaseous stream and that in the outlet gaseous stream).

Procedure 2: This is an experimental approach. Here H_2 consumption is determined by means of H_2 balance in the liquid feed and liquid product (i.e. based on the difference between the amount of H_2 in the liquid feed and that in the liquid products).

Procedure 3: Similar to Procedure 2; however, the increase in liquid product's H_2 content is determined based on the decrease in the aromatic carbon content instead of the elemental analysis as in procedure 2. According to a study by Hisamitsu et al. (1976), comparing to procedures 1 & 2, procedure 3 yielded more accurate results and it was the most convenient in situations where hydrocracking is small. Procedure 3 is expressed mathematically in Equation 2.4 (adopted from Hisamitsu et. al. (1976) and McCulloch and Roeder, 1976).

$$\text{Chemical } H_2 \text{ consumption} = \frac{[(C_A)_f - (C_A)_p] \times \text{density}_{\text{feed}}}{100 \times 2 \times 12} \times 379 + H'_{H_2S} + H'_{NH_3} + H_{H_2S} + H_{NH_3} \quad (2.4)$$

$$H'_{H_2S} \approx H_{H_2S} = \frac{[(S)_f - (S)_p] \times \text{density}_{\text{feed}}}{100 \times 32} \times 379 \quad (2.4.a)$$

$$H'_{NH_3} \approx H_{NH_3} = \frac{[(N)_f - (N)_p] \times \text{density}_{\text{feed}}}{100 \times 14} \times 379 \quad (2.4.b)$$

where:

C_A, S, and N = aromatic carbon, sulfur, and nitrogen contents (wt.%), respectively, and subscripts "f" and "P" = feed and products, respectively; H'_{H_2S} and H'_{NH_3} = amount of H_2 necessary to form hydrocarbon during HDS and HDN (scf/bbl), respectively; H_{H_2S} and H_{NH_3} = H_2 content of H_2S and NH_3 in the product gas (scf/bbl) , respectively; 379 = number of standard cubic feet in a mole of an ideal gas (scf/mole); $\text{density}_{\text{feed}}$ = 346 lb/bbl. The units for H_2 consumption is scf/bbl.

Procedure 4: Another approach for determining chemical H_2 consumption is to use typical hydrogen consumption found in the literature (Speight, 1999; Ancheyta and Speight, 2007). According to this approach, chemical hydrogen consumptions for HDS, HDN, and HDA are 90-100 scf/bbl per wt. % S, 300-350 scf/bbl per wt. % N, and 27 scf/bbl per vol. % aromatics. H_2 consumption is calculated by first determining the amount of the reduction in S, N, and aromatics then multiplying these quantities by the appropriate unit H_2 consumption.

2.9.1.2 Dissolved H_2 losses

Dissolved H_2 losses can be determined from VLE calculations using HYSYS. For hydrotreating applications, the appropriate thermodynamic models for VLE are Peng–Robinson equation (original and modified), the Soave–Redlich–Kwong equation and the Grayson–Streed method (Lal et al., 1999). In several studies, H_2 solubility in various hydrocarbons determined using these thermodynamic models were compared against those obtained experimental, and the authors concluded that these thermodynamic models yielded accurate predictions (Ramanujam et al. 1985, Wilson et al., 1981, Lal et al., 1999). For instance, Lal et al. (1999) measured H_2 in Athabasca bitumen using a batch autoclave at temperature range of 50 to 300°C and H_2 partial pressure up to 24.8 MPa. The authors concluded that the aforementioned thermodynamic equations yielded accurate results. The most accurate among them were the modified Peng–Robinson equation (see Figure 2.12).

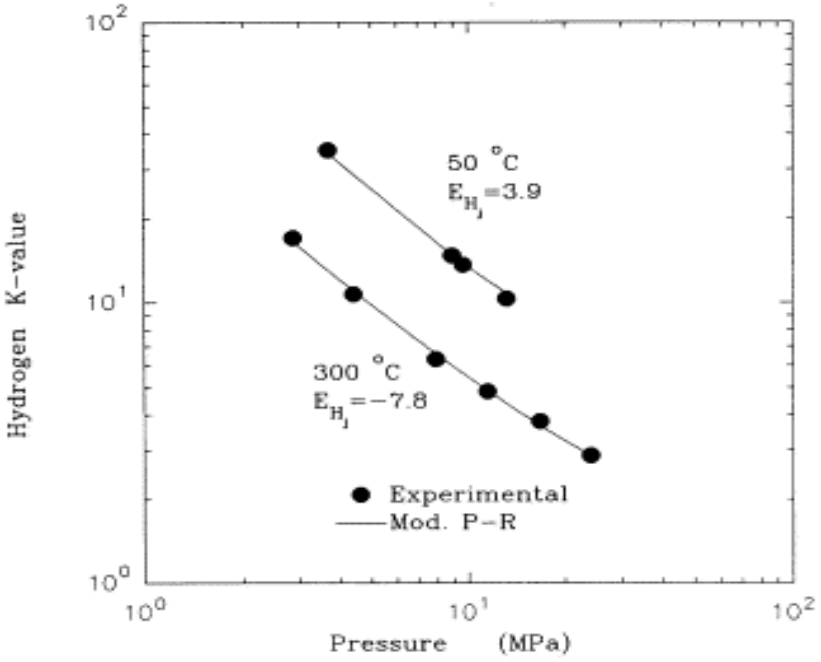

Figure 2.12: Experimental and pdicted H_2 K-values in Athabasca Bitumen (Lal et al. 1999).

2.9.2 Determination of inlet and outlet H_2 partial pressure

In situations where there is considerable H_2 consumption inlet and outlet hydrogen partial pressures may differ considerably. In this section a step by step method of determining H_2 partial pressure is shown (Adopted from McCulloch and Roeder, 1976).

Step 1: Use HYSYS to determine the VLE at the reactor inlet. For this task the following input data is needed: temperature, pressure, gas flowrate and composition, feed rate and properties. Since feeds such as heavy gas oil may not be available in the HYSYS package, boiling range distribution information (obtained from simulated distillation) of the feed may be used to simulate the feed in HYSYS. The above information is fed into HYSYS and the appropriate thermodynamic model is selected (in this case Peng–Robinson equation (original and modified), the Soave–Redlich–Kwong equation or the Grayson–Streed method can be selected). The software yields the resultant vapor/liquid split of all components.

The inlet H_2 partial pressure is then the product of H_2 mole fraction in the vapor phase and system's pressure. For heavy feed, inlet H_2 partial pressure can simply be approximated as the product of inlet H_2 purity and the system's pressure.

Step 2: Determine the H_2 consumption. For this step hydrotreating experiments are carried out and the products (gas or/and liquid) are analyzed. The results of the analysis are then used to calculate H_2 consumption; refer to section 2.8.1 for H_2 consumption calculation.

Step 3: Use HYSYS to determine the VLE at the reactor outlet. Notice that at the outlet condition, the gaseous compositions must account for the produced H_2S and NH_3, present CH_4, and the decrease in H_2 due to H_2 consumption. H_2S and NH_3 are produced as a result of HDS and HDN, respectively. Moreover, liquid product (s) properties are used instead of the feed properties. By running the flash calculations in HYSYS the resultant vapor/liquid split of all components at the reactor outlet are obtained. The outlet H_2 partial pressure is then the product of the product of H_2 mole fraction in the vapor phase and system's pressure.

2.10 Laws and Principles explaining gas-gas and gas-liquid interactions

To observe the interaction between the H_2 gas and the liquid hydrocarbon feedstock and the liquid and gaseous products, it is important to understand the possible liquid-liquid and gas-liquid interactions that may take place among these species. There are several principles and Laws that describe gas-gas and gas-liquid interactions. Some of these principles and Laws are briefly discussed below (Swarbrick and Boylan, 2002).

2.10.1 Le Chatelier's Principle

Le Chatelier's Principle states that when a system at equilibrium is subjected to a change the equilibrium shifts to counter-act the change. For instance, in a vapor-liquid equilibrium an increase in pressure will cause the equilibrium to shift toward formation of more liquid because liquid occupies less space than vapor.

2.10.2 Dalton's Law

Dalton's Law states that the partial pressure of a gas in a mixture of gases is equal to the product of the system's total pressure and the gas' vapor mole fraction. For real gases, especially at high pressure, Dalton's Law is not an absolute empirical law, and deviations may be observed due to the interactions among real gases. Nonetheless, these deviations are generally considered small.

2.10.3 Henry's Law

Henry's law states that at equilibrium and at a given temperature, dissolution of a gas in a constant volume of liquid is directly proportional to the gas' partial pressure. If the liquid volume is increased then the amount of the dissolved gas will increase and a new equilibrium is formed.

2.10.4 Raoult's Law

Raoult's Law states that in an ideal solution (no interactions, repulsion nor attraction, among the constituents), the partial vapor pressure of each constituent is directly proportional to the product of the vapor pressure of the pure component and that constituent's mole fraction in the solution. Real solutions tend to deviate from this law. The deviation can be either a positive deviation or a negative deviation based on the nature of the interactions among the solution's constituents.

2.10.4.1 Positive Deviation

When the interactions among the constituents in the solution are repulsive due to the dissimilarities in the constituents' polarities (e.g. a mixture of ethanol and diethyl

ether) then the constituents can escape the solution more easily. As a result, constituent's vapor pressures observed are greater than those predicted by Raoult's Law.

2.10.4.2 Negative Deviation

It is the opposite of the positive deviation. Here, the interactions are attraction due to likeness in the constituents' polarities (e.g. a mixture of nitric acid and water). As a result, constituent's vapor pressures observed are lower than those predicted by Raoult's Law due to decreases in their escaping tendencies.

2.11 Effects of H_2 partial pressure on hydrotreating activities

H_2 partial pressure is a key operating variable. Increasing H_2 partial pressure increases hydrotreating activities (Matar and Hatch, 2001, Speight, 1981). Many studies look at the effects of the H_2 partial pressure on hydrotreating activities using model and real feeds. In this section, some of these studies are reported and critically examined.

2.11.1 Effect of H_2 partial pressure on HDA

HDA is favored by low temperature and high H_2 partial pressure. High temperatures favors the dehydrogenation reactions (i.e. the reversed reaction), consequently lead to low HDA conversions. On the contrary, high H_2 partial pressure favors the forward hydrogenation reaction; thus enhance HDA conversions. For instance, Girgis and Gates (1991) reported that studies by Frye (1962) and Frye and Weitkamp (1969) on hydrogenation of naphthalene had showed that increasing H_2 partial pressure from 9.7 to 37 atm increased naphthalene's equilibrium conversion from

17 to 84%. The reaction temperature was 396ºC; at such a temperature the dehydrogenation reaction is favorable.

Recent studies by Sidhpuria et al. (2008) on hydrogenation of toluene over Rh/ZSM-5 (2002) and over Rh/Hβ zeolite explained the positive effects of increasing H_2 partial pressure on hydrogenation reaction. The authors reported that increasing H_2 partial pressure increases H_2 dissociation on the active sites, meaning higher concentration of H_2 to hydrogenate toluene. However, at extremely high hydrogen partial pressures this enhancing effect becomes insignificant. In Sidhpuria et al. 2008, the authors showed that toluene hydrogenation increased linearly as H_2 partial pressure was increased from 1 to 3 MPa; however, further increase of H_2 partial pressure from 3 to 4 MPa did not significantly improve toluene hydrogenation.

Research works have also been done on real feedstocks. For example, Nagy et al. (2009) have looked at HDA of different light gas oils over PtPd/γ-Al_2O_3. The boiling ranges of the light gas oils ranged from 184-356°C to 212-367°C. The authors concluded that the aromatic content of the products decreased with increasing H_2 partial pressure.

2.11.2 Effect of H_2 partial pressure on HDN and HDS

In a study by Dufresne et al. (1987) on the hydrotreatment of Arabian light VGO, it was observed that the sulfur, nitrogen, and aromatics contents of the liquid product dropped as the H_2 partial pressure was increased from 70 to 140 bars. The sulfur content dropped from 200 to 40 ppm, the nitrogen content dropped from 10 to 1 ppm, and the aromatics content dropped from 31 to 9.6 wt.%. The sulfur, nitrogen, and aromatics contents in the feedstock were 24300 ppm, 650 ppm, and 47 wt. %, respectively. The authors also observed that HDN was more sensitive than HDS and HDA to H_2 partial

pressure. Similar observation was made by Fang (1999) as he studied the effect of H_2 partial pressure on HDS and HDN of Shengli VGO. The H_2 partial pressure range was 4 to 12 MPa, while the temperature, LHSV, and gas/oil ratio were 380°C, 1.0 h^{-1}, and 1000 mL/mL, respectively. The author observed that both HDS and HDN activities improved as H_2 partial pressure was increased. However, HDN was more sensitive than HDS to the change in H_2 partial pressure. This observation was attributed to the differences in the mechanisms of HDS and HDN. HDS reaction may proceed without pre-hydrogenation of the heteroring. However, for an HDN reaction to take place, pre-hydrogenation of the heteroring is necessary.

Some of the research works used model feed to study the effects of H_2 partial pressure on hydrotreating activities. For instance, Yang and Satterfield's (1984) study on the HDN of quinoline found that the activity increased as the H_2 partial pressure was increased from 3.5-10.5 MPa and leveled-off at 14.0 MPa. A somewhat different finding was reached by Hanlon (1987), as he studied the HDN of pyridine. He concluded that hydrogenolysis step, and thus the overall HDN, was dependent on the H_2S partial pressure to H_2 partial pressure ratio (P_{H2S}/P_{H2}). As the H_2 partial pressure was increased (i.e. P_{H2S}/P_{H2} was decreased) hydrogenolysis decreased and so did the overall HDN in the high-pressure regime (5-10 MPa), which is hydrogenolysis-controlled. The contrary was observed in the low-pressure regime (<5MPa), which is hydrogenation controlled. Similar findings were reported by Paal and Menon (1987); the authors commented that hydrogenolysis is either enhanced or retarded depending on the range of the H_2 partial pressure under consideration. Nonetheless, for real feedstock hydrotreated under industrial conditions, the overall effect of increasing H_2 partial pressure increases the

HDS, HDN, and HDA activities (Speight 1981, 2000). Lower H_2 partial pressure accelerates catalyst deactivation.

All the aforementioned studies looked at the inlet H_2 partial pressure. McCulloch and Roeder (1976) objected to this approach. They argued that hydrotreating activities should be correlated to outlet H_2 partial pressure when the effects of H_2 partial pressure are studied. They insisted that from the catalyst deactivation standpoint outlet H_2 partial pressure is more important than inlet H_2 partial pressure since it approximates the average H_2 partial pressure over the catalyst bed. When the H_2 consumption is significant there may be a considerable difference between inlet and outlet H_2 partial pressure. As highlighted by Heinemann and Somorja (1985), the outlet H_2 partial pressure could be as low as 50% that of the inlet due to H_2 consumption; when hydrotreating heavy feedstocks using gas/oil ratio of 80. This means that a good portion of the catalyst bed is at H_2 partial pressure considerably lower than that at the inlet. By focusing only on the inlet H_2 partial pressure this fact can go undetected.

2.12 Kinetics Models for HDS, HDN, and HDA

For reactive processes kinetics studies are crucial in the design of commercial reactors, pilot plant study, process improvements, and optimization of operating conditions (Lee, 1999). The effects of operating variables such as temperature, pressure, LHSV, and gas/oil ratio on a catalyst's hydrotreating performance can be predicted by a suitable kinetic expression or model (Ferdous et al. 2006, Knudsen et al. 1999). Kinetic studies can be approached in two ways: intrinsically or apparently. Intrinsic kinetic study is based on the detailed mechanistic understanding of all the reactions involved

(Lee, 1999). Apparent Kinetics is based on the overall representative stoichoimetric reaction. Generally, the difference between intrinsic and apparent kinetics is that the former is free of diffusion or any other mass transfer limitations.

Two of the commonly used models in kinetic studies of hydrotreating of real feed are the power law model (P-L) and the Langmuir-Hinshelwood (L-H) type model (Girgis and Gates 1991, Ancheyta et al., 2002). P-L is used to describe overall rate law, while L-H is used to account for inhibitions that take place during reactions. Another effective but seldom used model is the multi-parameter kinetic model (Ai-jun et al., 2005). These three models are discussed in the following sub-sections.

2.12.1 Power Law Model

Power law model assume the mechanism described by equilibrium reaction in equation 2.5. By assuming $k_f >> k_r$, then the rate expression can be described by equation 2.6. For HDS and HDN of HGO, this assumption is valid at temperature greater than 425ºC, however, for HDA the reversible reaction becomes significant at temperature greater the 380ºC.

$$A + x\,H_2 \underset{k_r}{\overset{k_f}{\rightleftharpoons}} AH \qquad (2.5)$$

Where: A is the sulfur, nitrogen, or aromatic compounds, AH is the saturated products, and k_f and k_r are the rate constants for the forward and reverse reactions, respectively

Power law model is often preferred due to its simplicity (Ferdous et al., 2006). Compared to the Langmuir-Hinshelwood type model or the multi-parameter type model,

the power law model has fewer parameters which must be determined. Kinetic parameters that can be determined using this model are apparent rate constant and reaction order:

$$\frac{dC}{dt} = -kC^n \qquad (2.6)$$

where: C = sulfur, nitrogen, or aromatics content; t = residence; k = apparent rate constant; n = reaction order;

And its solutions are:

$$C_f - C_p = \frac{k_i}{LHSV} \qquad for\ n = 0 \qquad (2.6, a)$$

$$\ln\left(\frac{C_p}{C_f}\right) = -\frac{k_i}{LHSV} \qquad for\ n = 1 \qquad (2.6, b)$$

$$\left[\frac{1}{C^{n-1}{}_p} - \frac{1}{C_f{}^{n-1}}\right] = (n-1)\frac{k_i}{LHSV} \qquad for\ n \neq 0,1 \qquad (2.6, c)$$

where: n = reaction orders; k_i = apparent rate constant for species "i"; C_p = concentration of the product, wt. %; C_f = concentration of the reactant, wt%; LHSV = liquid hourly space velocity.

The activation energies can then be determined using the Arrhenius equation, Equation 2.7.

$$k_i(T) = k_o e^{-E/RT} \qquad (2.7)$$

where: k_o = Arrhenius constant; E = activation energy (kJ/mol); R = gas constant; kJ/mol.K; T = temperature, K.

Based on the power law model, kinetics studies of model feeds generally follow first order (Botchwey, 2003; Girgis and Gates, 1991; Speight, 2000; Ancheyta et al., 2002). For real feeds, the reaction order depends on the type of feed and the catalyst, and can range between 1-2.5 for HDS and 1-2 for HDN. Generally, the reaction order for HDA is assumed to be pseudo-first order (Owusu-Boakye, 2005). A summary of kinetic studies of real feedstocks are presented in Table 2.3.

2.12.2 Langmuir-Hinshelwood Model

Generally this model is based on the following mechanistic steps (Owusu-Boakye, 2005):

1. The reactants adsorb onto the active sites present on the catalyst's surface.
2. Surface reaction takes place among adsorbed reactants or among absorbed reactants and those reactants present in the bulk solution to form products.
3. Products desorption from the active sites into the bulk solution.

The use of the Langmuir –Hinshelwood type model for kinetic modeling of real industrial feed is very complicated due to the many coefficients that must be determined,

Table 2.3: Summary of reaction orders and activation energies for NiMo- Al_2O_3 as found in the literature.

References	Boiling range feed, °C	Kinetic model	Reaction order			Activation energy, kJ/mol		
			HDS	HDN	HDA <380°C	HDS	HDN	HDA <380°C
Yui and Dodge, 2006	286-541	P-L	1.5	1	1	151	132	72
Ai-jun et al., 2005	214-559	M-P	1.5	1.6	-	141	94	-
Owusu-Boakye et al., 2006	170-439	L-H	Pseudo 1st	-	Pseudo 1st	55	-	85
Ferdous et al., 2006	185-576	L-H	1	1.5	-	87	74	-
Bej et al., 2001a	210-655	P-L	1.5	-	-	28	-	-
Bej et al., 2001b	210-655	P-L	-	2	-	-	80	-
Mann et al., 1987	345-524	P-L	1.5	2	-	87	105	-
Yui and Sanford, 1989	196-515	P-L	1	1.5	-	138	92	-
Botchwey et al., 2004	210-600	L-H	Pseudo 1st	Pseudo 1st	-	114.2	93.5	-
Marin et al., 2002	LGO/SRGO	P-L	Pseudo 1.5	Pseudo 1st	Pseudo 1st	77.8	64.2	51.4

as well as the difficulty in their determination (Botchwey et al., 2006). However, it is thought to be a better approach than the other two models since it accounts for the inhibition caused by H_2S and other species under hydrotreatment. Two simpler versions of this model were frequently cited in the literature; they are Equations 2.8 and 2.9. Equation 2.8 is used to describe HDS and HDN kinetics (Ferdous et al., 2006, Botchwey et al., 2006), while Equation 2.9 was used to describe HDA kinetics (Owusu-Boakye, 2005). Assumptions that were made in the development of Equation 2.8 & 2.9 are (Owusu-Boakye, 2005):

- Surface reactions are the rate limiting
- All reactions are pseudo-first order
- The reactions take place in a plug flow regime
- H_2S inhibit HDS, HDN, and HDA reactions

$$-r_i = \frac{k_i K_i K_{H_2} P_{H_2} C_i}{1 + K_i C_i + K_{H_2} P_{H_2} + K_{H_2S} P_{H_2S}} \qquad (2.8)$$

$$-r_i = \frac{k_f K_i K_{H_2} P_{H_2} C_i}{1 + K_i C_i + K_{H_2S} P_{H_2S}} \qquad (2.9)$$

Equations 2.8 and 2.9 are solved using Maple V software which yields the following solutions (Ferdous et al., 2006):

For Equation 2.8, the solution is:

$$\mathbf{C_i(t)} = \frac{(1+K_{H_2}P_{H_2}+K_{H_2S}P_{H_2S})\,\text{LambertW}\left(\frac{K_i \exp\left(\frac{\left(t+\frac{C_{io}K_i+\ln(C_{io})+\ln(C_{io})K_{H_2}P_{H_2}+\ln(C_{io})K_{H_2S}P_{H_2S}}{K_{H_2}P_{H_2}K_ik_i}\right)K_{H_2}P_{H_2}K_ik_i}{1+K_{H_2}P_{H_2}+K_{H_2S}P_{H_2S}}\right)}{1+K_{H_2}P_{H_2}+K_{H_2S}P_{H_2S}}\right)}{K_i} \quad (2.8.a)$$

where:

$$\text{LambertW}(x) = x - x^2 + \frac{3}{2}x^3 - \frac{8}{3}x^4 + \frac{125}{4}x^5 - \frac{54}{5}x^6 + (0)^7 \quad (2.8.b)$$

and

$$x = \left(\frac{K_i \exp\left(\frac{\left(t + \frac{C_{io}K_i + \ln(C_{io}) + \ln(C_{io})K_{H_2}P_{H_2} + \ln(C_{io})K_{H_2S}P_{H_2S}}{K_{H_2}P_{H_2}K_i k_i} \right) K_{H_2}P_{H_2}K_i k_i}{1 + K_{H_2}P_{H_2} + K_{H_2S}P_{H_2S}} \right)}{1 + K_{H_2}P_{H_2} + K_{H_2S}P_{H_2S}} \right) \quad (2.8.c)$$

For Equation 2.9, the solution is:

$$C_i(t) = \frac{(1+K_{H_2S}P_{H_2S})\,\text{LambertW}\left(\frac{K_i \exp\left(\frac{\left(t+\frac{C_{io}K_i+\ln(C_{io})+\ln(C_{io})K_{H_2S}P_{H_2S}}{K_{H_2}P_{H_2}K_ik_i}\right)K_{H_2}P_{H_2}K_ik_i}{1+K_{H_2S}P_{H_2S}}\right)}{1+K_{H_2S}P_{H_2S}}\right)}{K_i} \qquad (2.9.a)$$

where:

$$\text{LambertW}(x) = x - x^2 + \frac{3}{2}x^3 - \frac{8}{3}x^4 + \frac{125}{4}x^5 - \frac{54}{5}x^6 + (0)^7 \qquad (2.9.b)$$

and:

$$x = \left(\frac{K_i \exp\left(\frac{\left(t + \frac{C_{io} Ki + \ln(C_{io}) + \ln(C_{io}) K_{H_2S} P_{H_2S}}{K_{H_2} P_{H_2} K_i k_i} \right) K_{H_2} P_{H_2} K_i k_i}{1 + K_{H_2S} P_{H_2S}} \right)}{1 + K_{H_2S} P_{H_2S}} \right) \qquad (2.9.c)$$

Excel solver is then used to solve Equation 2.9.a and 2.9.a. The apparent rate constants and adsorption equilibrium constants are obtained by the means of trial- and- error method (Ferdous et al. 2006). The partial pressures of H_2 and H_2S can be obtained from the HYSYS analysis.

2.12.3 Multi-parameter Model

The mechanism for this model is that of power law the only difference is on how the rate equation is expressed. According to The multi-parameter model, hydrogen pressure and gas/oil ratio are taken into account in the rate expression, along with temperature and LHSV. The multi-parameter model is a better model than the overly simplified power law model as it includes more process variables, and thus the effects of more variables on hydrotreating activities can be observed. The multi-parameter model is shown below, Equation 2.10 (Ai-jun et al., 2005).

$$-\frac{dC}{dt} = k_i \times P_H{}^m \times C^n \times (G/O)^q \qquad (2.10)$$

Equation 2.10 solution is:

$$\ln\frac{C_f}{C_p} = \frac{k_o \times e^{(-s/T)} \times P_H{}^m \times (G/O)^q}{LHSV^C} \;;\; n = 1 \qquad (2.10.a)$$

$$\frac{1}{n-1}\left[\frac{1}{C_p{}^{n-1}} - \frac{1}{C_f{}^{n-1}}\right] = \frac{k_o \times e^{(-s/T)} \times P_H{}^m \times (G/O)^q}{LHSV^C} \;;\; n > 1 \qquad (2.10.b)$$

where: C_f and C_p = the nitrogen, sulfur, or aromatics in feed and product, respectively; k_o = pre-exponential factor; s = E/R, where E = activation energy and R = gas constant; n = reaction order; m, q, and c = empirical regression factors. P_H = H_2pp (in this work outlet H_2pp); G/O = gas/oil ratio; LHSV = liquid space velocity.

2.12.4 Mass transfer limitation

The basic assumption in the kinetic studies is that the system operates under isothermality and plug flow conditions. Laboratory-scale trickle bed reactor can significantly deviate due to poor catalyst wetting, higher liquid back-mixing, and wall effect (Ferdous et al. 2006; Bej et al. 2001). These effects can greatly be improved upon by diluting the catalyst with fine inert particle such as SiC. Table 2.4 shows the hydrodynamic evaluation of a diluted versus an undiluted catalyst beds packed following the method illustrated in Bej et al. (2000); the evolution is carried out based on criteria found in Ramirez et al. (2004). This table shows that dilution the catalyst bed with SiC (90 Mesh) helps eliminate wall, wetting, and back-mixing effects, however, deviation from plug flow regime cannot be totally neglected.

Table 2.4: Evaluation of hydrodynamic parameters (Ranirez et. al., 2004).

Phenomena	Correlations	Cut off*	Results of calculation under un-diluted conditions	Results of calculation under diluted conditions	Is this phenomena negligible under diluted conditions?
Back-mixing	$\frac{L}{d_p} > 100$	>100	80	731	yes
Wetting	$W = \frac{\eta_L u_L}{\rho_L d^2{}_p g} > 5*10^{-6}$	$>5*10^{-6}$	$4.8*10^{-6}$	609	yes
Wall effect	$\frac{D_b}{d_p} > 25$	>25	6.7	61	yes
Plug flow	$Pe_L > 8n\left[\ln\left(\frac{1}{1-X}\right)\right] = Pe$	>27	0.002	0.0007	No

* This values are results of calculation using the correlations

The reactor's internal mass transfer is greatly affected by the catalysts' size. Smaller catalyst's sizes are required to minimize pore diffusion effects; however, when it gets too small the reactor experiences excessive pressure drops, and consequently liquid misdistribution (Gruia, 2006). For instance, Trytten (1989) (Found in Gray R. 1994) studied the internal diffusion resistance during hydrotreating of coker gas oil in a continuous-flow stirred reactor. The author used two different sizes (0.93 and 0.5 mm diameter) of NiMo-γAl_2O_3 catalyst. H_2 partial pressure, temperature, and LHSV were 13.9 MPa, 400°C, and 12.5 mL/h-g catalyst, respectively. The agitation rate was maintained at 1100 rpm to eliminate external mass transfer. The author concluded that to eliminate diffusion limitations for both HDS and HDN the catalyst diameter should be less than 0.5 mm. Such a small catalyst diameter leads to high pressure drops in the reactor (Gruia, 2006). The commercial MiNo/γ-Al_2O_3 catalyst has a diameter of 1.5 mm therefore some internal diffusion limitation is expected when it is used in such a system.

Beside the possibility of presence of internal diffusion limitation, Treating feeds such as coker gas oil (with components ranging for naphtha to heavy gas oil and having molecular weights of 84 to 500 g/mol) as a single component when conducting kinetics studies involves a lot of approximations (Gray R., 1994), and thus conducting intrinsic kinetic studies is difficult. Obtaining true intrinsic kinetics involves accounting for all mechanistic steps and rates of chemisorptions and desorption (Lee, 1999), which a very difficult thing to do when dealing which real feedstocks. Often apparent kinetics based on statistical and experimental analysis are adequate for industrial and chemical engineering applications (Lee, 1999).

2.12.5 Heat transfer evaluation

HDS, HDN, and HDA reactions are exothermic and the heat generated may lead to formation of hot spots. The use of high gas flowrate quickly dissipates this heat (Botchwey et al. 2006). Moreover, diluting the catalyst with SiC greatly improves the heat transfer rate in the catalyst bed (Giermen, 1988). Often in the literature isothermality assumption is achieved when carrying out kinetic studies in micro-trickle bed reactors. However, a simulation work by Botchwey et al. (2006) has shown that the temperature between the reactor wall and centre could be as high as 9 K, and that the temperature is higher at the reactor's outlet than its inlet.

3.0 EXPERIMENTAL

In this chapter experimental plan and operating procedure of the trickle bed reactor are discussed in detail. Also discussed are the analytical techniques used for feed and products analysis.

3.1 System description

The micro-reactor was made of 304 stainless steel tube with internal diameter of 10 mm and length of 240 mm, which was heated by means of a furnace system (Vinci Technologies SA, Nanterre, France) and monitored by a temperature controller (Eutherm 2216e, Moyer instruments, Inc., Tamaqua, PA, USA). A positive displacement pump (Model: A-10-S, Hurst, Emerson Electric Co., IN, USA) was used to pump the liquid feed. The gas flow was regulated with a mass flow controller (Model: 5850 series, Brooks Instruments, Hatfield, PA, USA). The schematic diagram of the experimental set up is shown in Figure 3.1.

3.2 Catalyst loading

Before loading the reactor, the commercial Ni-Mo/γ-alumina was dried at 200°C for 3 hr in an oven, and cooled in a desiccator. For loading the catalyst, the bottom end of the reactor was sealed with a Swagelok 60 micron stainless filter (Solon, OH, USA) and then packed from bottom to top in three parts. The bottom part was loaded with 22 mm of glass beads of size 3 mm diameter followed by 25 mm, 10 mm, and 10 mm of 16

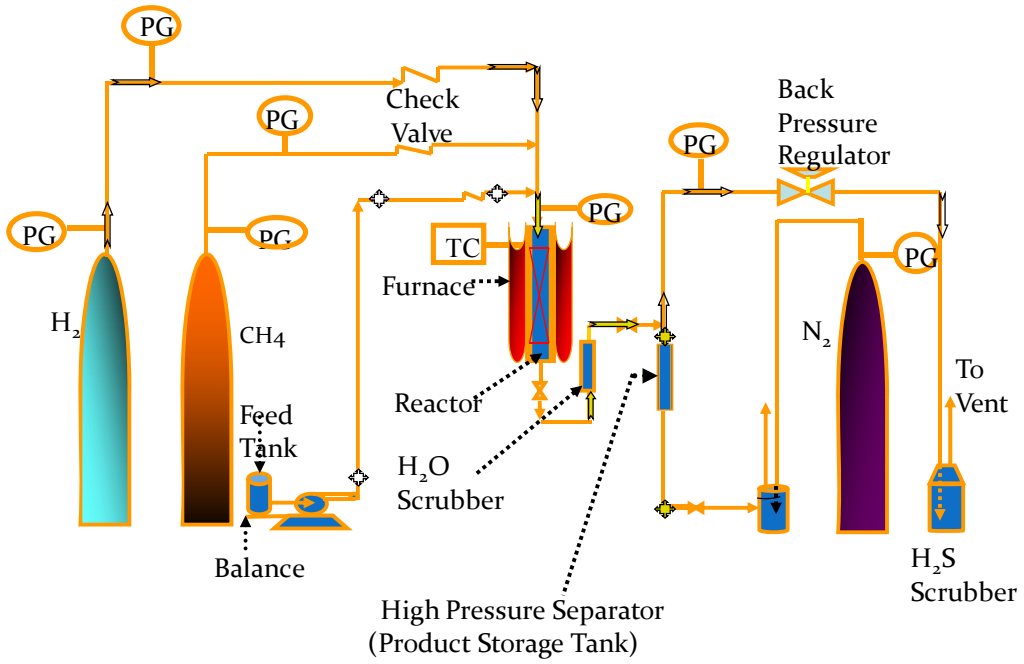

Figure 3.1: Experimental setup (PG= pressure gauge; TC = Temperature controller)

mesh, 46 mesh, and 60 mesh SiC, respectively. In the middle part of the reactor, 5 mL of catalyst and 12 mL of 90 mesh SiC were loaded alternately; small quantity of each at a time, for a total number of 10 - 12 layers. Finally, the top part was loaded with 8 mm of SiC of 60 mesh followed 8 mm, 8 mm, and 20 mm of 46 mesh SiC, 16 mesh SiC, and 3 mm diameter glass beads. The top 20 mm of the reactor was kept empty. A schematic description of the catalyst loading in the reactor is shown in Figure 3.2. Earlier study on a similar reactor with such loading technique has shown establishment of trickle flow in the catalyst bed (Bej et al. 2001). Subsequently, the reactor was connected to the system and was pressurized to 90 bar using helium gas. Pressure was built up by adjusting the back pressure regulator to hold the pressure in the system. Swagelok liquid leak detector (Snoop Solution) was used to detect any leaks. The reactor was left at this pressure for a

period of 24 hr and was re-tested for leaks. After ensuring that no leaks existed, the reactor's temperature was increased to 100°C.

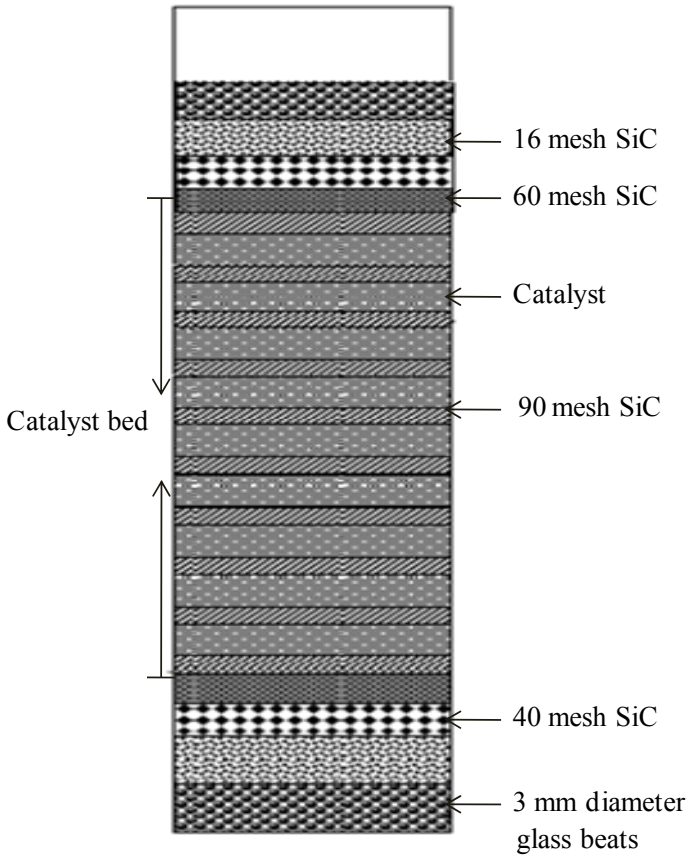

Figure 3.2: Catalyst loading schematic.

3.3 Experimental procedure

After the reactor was loaded and ensured that no leaks existed, the sulfidation process was started. The sulfiding solution was made of 2.9 vol. % butanethiol, a commonly used sulfiding agent (Andari et al., 1996), in electrical insulating oil (VOLTESSO 35). 100 mL of the sulfiding solution was pumped into the reactor at a high flowrate (~ 2.5 mL/min) to wet the catalyst. Subsequently, the flowrate was adjusted to 5 mL/h and maintained. Gas/oil ratio was operated at 600 mL/mL. The

catalyst bed temperature was gradually increased to 193°C. The reactor temperature was then maintained for 24 h. Next, the temperature was further increased to 343°C in steps and the reactor was kept at this temperature for another 24 h.

The catalyst was precoked for seven days after catalyst sulfidation by flowing heavy gas oil (HGO) into the reactor at the rate of 5 mL/h. The temperature of the reactor was increased to 375°C. The purpose of catalyst precoking was to stabilize its activity to ensure uniform activity across the catalyst surface before the experiments were conducted (Speight, 2000). Liquid products were collected every 24 h, stripped with nitrogen gas to remove dissolved NH_3 and H_2S, and analyzed for sulfur and total nitrogen contents. After the catalyst stabilization, the experiments were carried out as designed. Each run was conducted for three days, and product withdrawn every 24 h. A transient period of 24 h was allowed after a change in process conditions and samples taken within this period were discarded. Products collected in the second and third days were stripped off dissolved H_2S using nitrogen gas, and were analyzed for sulfur, nitrogen, and aromatics conversions.

3.4 Experimental plan

The following subsections give some details about each phase of the experiment are given. In all phases, commercial catalyst was used to hydrotreat heavy gas oil (HGO) (see Table 3.1 for HGO properties). The purity of the hydrogen gas was adjusted using methane.

Table 3.1: HGO properties

Boiling range, °C	258 - 592
Density @ 20°C, g/cm^3	0.988
Sulfur content, wppm	42,310
Nitrogen content, wppm	3,156
Aromatics content, wt %	31.4

3.4.1 Phase I – Effect of H_2 purity on hydrotreating activities

The effect of the hydrogen purity on the hydrotreating activities (HDS, HDN, and HDA), and on properties namely: density, viscosity, fractional distribution, aniline point, diesel index, and cetane index of the liquid product were studied in the H_2 purity range of 0 to 100 vol. % (namely: 0, 50, 80, 90, and 100%). Methane was used to dilute the hydrogen stream. The experiments were carried out at constant temperature and LHSV of 380°C and 1 h^{-1}, respectively (note: above 380ºC, HDA of HGO is reversible). The effect of H_2 purity on H_2 partial pressure was compared against that of pressure and gas/oil ratio. The outline of the phase I experimental plan is presented in Table 3.2.

Table 3.2: Phase I experimental plan (T = 380ºC; LHSV = 1h^{-1})

H_2 purity %	Pressure MPa	Gas/oil ratio mL/mL
0-100	9	800
100	9	400
50	10	800
50	9	1270

3.4.2 Phase II –Effect of H_2 partial pressure on hydrotreating activities

The H_2 partial pressure level in the reactor was adjusted by varying reactor pressure, H_2 purity, and gas/oil ratio. Reactor pressure, H_2 purity, and gas/oil ratio ranges were 7-11 MPa, 75-100 vol. %, and 400-1200 mL/mL, respectively, while temperature and LHSV were kept constant at 380ºC and 1 h^{-1}, respectively.

The experiments were statistically designed using with a standard Response Surface Methodology (RSM) design called a Central Composite Design (CCD). RSM is a procedure that combines the concept of experimental design and optimization theory. Its purpose is to determine optimal operating conditions by modeling the relationship between the independent variables and the response (s). CCD is an experimental design method for building **quadratic model** without the need of using the complete factorial design. While CCD is ideal for quadratic model, the factorial design is preferred for linear model. CCD's advantage over other approaches such as a factorial design is that it provides information on the effect of independent variables with minimum number of experimental runs. There are three types of CCD: Central Composite Circumscribed (CCC), Central Composite Inscribed (CCI), and Central Composite Face-centered (CCF)). When dealing with variables that have true limits such as purity (e.g. its upper limit is 100%), then Central Composite Inscribed method could be selected. CCD overall design is made up of three types of points (selected experimental runs): $2n$ axial points, 2^n cube points (factorial), and a single center point repeated six times (to improve precision and minimize prediction error); where n is the number of the input variables. For example, to study the effect of three input variables, the CCD will specify a total of 20 runs (i.e. $2 \times 3 + 2^3 + 6 = 20$). The cube points is to estimate the linear and interaction terms and the axial and center point(s) is to estimate the quadratic terms in the overall

model. The full matrix of the experimental design using pressure, H_2 purity, and gas/oil ratio as input variables is shown in Table 3.3.

Table 3.3: Phase II CCD experimental Design.

Run	Pressure psi	gas/oil mL/mL	purity %	X_N %	X_S %	X_A %	Inlet H_2pp MPa	Outlet H_2pp MPa
1	1305	800	75					
2	1133	1038	80					
3	1478	562	80					
4	1133	562	80					
5	1478	1038	80					
6	1305	400	88					
7	1305	1200	88					
8	1015	800	88					
9	1305	800	88					
10	1305	800	88					
11	1595	800	88					
12	1305	800	88					
13	1305	800	88					
14	1305	800	88					
15	1305	800	88					
16	1133	1038	95					
17	1133	562	95					
18	1478	562	95					
19	1478	1038	95					
20	1305	800	100					

X_N, X_S, X_A are total conversions of nitrogen, sulfur, and aromatics, respectively; H_2pp is H_2 partial pressure.

3.4.3 Phase III –Kinetic modeling

In this phase, the effects of temperature and LHSV on H_2 partial pressure and hydrotreating activities were studied. Data obtained from this part was combined with that from phases I & II, and the combined data was then used in the kinetic modeling of

HDS, HDN, and HDA. For study on the effects of temperature and LHSV, the temperature and LHSV ranges were 360 to 400°C and 0.65 to 2 h^{-1}, respectively. H_2 purity, pressure and gas/oil ratio were kept constant at 100%, 9 MPa, and 800 mL/mL, respectively. LHSV was kept constant at 1 h^{-1} when the effect of temperature was studied. Temperature was kept constant at 380°C when the effect of LHSV was studied.

3.5 Analysis of feed and liquid products

Several analytical instruments and techniques were to analyze the feed and liquid products, and they are discussed in the subsections below.

3.5.1 Nitrogen and sulfur analysis

Sulfur contents of the feed and the liquid products were determined using a combustion/fluorescence technique according to ASTM 5463 procedure. Total nitrogen contents of the feed and the liquid products were measured using a combustion/chemiluminiscence technique following ASTM D4629 procedure.

A total nitrogen/sulfur analyzer (Antek 9000, model: 9000NS) was used. The principal Chemistry is summarized in equations 3.1, 3.2, & 3.3 (Antek, 1998). The process starts with a high temperature oxidation of the sample (temperature in excess of 1000ºC). This results in conversion of sulfur and nitrogen into sulfur dioxide and nitric oxide, respectively. The sulfur dioxide is excited by an ultraviolet radiation of a specific wavelength, and as the electrons return to their original level light (fluorescent emission, i.e. absorbed originally from a light source) is emitted and detected at a specific wavelength by a photomultiplier. The nitric oxide is contacted with ozone, from an onboard ozone generator, to produce a metastable nitrogen dioxide species. As the

metastable nitrogen dioxide species decays, light (chemiluminescent emission, i.e. from a chemical reaction) is emitted and detected at a specific wavelength by a photomultiplier.

$$\text{R-N} + \text{R-S} + O_2 \longrightarrow CO_2 + H_2O + \bullet NO + SO_2 \quad (3.1)$$

$$SO_2 + h\nu' \longrightarrow SO_2 + h\nu'' \quad (3.2)$$

$$\bullet NO + O_3 \longrightarrow NO_2^* + O_2 \longrightarrow NO_2 + h\nu \quad (3.3)$$

The HDS and HDN conversions are calculated as follows:

$$\%\text{conversion of species (i)} = \frac{\text{species (i) in feed} - \text{species (i) in product}}{\text{species (i) in feed}} \times 100 \quad (3.4)$$

where: species (i) is sulfur, nitrogen, or aromatics.

3.5.2 ^{13}C NMR analysis

NMR stands for nuclear magnetic resonance. ^{13}C nucleus has a spin quantum number of ½, thus responds to a magnetic field. The process starts with placing the liquid sample in a special glass, and the glass is placed in a uniform magnetic field. An incremental radio frequency pulse of a known frequency range is sent through shielded cable to a coil wound around the test sample. Different chemical species absorb the RF at different frequencies (thus absorption information can be used to differentiate among the species). RF absorbed by the sample is monitored and measured. Information collected about the frequency of the RF and the absorption are used to construct the

NMR spectrum (ITM, 2008). Information on the chemical shift of the species in the sample can be used to differentiate between saturates (C-C) and aromatics (C=C). The chemical shift of C-C is between 0-50 ppm and for C=C it is between 100-150 ppm (Owusu-Boakye, 2005). Chemical shift is an absolute quantity defined as the frequency of absorption of the sample relative to the frequency of absorption of a reference standard (often TMS, Tetramethylsilane), is shown mathematically in the equation below (Carey, 2009):

$$\text{Chemical shift} = \frac{\text{Frequency reference} - \text{Frequency sample}}{\text{Frequency spectrometer}} \text{ x } 10^6 : \qquad (3.5)$$

Aromaticity, defined as the mole percent of carbon in a sample that is present as part of an aromatic ring structure of the feed and the liquid products, is determined by ^{13}C-NMR spectroscopy. The spectra were obtained in the Fourier Transform mode (i.e. the applied RF is not continuous but is an intense and short pulse), operating at a frequency of 500 MHz.

The instrumental conditions were as follows: a pulse delay of 2 sec, a sweep width of 27.7 kHz and gated decoupling. Overall time for each sample was 56 minutes for 1056 scans. Deuterated chloroform, $CDCl_3$, was used as a solvent. The resultant spectrum is composed of two distinct zones separated by the solvent bar. Total saturated hydrocarbons were located between 0 – 50 ppm; whereas the total aromatics were observed between 100 – 150 ppm (Owusu-Boakye, 2005). Equation 3.5 was then used to determine the aromatics content (%) of each sample. The integrals of the saturated

hydrocarbons zone, I_{sat}, and the total aromatics zone, I_{ar}, were determined using XWIN-NMR 3.5 software.

$$C_{ar} = \frac{I_{ar}}{I_{ar} + I_{sat}} \times 100 \qquad (3.6)$$

where: C_{ar} = aromatics content; I_{ar} = the integral of total aromatics; I_{sat} = the integral of total saturates.

3.5.3 Simulated distillation

The principle behind simulated distillation is separation of components based on their boiling point by a column; and can be performed using ASTM D6352 method. A Varian model CP3800 gas chromatograph coupled to a Varian CP 8400 auto sampler was used in this work. The hydrocarbons in the sample (s) were separated based on their boiling range by a capillary column 10 m (length) x 0.53 mm (diameter) x 0.88 mm (nominal film thickness). A flame ionization detector (FID) was used to detect the components' boiling ranges using He as a carrier gas at a flow rate of 30 mL/min. The air flow and H_2 were maintained at 400 mL/min and 35, respectively. The detector temperature and oven final temperature were maintained at 375 and 380ºC, respectively. The boiling fractions are identified by comparing them against calibration curve.

3.5.4 Cetane number, aniline point, and diesel index

Information on liquid products such as density, viscosity, fractional distribution, aniline point, diesel index, and cetane index may be very interesting for refiners (Wauquier et al., 1995; Botchwey, 2003)**.** Cetane index is substituent for cetane number

and is a measurement of the combustion quality of diesel fuel during compression ignition. The larger the cetane index the greater the fuel efficiency. Aniline point is the temperature at which equal volumes of aniline and diesel oil are completely miscible; and is inversely related to the aromatics content of the fuel. Diesel index correlates between the aniline point of a diesel fuel and its ignitability. The higher the diesel index the better the fuel quality.

The densities of the feed and the liquid products were measured using a digital precision density meter (model: DMA 35, Anton Paar, Austria, Europe). The viscosity of the feed and the liquid products were measured using a Brookfield digital viscometer (model: LVDV-I+CP, Middleboro, MA, USA). The fractional distributions were determined from the results of GC-simulated distillation and the fractional ranges are defined as follows: gasoline (G) 1BP-205°C, kerosene (K) 205-260°C, light gas oil (LGO) 260-315°C, heavy gas oil (HGO) 315-425°C, and vacuum gas oil (VGO) 425-600°C (Yang et al., 2002). The cetane indices were calculated according to ASTM D 4737.

$$CI = 45.2 + (0.0892)(T_{10N}) + [0.131 + 0.901(B)][T_{50N}] + [0.0523 - (0.420)(B)][T_{90N}] + [0.00049][(T_{10N})^2 - (T_{90N})^2] + 107(B) + 60(B)^2 \quad (3.7)$$

where:

CI = Cetane Index

D = density at 15 °C, kg/L

DN = D - 0.85

$$B = [e^{(-3.5)(DN)}]^{-1}$$

$T_{10N} = T_{10} - 215$ (T_{10N} is the temperature at 10 % recovery point)

$T_{50N} = T_{50} - 260$ (T_{50N} is the temperature at 50 % recovery point)

$T_{90N} = T_{90} - 310$ (T_{90N} is the temperature at 90 % recovery point)

Some empirical formulas directly correlate cetane index to aniline point and diesel index (Maples, 2000; Wauquier et al., 1995). Two of these correlations are Equation 3.7 and 3.8 (Maples, 2000).

$$CI = AP + 15.5 \qquad (3.8)$$

$$CI = 0.72 \text{ x } D.I. + 10 \qquad (3.9)$$

where:

AP = aniline point (°C); D.I. = Diesel index

3.5.5 Mild hydrocracking (MHC)

Mild hydrocracking (MHC), unlike conventional hydrocracking, occurs at lower pressures. MHC has an advantage over the latter in that it results in the production of less undesirable light products and also minimizes hydrogen consumption (Yang et al., 2002; Botchwey et al., 2003). However, it is associated with lower conversions (Yang et al., 2004). The MHC regime is usually said to take place at temperatures greater than 390°C. But, Botchwey et al. (2003) observed that MHC occurred simultaneously with hydrotreatment at temperature range of 340°C to 390°C. MHC conversion is defined as

the fraction of material with boiling temperatures of 343°C+ in the feed that is converted to lighter products (products with boiling temperature less than 343°C) (Yang et al., 2002). Fractions in the feed and the liquid products were determined using GC – simulated distillation (model: CP3800, Varian, Palo Alto, CA, USA), following standard procedure ASTM D2887, and the results were used to calculate MHC conversions using Equation 3.10:

$$\text{MHC Conversion} = \frac{[343°\text{C} + \text{material in feed (wt\%)} - 343°\text{C} + \text{material in product (wt\%)}]}{343°\text{C} + \text{material in feed (wt\%)}} \tag{3.10}$$

The densities of the feed and the liquid products were measured using a digital precision density meter (model: DMA 35, Anton Paar, Austria, Europe). The viscosity of the feed and the liquid products were measured using a Brookfield digital cone and plate viscometer (model: LVDV-I+CP, Middleboro, MA, USA). The fractional distributions were determined from the results of GC-simulated distillation (see section 3.5.3).

4.0 RESULTS AND DISCUSSION

4.1 Phase I: Effect of H_2 purity on hydrotreating activities

4.1.1 Effect of the Hydrogen Purity The effect of the hydrogen purity on the HDS, HDN, and HDA of HGO was studied in the purity range of 0-100%. Methane was used to dilute the hydrogen stream. The experiments were carried out at constant temperature, pressure, gas/oil ratio, and LHSV of 380°C, 9 MPa, 800 mL/mL, and 1 h^{-1}, respectively. The results are presented in Figure 4.1. Figure 4.1 shows that increasing H_2 purity enhances the activities of HDS, HDN, and HDA. However, HDN and HDA are better improved by increasing H_2 purity than HDS; no further improvement because HDS conversion was already very high. One of the principal hydrotreating variables is hydrogen partial pressure. In general, increasing hydrogen partial pressure increases HDS, HDN, and HDA conversions and vice versa (Gary H. et al., 2007). According to Dalton's law, the partial pressure of any component in a gas mixture is equal to its vapor-phase mole fraction multiplied by the system total pressure (Fogler, 1999). As the purity decreased, more and more methane was present in the gas phase, which consequently led to a decrease in the hydrogen mole fraction and ultimately hydrogen partial pressure. The decrease in hydrogen partial pressure resulted in decreases in HDN and HDA activities.

HDS activity did not show a significant decrease under these experimental conditions because the conversions was already very high especially when the results are

expressed as percentage conversions, such as in Figure 4.1. Often HDS conversion is expressed as a percentage (Equation 3.4, see Chapter 3) (Bej et al. 2001; Botchwey et al.,2003) which is not a fair representation, especially when compared to HDN, because the sulfur content is more than 10-folds that of the nitrogen content. A better way of presenting HDS is simply reporting the sulfur content in the product oil. This allows the effect of the variables to be clearly observed (see Table 4.1). Table 4.1 shows that, as the H_2 purity is lowered, which means a decrease in H_2 partial pressure, more sulfur remains in the product oil and, thus, HDS conversion decreases. Nonetheless, it is generally agreed upon that the effect of the H_2 partial pressure on HDN is more significant than that on HDS (Botchwey et al. 2003; Knudsen et al. 1999) and this fact is often explained in terms of the HDS mechanism versus the HDN mechanism.

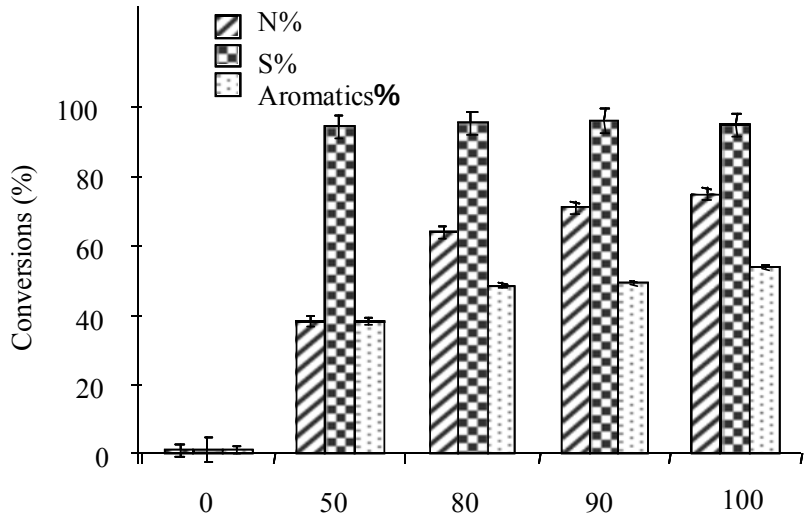

Figure 4.1: Effect of the hydrogen purity on HDS, HDN, and HDA of HGO. The experiments were carried out at temperature, pressure, gas/oil, and LHSV of 380 °C, 9 MPa, 800 mL/mL, and 1 h^{-1}, respectively.

Table 4.1: Effect of Hydrogen Purity on HDS

H_2 purity (%)	Inlet H_2 pp (MPa)	Feed sulphur content (ppm)	Product sulfur content (ppm)
100	9.0	42,310	1,353
90	8.1	42,310	1,691
80	7.2	42,310	1,785
50	4.5	42,310	3,474

Hydrogenation of a N-containing ring occurs prior to C-N bond scission over conventional catalysts. Thus, the HDN rate can be affected by the equilibrium of N-ring hydrogenation because N-ring hydrogenation occurs before nitrogen removal (hydrogenolysis). HDS does not always require hydrogenation. HDS can proceed via two possible mechanisms, as shown in Figure 4.2 (Botchwey et al. 2003; Knudsen et al. 1999) (i) ring hydrogenation followed by hydrogenolysis or (ii) direct hydrogenolysis. In general, HDN is more difficult to carry out than HDS. Thus, HDN reactions are operated under more severe conditions, i.e., higher temperature and hydrogen pressure, than HDS (Kabe et al., 1999). To understand the difference between the HDS mechanism and that of HDN, the bond energies of C=S, C-S, C=N, and C-N must be compared. The bond energies of C=S and C-S are equal to 536 kJ/mol. However, the bond energies of C=N

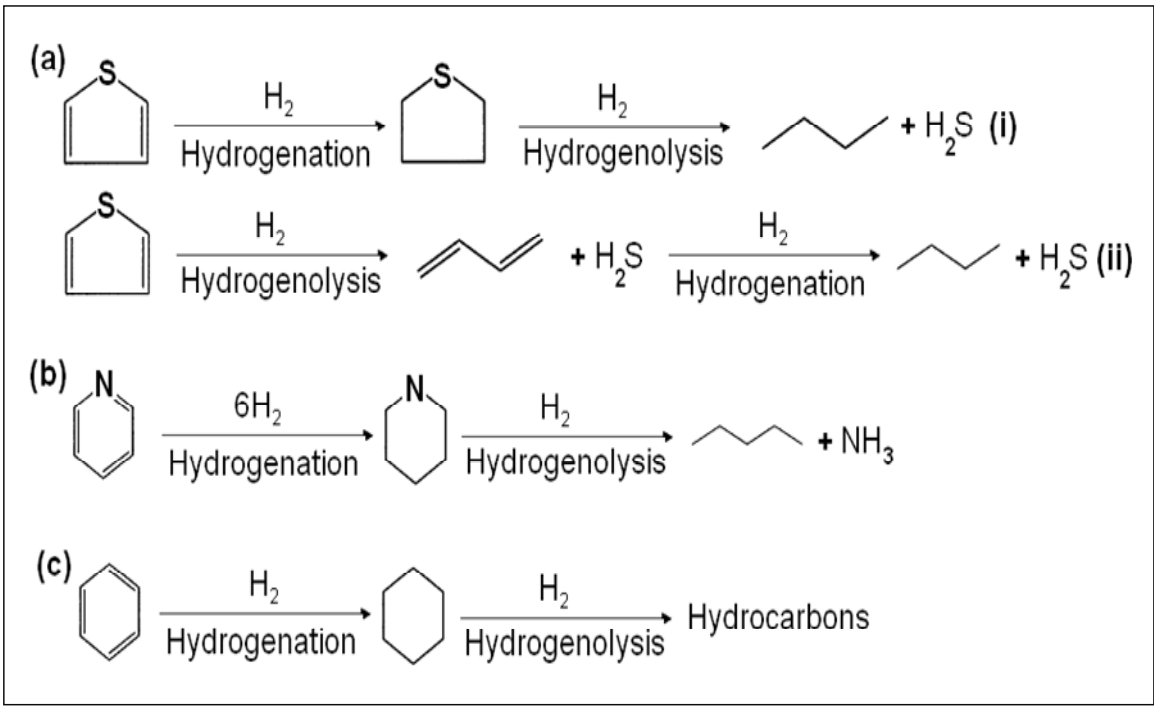

Figure 4.2: Reaction pathways for HDS, HDN, and HDA (Botchwey et al. 2003; Knudsen et al. 1999).

and C-N are 615 and 389 kJ/mol, respectively. Thus, it is energetically favorable to hydrogenate C=N to C-N before C-N bond scission. There is no particular preference for C=S and C-S (Kabe et al., 1999).

The mechanism for HDA is hydrogenation, and a decrease in the hydrogen partial pressure results in a reduction of the hydrogenation rate. Consequently, a decrease in HDA conversion is observed as H_2 partial pressure is reduced (Girgis and Gates 1991). The purity range between 0 and 50% was not looked at because at 50% purity the HDN had fallen beyond a practically acceptable Hydroprocessing conversion range (60-80%) (Speight, 2000). Hydrotreatment is not practical unless the conversions of all three processes (HDS, HDN, and HDA) are within the acceptable ranges.

The most interesting finding in this section was the level of decrease in the conversions as the purity was reduced. It is well known and rather intuitive that, as the hydrogen partial pressure or hydrogen purity drops, the conversions drop. However, it remains important to know how much and how significant these decreases in the hydroprocessing conversions are. Hydroprocessing conversions decreased as follow: HDS from 97 to 96%, HDN from 75 to 67%, and HDA from 54 to 48%, as the purity dropped from 100 to 80% (see Figure 4.1). These conversions are within reasonable ranges. The practical importance of this finding is that the recycle hydrogen stream does not need to be ultra-purified to obtain reasonable hydroprocessing conversions. Moreover, for hydrogen recovery units, such as PSA, if the hydrogen purity criteria are relaxed (i.e., accepting lower product purities), higher hydrogen recoveries can be attained (Voss, 2005). This may mean less hydrogen losses and better overall process economics.

The effect of purity on MHC was also examined. The experiments were carried out at constant temperature, pressure, gas/oil ratio, and LHSV of 380 °C, 9 MPa, 800, and 1 h^{-1}, respectively; H_2 purity was varied between 0 and 100% (with the rest methane). MHC conversions were determined using Equation 3.10 (see chapter 3), and the results are presented in Figure 4.3. This figure shows that MHC conversion decreased from 20 to 19% as the purity was decreased from 100 to 80%. However, with a further decrease in purity to 50%, the MHC conversion dropped to 17%. Here, it can be seen that H_2 MHC conversion did not suffer considerably as the H_2 purity was reduced from 100 to 80%. Information on liquid products, such as density, viscosity,

fractional distribution, aniline point, diesel index, and cetane index may be very interesting for refiners (Botchwey et al., 2003; Wauquier et al., 1995).

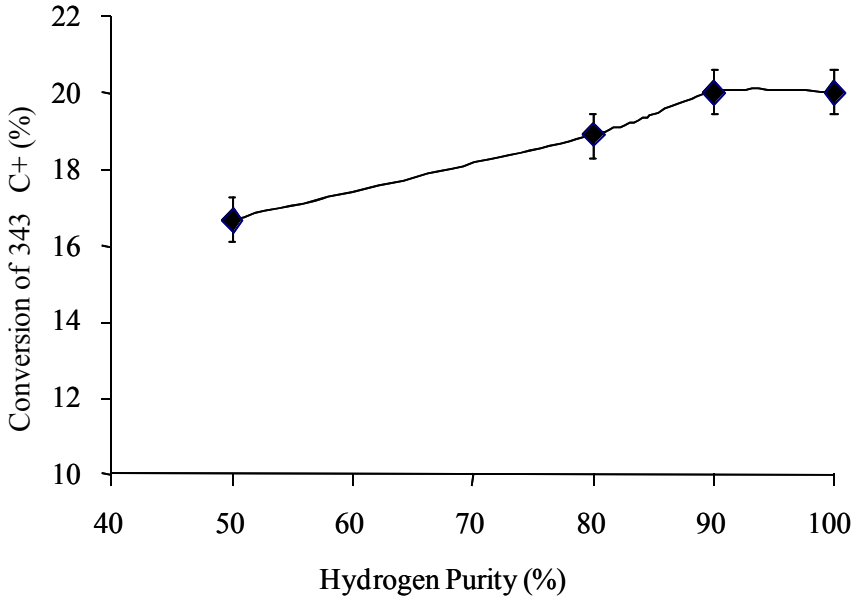

Figure 4.3: Effect of the hydrogen purity on MHC.

The following highlights the effect of H_2 purity on the product quality as it undergoes hydrotreating and MHC. The fractional distributions, densities, viscosities, and cetane indices of the products are shown in Figures 4.4-7, respectively, and the aniline point and diesel index are shown in Figure 4.8. Figure 4.4 shows that, as hydrogen purity was dropped from 100 to 80%, there was no significant difference in the fractional distributions of the liquid products. Figure 4.5 shows that density is closely linearly related to hydrogen purity. Figure 4.6 shows that viscosities of the liquid products decreased with an increasing H_2 purity. Figure 4.7 shows that cetane indices of the liquid products decreased with a decreasing H_2 purity. At 100% H_2 purity, the

product cetane index was 34.2, which dropped slightly to 33.5 as H_2 purity was decreased to 80% and further to 31.6 as the H_2 purity was lowered to 50%. Figure 4.8 shows that both calculated aniline points and diesel indices of the liquid products increased with increasing H_2 purity. There is a known correlation between the aniline point and the aromatics content of a petroleum product: the higher the aniline point, the lower the aromatics (Owusu-Boakye, 2005). As was observed in this work, while the aromatics content of the liquid products decreased (increase in HDA) with an increasing H_2 purity, the aniline point increased.

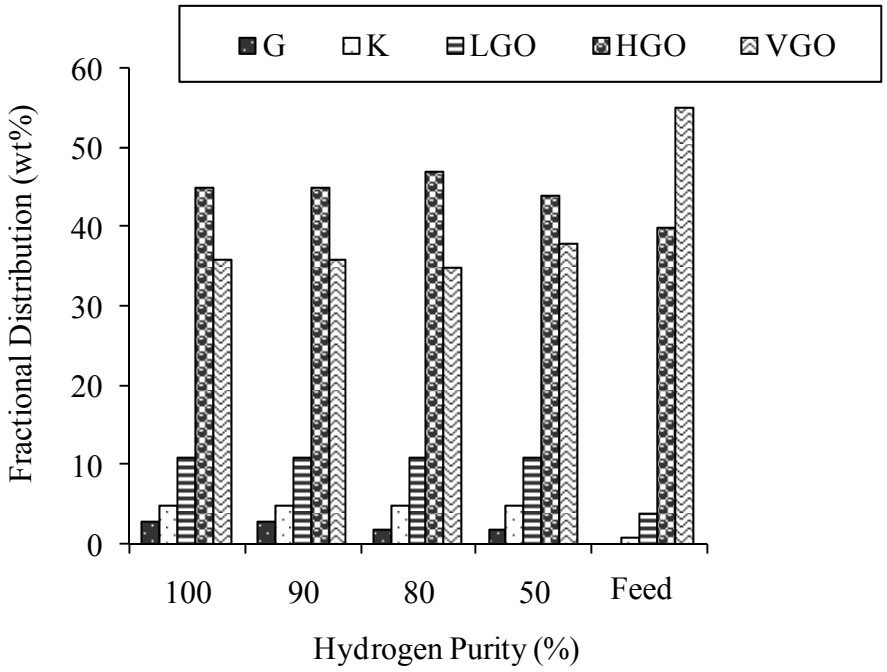

Figure 4.4: Effect of the hydrogen purity on the fractional distribution of the products.

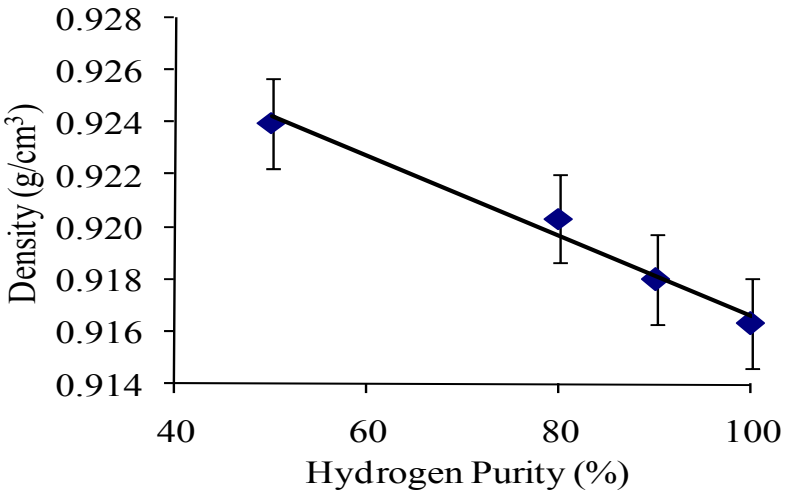

Figure 4.5: Effect of the hydrogen purity on the density of the products. Measurements were taken at 20 °C.

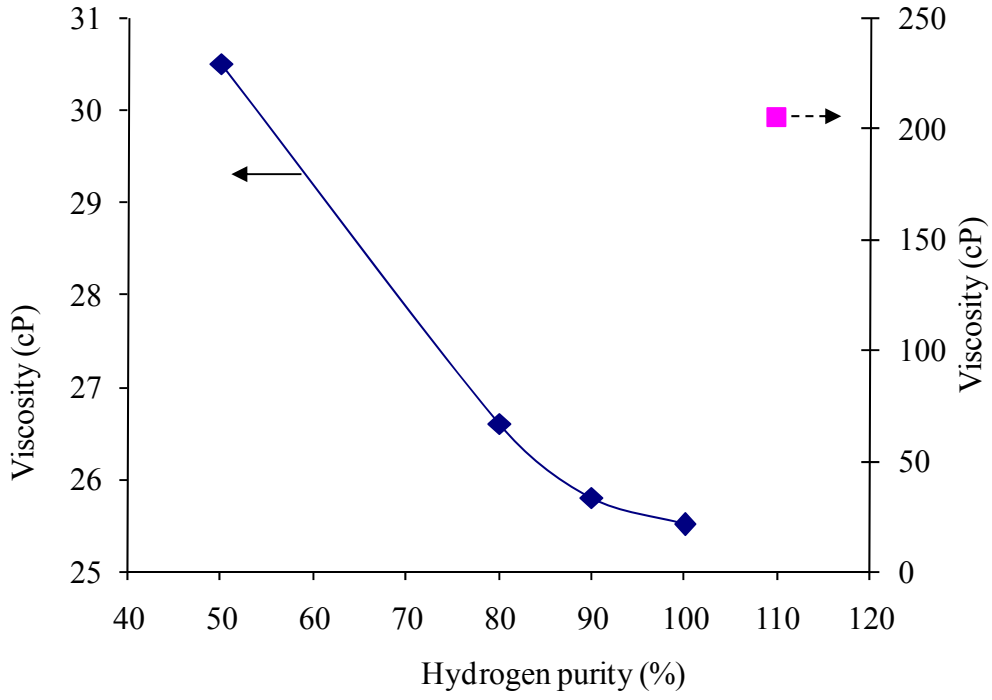

Figure 4.6: Effect of the hydrogen purity on the viscosity of the products. Measurements were taken at 40 °C.

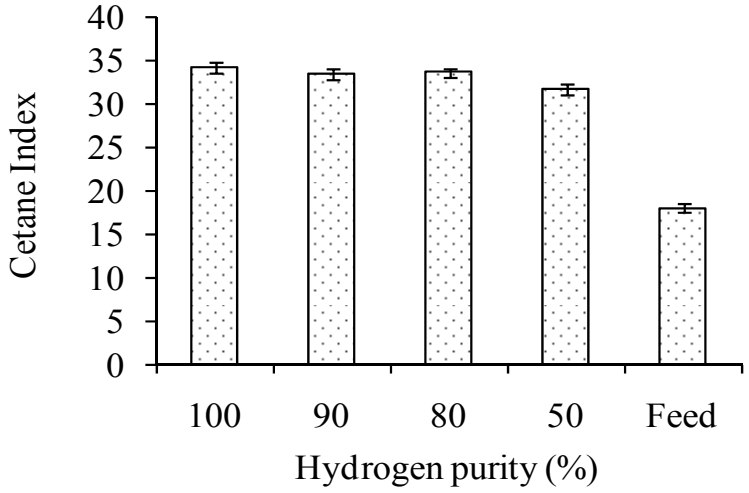

Figure 4.7: Effect of the hydrogen purity on the cetane index of the products.

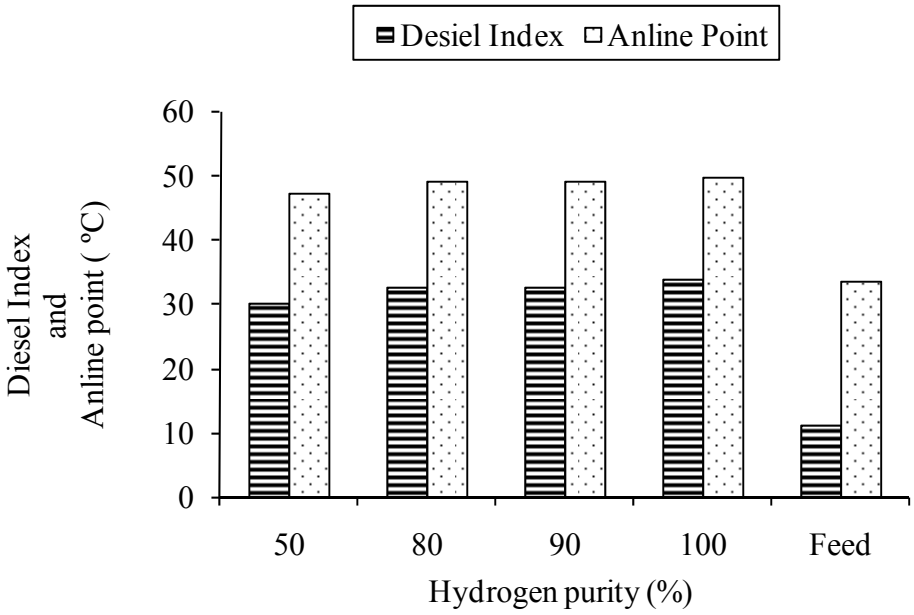

Figure 4.8: Effect of the hydrogen purity on the diesel index and aniline point of the products.

4.1.2 Effect of Methane on catalyst performance

As mentioned in the introduction, methane is the second most abundant constituent of the hydrotreating exit and recycle gas stream after hydrogen. To observe the impact of the H_2 purity on the catalyst performance, one must study the effect of methane content. Consequently, experiments were performed at progressively decreasing H_2 purity (with the rest methane). All experiments were conducted at constant temperature, pressure, gas/oil ratio, and LHSV of 380°C, 9 MPa, 800 mL/ mL, and 1 h^{-1}, respectively. To detect if there were any changes in the catalyst activity as the purity was progressively decreased, an experiment at 100% H_2 purity, named "control", was intermittently repeated before and after each experiment. To clearly illustrate this process, as a part of the same run, the H_2 purity was first set at 100%, the experiment was carried out, and samples were collected. H_2 purity was then reduced to 90% (with the rest methane); the experiment was carried out; and samples were collected. Next, the H_2 purity was reset back to 100%; the experiment was carried out; and samples were collected. This procedure was repeated for each of the subsequent experiments.

The results of HDS, HDN, and HDA conversions are shown in Figures 4.9-11, respectively. The results show that, as the hydrogen purity was decreased to 80%, the catalyst did not suffer considerable HDS, HDN, and HDA activity losses; the hydroprocessing conversions at the "control" condition before and after the experiments were unchanged. However, as the H_2 purity was further dropped to 50%, the HDN and HDA conversions at the "control" conditions dropped. The decrease in the HDS, HDN, and HDA activities was not directly caused by methane but by the deficiency in the

hydrogen partial pressure, which caused catalyst deactivation because of coke formation (Antos et al., 2004).

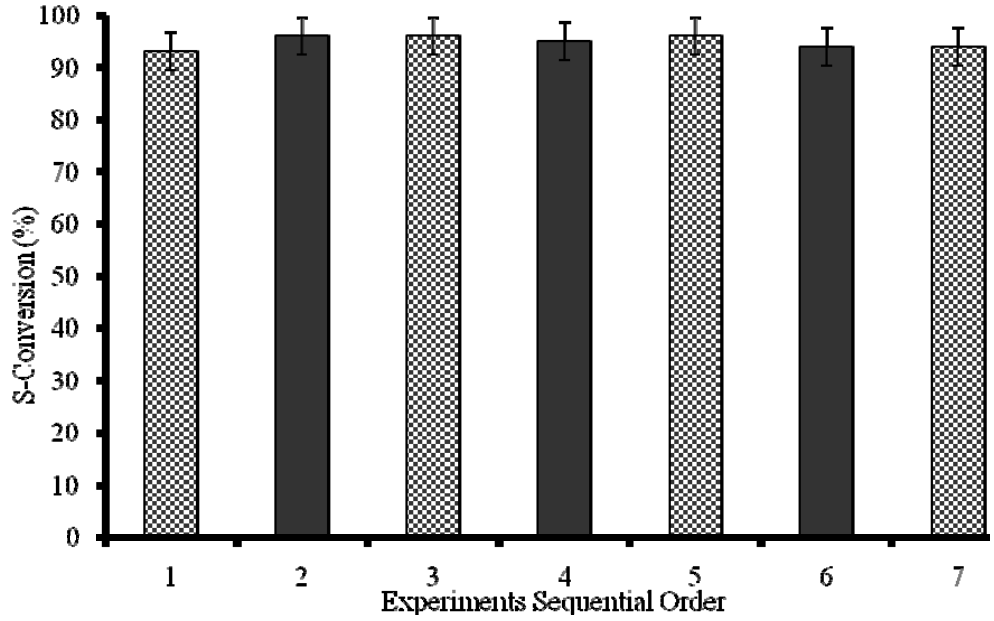

Figure 4.9: Change in catalytic activities with H_2 purity for HDS. The experiments were carried out at temperature, pressure, gas/oil ratio, and LHSV of 380 °C, 9 MPa, 800 mL/mL, and 1 h-1, respectively. H_2 purities for experiments 1, 3, 5, and 7 were 100% and were 90, 80, and 50% for experiments 2, 4, and 6, respectively.

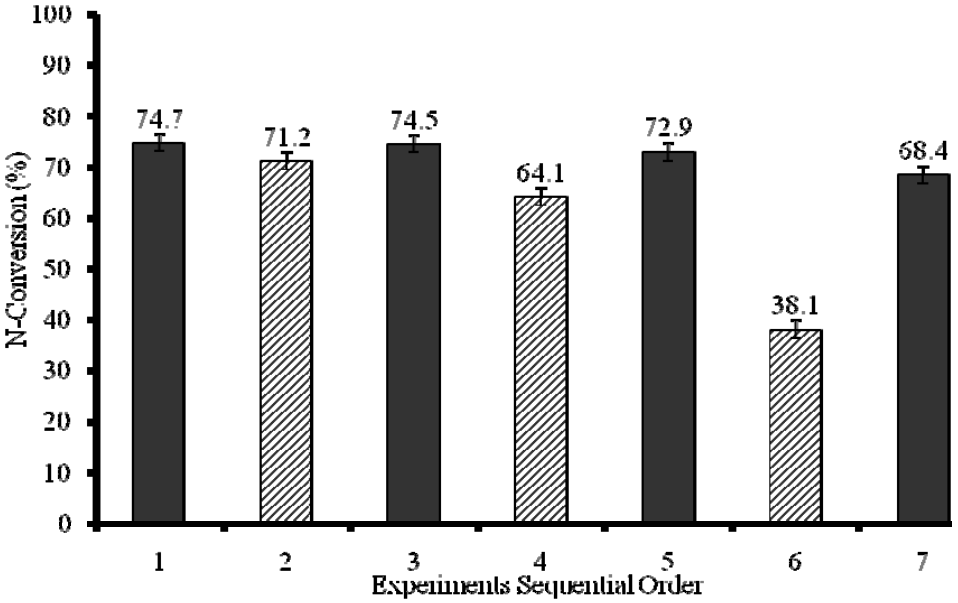

Figure 4.10: Change in catalytic activities with H_2 purity for HDN. Experimental conditions were the same as shown in Figure 4.9.

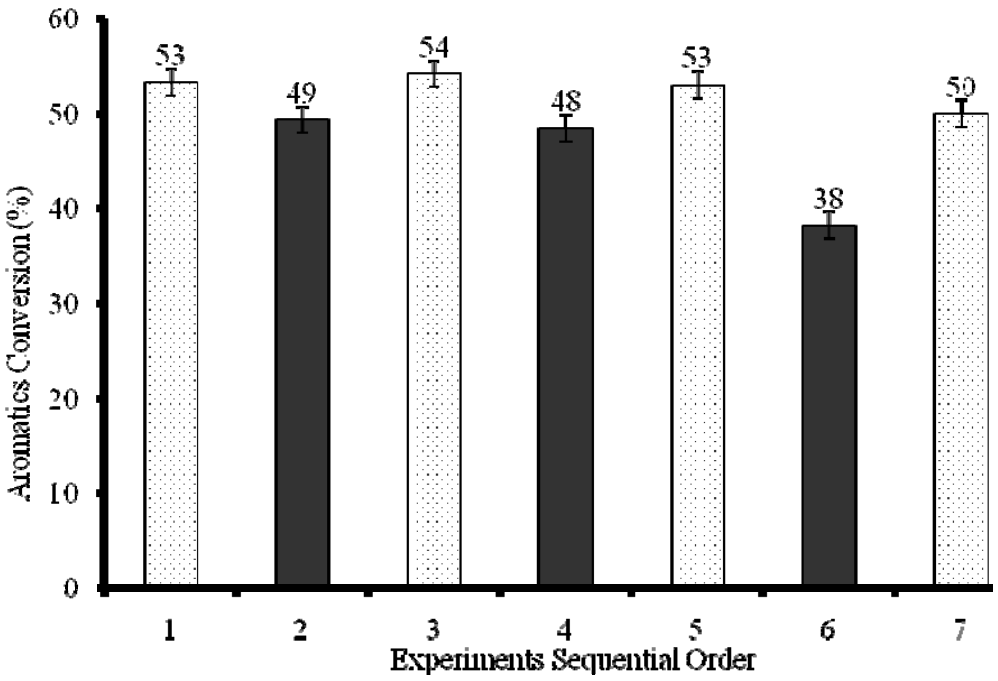

Figure 4.11: Change in catalytic activities with H_2 purity for HDA. Experimental conditions were the same as shown in Figure 4.9.

To verify the above claim, the effect of methane on the catalyst performance was studied by contrasting methane against helium. Helium is known to be inert toward Hydroprocessing catalysts (Bej et al., 2001b). Two experiments were conducted at 50 and 80% H_2 purity (with the rest either methane or helium). The "control" experiment was intermittently repeated before and after each of these two experiments. All experiments were conducted at constant temperature, pressure, gas/oil ratio, and LHSV of 380 °C, 9 MPa, 800 mL/mL, and 1 h^{-1}, respectively. The results are shown in Figure 4.12. It can be seen in this figure that there were no differences in hydroprocessing activities when methane was replaced by helium. Thus, it can be concluded that methane is inert toward the Ni-Mo/γ-alumina catalyst under these experimental conditions. Therefore, the use of lower purity hydrogen to carry out hydrotreatment will not have any adverse effect besides lowering the hydrogen partial pressure in the system.

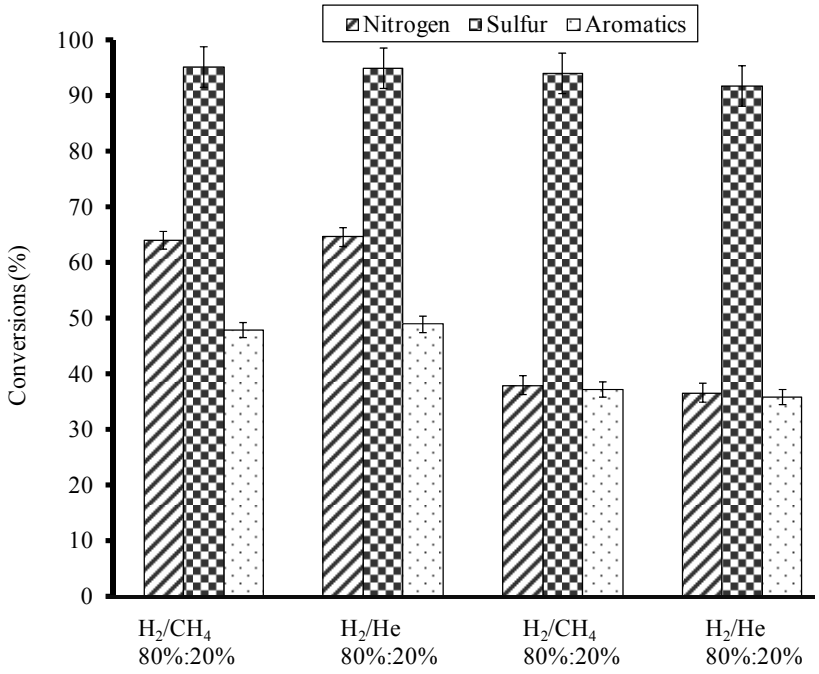

Figure 4.12: Methane versus helium effect on hydroprocessing conversions.

This decrease in hydrogen partial pressure can be countered by increasing the system total pressure, as shown in Figure 4.13. The results in this figure were generated using two experiments. In one experiment, the system total pressure was set at 7.2 MPa and the hydrogen purity was set at 100%. In the other experiment, the hydrogen purity was maintained at 80%. However, to keep the inlet hydrogen partial pressure the same, the total pressure of the system was increased to 9 MPa. The results show that both experiments produced similar hydrotreating conversions. Thus, pressure can be used to offset the use of lower hydrogen purity to achieve any desired hydrogen partial pressure without affecting HDS, HDN, and HDA conversions.

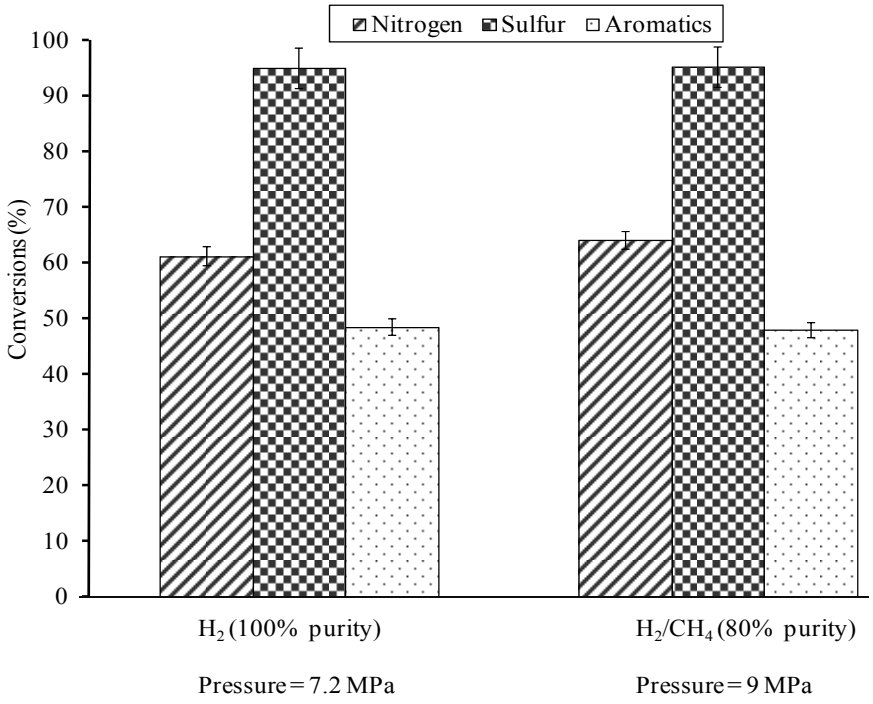

Figure 4.13: Pressure versus purity effect on hydroprocessing conversions. The experiments were carried out at temperature, gas/oil ratio, and LHSV of 380 °C, 800 mL/mL, and 1 h^{-1}, respectively.

4.1.3 Long term effect of Methane on catalyst performance

A catalyst deactivation study was conducted to observe the long-term effect of methane on catalyst performance. The catalyst was loaded, and experiments were conducted for a period of 66 days at increasing methane concentrations (with the rest H_2). The methane concentration was increased as follows: 0% for 3 days, 5% for 12 days, 12% for 30 days, 20% for 12 days, and 25% for 6 days; it was then decreased back to 0% for 3 days. Temperature and LHSV were kept constant at 380°C and 1 h^{-1}, respectively. The average conversions of HDS, HDN, and HDA at 0% methane at days 2 and 3 and days 65 and 66 were 96.8, 75.2, and 54.0% and 96.5, 74.5, and 52.4%, respectively. Thus, it can be concluded that the catalyst activities of HDS, HDN, and

HDA did not suffer significantly after being subjected to methane concentrations as high as 25 vol. % for a period of 66 days.

4.1.4 Variables affecting H_2 partial pressure

The increase of hydrogen partial pressure has a positive effect on hydroprocessing conversions (Girgis and Gates, 1991; Gary H. et al., 2007). To increase hydrogen partial pressure, one must increase total pressure, gas/oil ratio, or purity (amount of hydrogen in the gaseous phase) (Turner and Reisdorf, 2004). In this work, the effects of these three variables on the Hydroprocessing of HGO were also evaluated. Three additional experiments were conducted, and their results were compared to that of an experiment (shown as b in Figure 4.14) conducted at H_2 purity, pressure, and gas/oil ratio of 50% (with the rest methane), 9 MPa, and 800 mL/mL, respectively. All experiments were conducted at constant temperature and LHSV of 380°C and 1 h^{-1}, respectively. The full results are shown in Figure 4.14, and the four experiments are labeled a-d. Also, Table 4.2 contains HDS results expressed in parts per million (ppm) rather than percentages, for clarity purposes. In experiment a, H_2 purity was increased from 50 to 100% and the gas/oil ratio was reduced to 400 mL/mL. In experiment c, the pressure was increased from 9 to 10 MPa, and in experiment d, the gas/oil ratio was increased from 800 to 1270 mL/mL. Keep in mind that experiment b is used as a reference. The results show that increases in purity or pressure have positive effects on HDS, HDN, and HDA. At a constant H_2 purity of 50%, increasing the gas/oil ratio from 800 to 1270 mL/mL did not show promoting effects on HDS, HDN, or HDA.

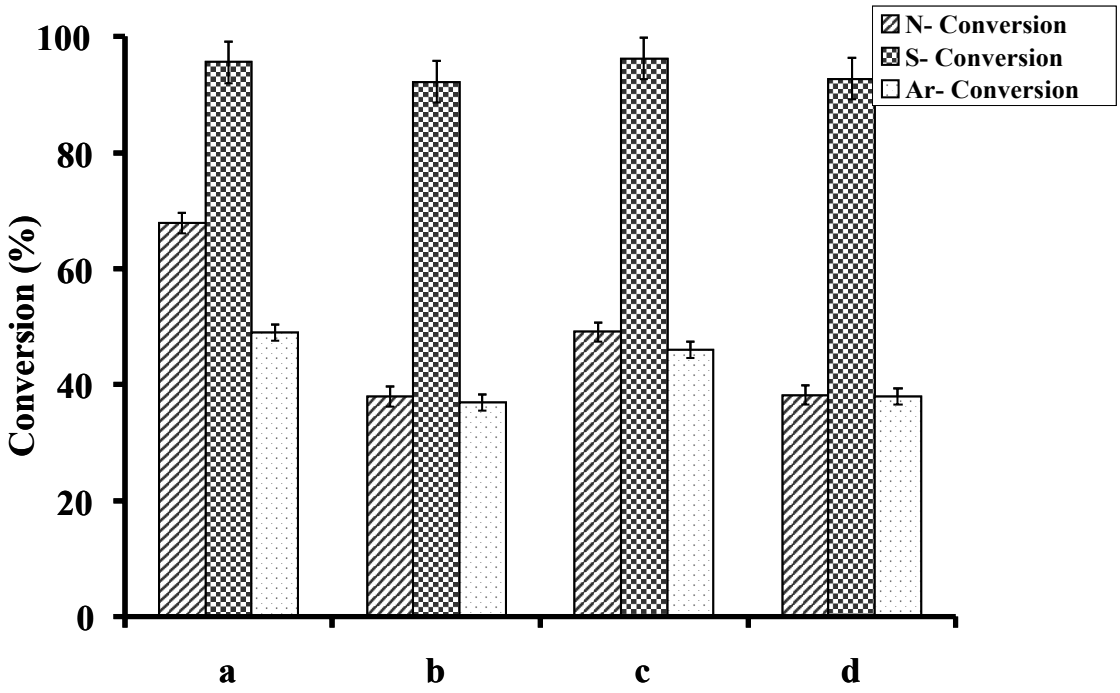

Figure 4.14. Comparison of the effects of (a) H_2 purity, (c) pressure, and (d) gas/oil ratio on hydroprocessing of HGO. The experimental conditions for a-d are stated in Table 4.2.

Table 4.2: Effect of the H_2 Purity, Gas/Oil Ratio, and Pressure on HDS

Exp.	Purity (%)	Gas/oil ratio (mL/mL)	Pressure (MPa)	Feed sulfur content (ppm)	Product sulfur content (ppm)
a	100	400	9	42,310	1,353
b	50	800	9	42,310	3,474
c	50	800	10	42,310	1,338
d	50	1,270	9	42,310	3,057

Similar results to those above were observed by Andari et al. (1996) and Bej et al. (2001a, 2001b). They found that the gas/oil ratio had an optimal value, depending upon the other process variables, after which a further increase in this ratio did not result in hydroprocessing improvement. A notable point is that, by increasing the gas/oil ratio from 800 to 1270 mL/mL, there was 60% (by volume) more hydrogen increase in the reactor but there were no corresponding increases in HDS, HDN, or HDA conversions. However, when the amount of hydrogen delivered into the reactor was kept constant and either the purity or the pressure was increased, both of which can increase the hydrogen partial pressure, improvement in hydroprocessing conversions were observed. Thus, hydrogen partial pressure is rather important than the amount of hydrogen present in a reactor, provided that the stoichoimetric amount of hydrogen is met.

4.2 Phase II: Effect of H_2 partial pressure on Hydrotreating activities

In this section the effects of the independent variables (pressure, temperature, LHSV, gas/oil, and H_2 purity) on feed vaporization, hydrogen dissolution, hydrogen consumption, and inlet and outlet H_2 partial pressure were studied. Also studied were the correlations between inlet and outlet H_2 pp and hydrotreating conversions. As mentioned in the introduction H_2pp is significantly more affected by pressure, gas/oil ratio, and H_2 purity than by temperature and LHSV (Antos et al., 2004). Therefore, these three important variables were used in the central composite inscribed method (using Expert design 6.0.1, which uses Derringer and Suich optimization method (Myers and Montgomery) to design the experiments. Their ranges were as follows: pressure was 7 to

11 MPa, H_2 purity was 75 to 100 vol. %, and gas/oil ratio was 400-1200 mL/mL (with the rest methane). In our previous work it was found that methane was inert towards commercial Ni-Mo/γ-alumina under these experimental conditions (Mapiour et al., 2009). Temperature and LHSV were kept constant at 380°C and 1 h^{-1}, respectively.

In a separate set of experiments the effects of temperature and LHSV on feed vaporization, hydrogen dissolution, hydrogen consumption, and H_2pp were studied. Temperature and LHSV ranges were 360 to 400°C and 0.65 to 2 h^{-1}, respectively. H_2 purity, pressure and gas/oil ratio were kept constant at 100 %, 9 MPa, and 800 mL/mL, respectively. LHSV was kept constant at 1 h^{-1} when the effect of temperature was studied. Temperature was kept constant at 380°C when the effect of LHSV was studied.

4.2.1 Effect of pressure, H_2 purity, and gas/oil ratio on feed vaporization, H_2 dissolution, H_2 consumption, and H_2pp

The data on the effect of reactor pressure, H_2 purity, and gas/oil ratio on feed vaporization, H_2 dissolution, H_2 consumption, and H_2 pp was analyzed using a non-linear regression. The regression analysis of experimental data generated the generalized equation below (Equation 4.1). The coefficients of this equation are summarized in Table 4.3.

$$X = i + a * \text{Purity} + b* \text{Pressure} + c * \text{Gas/oil} + d* \text{Gas/oil}^2 + e * \text{Purity x Pressure} + f * \text{Purity x Gas/oil} + g * \text{Purity}^2 + h * \text{Pressure}^2 \quad (4.1)$$

Where : X is inlet H_2 pp, outtlet H_2 pp, vaporized feed, Dissolved H_2, or H_2 consumption; a,b , c, d, e, f, g, h, i are coefficeints, and are summarized in Table 4.1. Purity, pressure, gas/oil are in vol. %, MPa, and mL/mL, respectively. *The equations are valid within the operating conditions studied*

Table 4.3 : The summary of the coefficients of Eqaution 4.1.

Coefficients	Inlet H_2 pp (MPa)	Outlet H_2 pp (MPa)	Vaporized Feed (g/h)	Dissolved H_2 (scf/bbl)	H_2 consumption (scf/bbl)
a	-2.401×10^{-3}	-0.339	-9.531×10^{-3}	0.675	5.677
b	7.289×10^{-3}	-4.965	0.150	-3.565	33.997
c	9.889×10^{-3}	-2.561×10^{-3}	3.883×10^{-3}	2.160×10^{-3}	0.085
d	-	-4.653×10^{-6}	-	-	-
e	-	0.051	-	0.113	-
f	-	1.326×10^{-3}	-3.094×10^{-4}	1.697×10^{-4}	-
g	-	-	-	-3.948×10^{-3}	-
h	-	-	-	0.233	-
i	0.149	36.589	-0.517	-23.958	336.133

Two statistical tests (test of significance of factors and R^2 test) were used to evaluate how well the experimantal data was represented by the models. The use of the test of significance of factors means that insignificant factors or interactions must be excluded from the model (Lazic, 2004). Significance of the factors or the interactions are evaluated using *p*-value (probability value). When a *p*-value of a factor or an interaction is greater than 0.05, it is certain at a 95% confidence level that that factor or interaction is insignificant and can therefore be excluded from the final mathematical model. The reduced models are presented in Equation 4.1.

R^2 , a value that always falls between 0 and 1, is the relative predictive power of a model (Lazic, 2004). The closer to 1 the R^2 is the better the model represents the expreimental observations. However, note that by simply incorporating more factors or

interactions R^2 could be increased while the predictive power of the model is not improved. Due to this shortcoming of R^2 , the use of adjusted R^2 is adviced. Adjusted R^2 is a modification of R^2 , but unlike R^2 it only increases when the newly included factor(s) or interaction(s) are significant (Montgomery, 1997). Another quantity is predicted R^2 . While R^2 indicates how well the model fits the experimental data at hand, predicted R^2 indicates how well the model predicts responses for new observations. The R^2, adjusted R^2, and predicted R^2 values of the factors and interactions of the developed models are summarized in Table 4.4.

Table 4.4: *R*-Squared statistics for the models

Model	R^2	Adjusted R^2	Predicted R^2
Vaporized feed	0.8793	0.8471	0.7311
Dissolved H_2	0.9995	0.9992	0.9987
H_2 consumption	0.9220	0.9074	0.9074
Inlet H_2 partial pressure	0.9994	0.9993	0.9988
Outlet H_2 partial pressure	0.9513	0.9288	0.8002

To test the predictive ability of the generatered models three experiment, (at conditions that were different than those of the expreimental design used to generate the data for the models development) were conducted. In these three experiments pressure, temperature, LHSV, gas/oil ratio were kept constant at 9 MPa, 380°C, 1 h^{-1}, and 800 mL/mL, respectively, while H_2 purity was varied as follows: 50, 80, and 90 vol. % (with the rest methane) . At these conditions quantities such as inlet H_2, outlet H_2, and vaporized feed, dissolved H_2, and H_2 consumption were experimentally determined and

compared to those predicted by the models, shown in Table 4.5. The maximum percentage differences for inlet H_2 and outlet H_2 partial pressure were 2.2% 15.3%, respectively. However, this relatively high percentage difference, 15.3%, was observed at the extrapolated experimental condition, i.e. at 50 % H_2 purity. When the comparisons were done solely within the range of conditions used to develop the models the maximum percentage differences for inlet H_2 and outlet H_2 partial pressure were 0.4 % and 0.9 %, respectively. Figure 4.15a and 4.15b are three-dimensional plots of the effects of pressure, H_2 purity and gas/oil ratio on inlet H_2 pp. These figures show that inlet H_2pp increases with increasing pressure and H_2 purity, but is not affected by the gas/oil ratio. The effect of pressure and H_2 purity are explained by Dalton's law. Gas/oil ratio does not affect inlet H_2 pp because as the amount of treat gas increases so does the amount of feed vaporization, thus vapor composition stays the same (McCulloch and Roeder, 1976).

Table 4.5: Comparison between the predicted and observed values

Model	R^2	Adjusted R^2	Predicted R^2
Vaporized feed	0.8793	0.8471	0.7311
Dissolved H_2	0.9995	0.9992	0.9987
H_2 consumption	0.9220	0.9074	0.9074
Inlet H_2 partial pressure	0.9994	0.9993	0.9988
Outlet H_2 partial pressure	0.9513	0.9288	0.8002

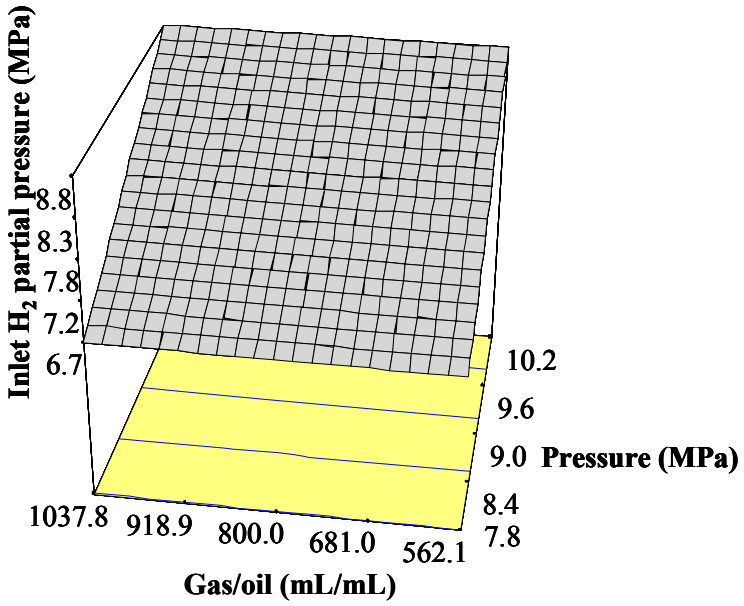

(a)

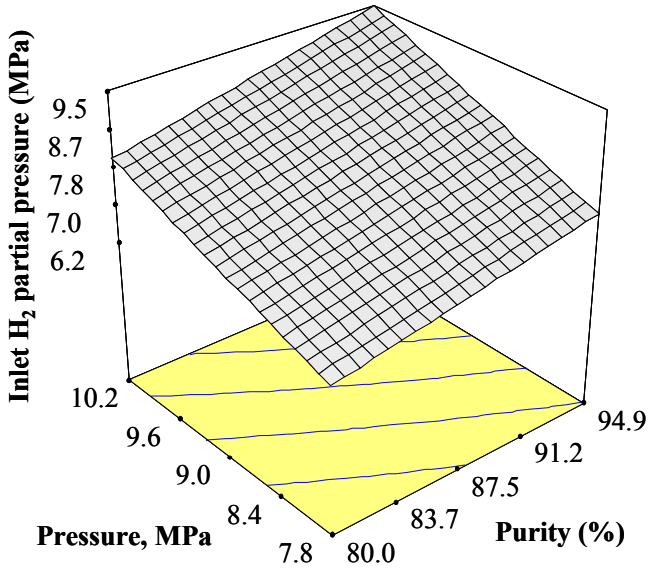

(b)

Figure 4.15: Surface response of the effect of pressure, H_2 purity, and gas/oil ratio on inlet H_2 partial pressure. Temperature and LHSV were constant at 380°C and 1 h^{-1}, respectively

Figure 4.16a and 4.16b show the effect of pressure, H_2 purity and gas/oil ratio on outlet H_2 pp. Outlet H_2pp increases with increasing pressure, H_2 purity and gas/oil ratio. However, the enhancing effect of the gas/oil ratio tends to plateau at higher values (approximately 800 mL/mL and above). To fully explain the effects of pressure, H_2 purity, and gas/oil ratio on inlet and outlet H_2 partial pressure one must first study their effects on the factors that influence inlet and outlet H_2 partial pressure, namely: feed vaporization, H_2 dissolution, and H_2 consumption.

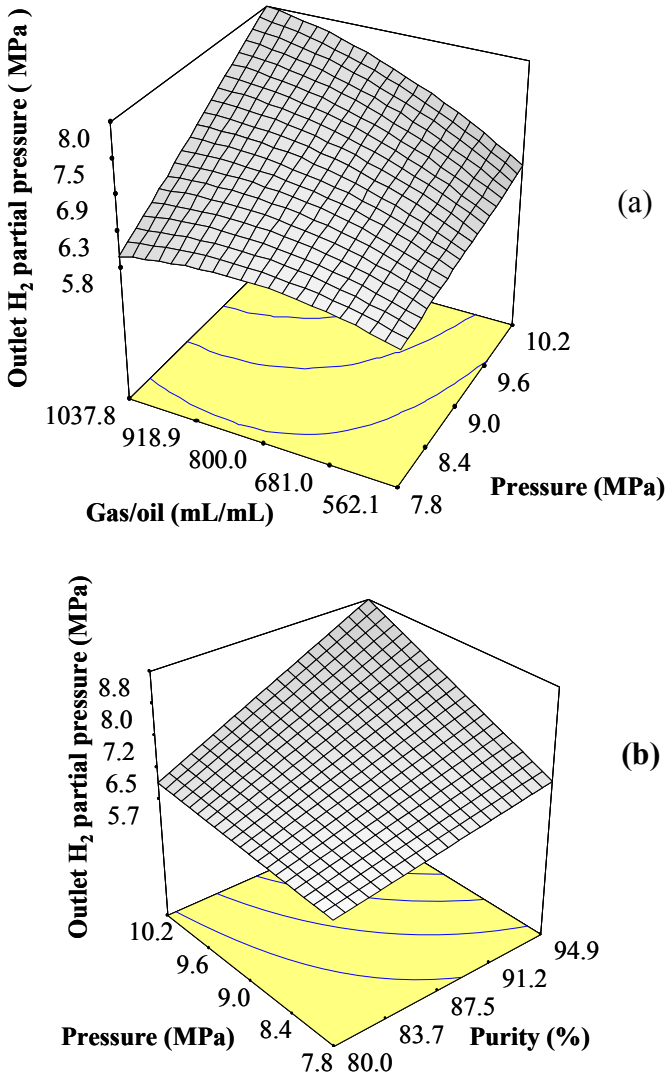

Figure 4.16: Surface response of the effect of pressure, H_2 purity, and gas/oil ratio on outlet H_2 partial pressure. Temperature and LHSV were constant at 380°C and 1 h^{-1}, respectively.

Figures 4.17, 4.18, and 4.19 depict the effects of pressure, H_2 purity, and gas/oil ratio on feed vaporization, H_2 dissolution, and H_2 consumption, respectively. In Figure 4.17 (a and b) and 4.18 (a and b) it can be observed that increasing pressure and H_2 purity and decreasing gas/oil ratio result in increases in H_2 dissolution and decreases in feed vaporization. The effect of pressure on feed vaporization can be explained by Le-Chatelier's principle. As the pressure increases the equilibrium counters this change by converting more gas into liquid since liquid takes less space (Tro, 2009). The effect of pressure on H_2 dissolution can be explained by Henry's Law. This law states that the concentration of dissolved gas is directly proportional to its partial pressure at a constant temperature. Therefore if the pressure is increased, causing an increase in the gas' partial pressure, the amount of the dissolved gas increases (Tro, 2009). Hence, an increase in H_2 dissolution is observed.

The effect of decreasing gas/oil ratio on feed vaporization can be explained in terms of mass transfer driving force. At a constant oil flowrate, gas/oil ratio is decreased by decreasing gas flowrate. As the gas flowrate is decreased less vaporization takes places due to decrease in mass transfer driving force (Wankat, 2007). Observed results of the effect gas/oil ratio on H_2 dissolution is counter-intuitive, one would expect that as gas/oil ratio increase more H_2 would be dissolved. Since increasing gas/oil ratio increases H_2 partial pressure, and according to Henry's Law, forces additional H_2 dissolution. However, the results suggest that increasing gas/oil ratio leads to decreases in H_2 dissolution. The reason for this is that both feed vaporization and H_2 dissolution occur simultaneously, and as the gas/oil ratio is increased more liquid feed is vaporized

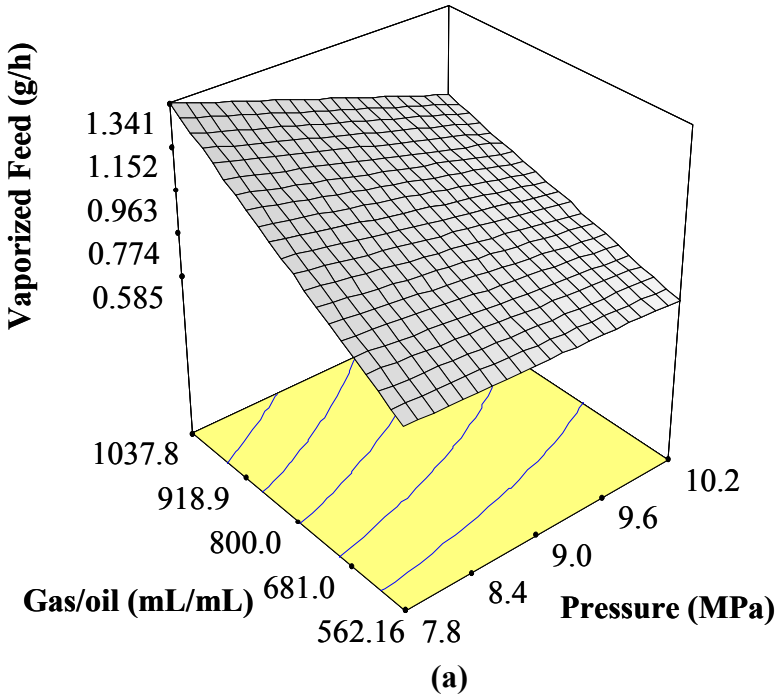

(a)

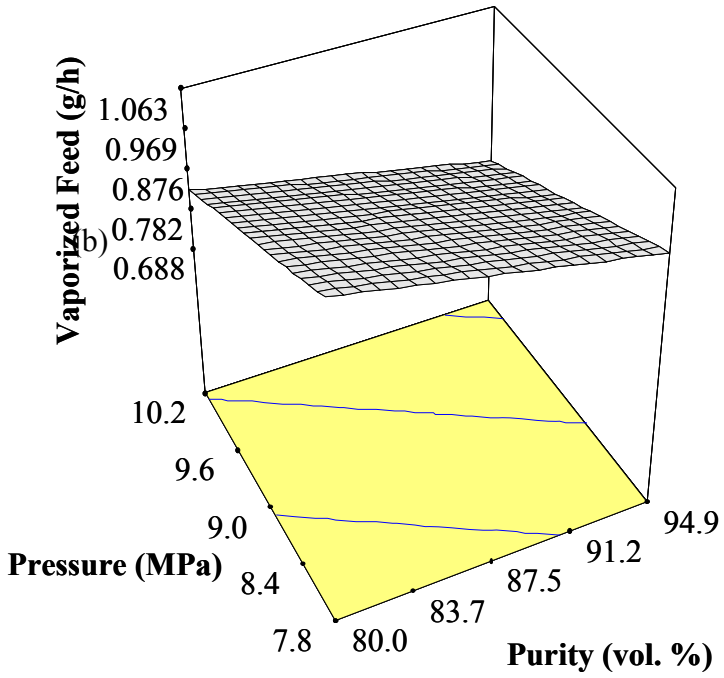

(b)

Figure 4.17: Surface response of the effect of pressure, H_2 purity, and gas/oil ratio on vaporized feed. Total liquid flow is 5 g/h.

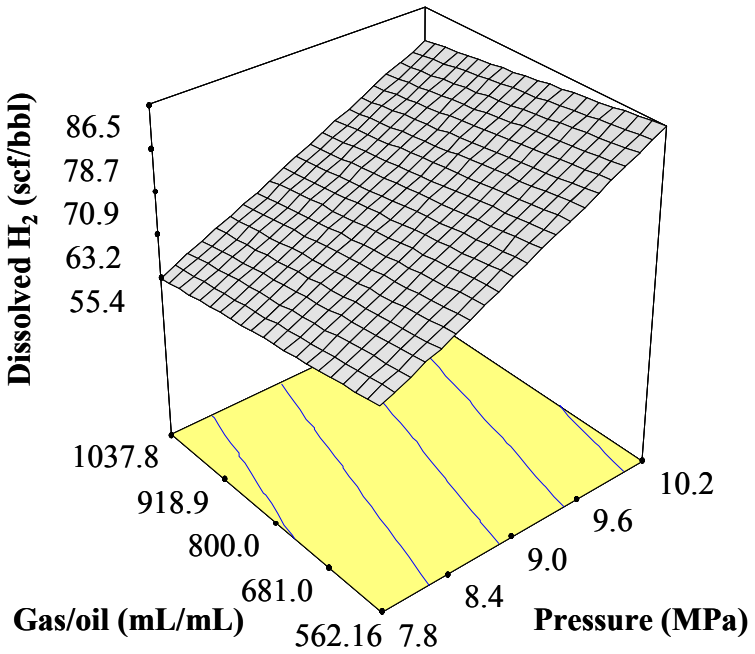

(a)

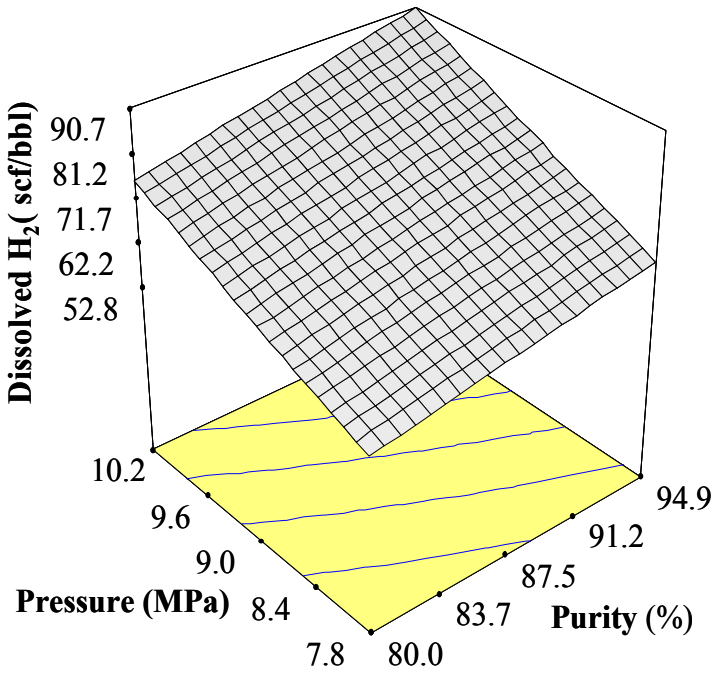

(b)

Figure 4.18: Surface response of the effect of pressure, H_2 purity, and gas/oil ratio on dissolved H_2.

leaving a smaller liquid volume for H_2 to dissolve in. Consequently the amount of the dissolved H_2 decreases. Similar results were observed by McCulloch and Roeder 1976.

Increasing the H_2 purity means that methane is replaced with H_2. Wilson et al. (1981), in an attempt to examine volatility of coal liquids, determined the interactions of CH_4 and H_2 with coal liquids. The authors found that the binary interaction constants for CH_4/coal liquids and H_2/coal liquids were 0.08 and 0.25, respectively. It is therefore reasonable to expect that the interaction between H_2 and other heavy hydrocarbons such as HGO would be higher than that of CH_4. Based on this assumption, H_2/HGO binary mixing is expected to exhibit more negative deviation from Raoult's Law, i.e. the molecules in the binary mixture have lower escaping tendency. Hence, lower feed vaporization was observed as H_2 purity was increased. Increasing the H_2 purity also led to increase in H_2 partial pressure. As explained by Henry's Law, increases in a gas' partial pressure leads to increases in its dissolution. Hence, increases in a H_2 partial pressure, caused by increasing the H_2 purity, led to increases in H_2 dissolution.

Figure 4.19a and 4.19b show that H_2 consumption increases with increasing pressure, H_2 purity and gas/oil ratio. In general, increasing pressure, H_2 purity and gas/oil ratio enhance hydrotreating conversions leading to higher H_2 consumption

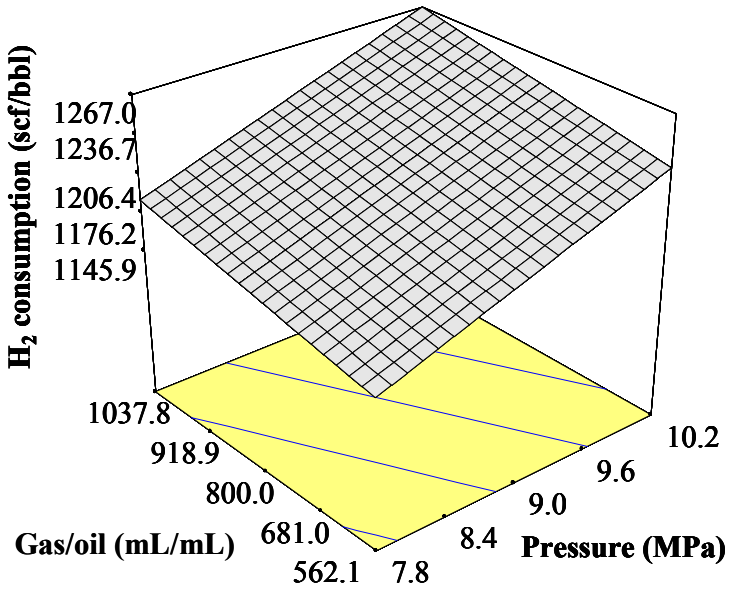

(a)

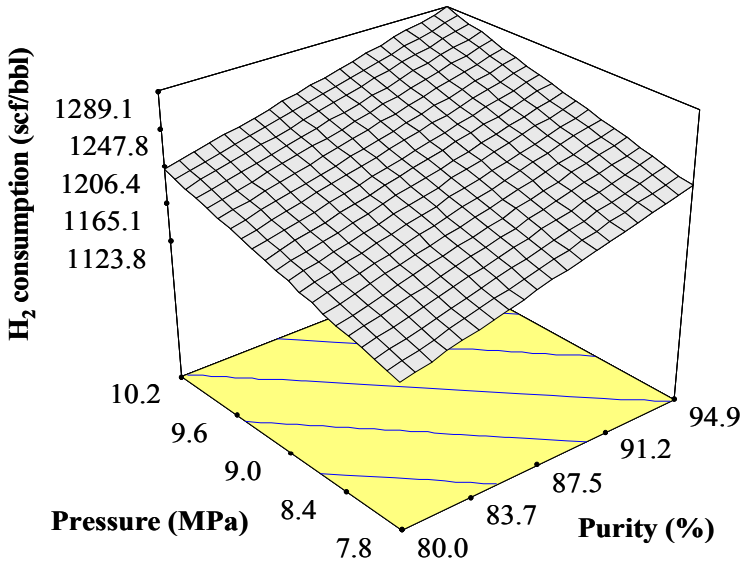

(b)

Figure 4.19: Surface response of the effect of pressure, H_2 purity, and gas/oil ratio on outlet H_2 consumption.

4.2.2 Effect of temperature and LHSV on feed vaporization H_2 dissolution, H_2 consumption, and H_2 partial pressure

The results of the effects of temperature and LHSV on feed vaporization, hydrogen dissolution, hydrogen consumption, and inlet and outlet H_2 partial pressure are given in Table 4.6. The results show that increasing temperature leads to increases in feed vaporization and very slight decreases H_2 dissolution. Increasing temperature causes increases in the species' kinetic energies leading to increases in feed vaporization. Also, the higher the temperature the more a gas expands and the harder it is for a gas to dissolve in a liquid. As a result decrease in H_2 dissolution was observed (Martin; Bustamante, 1993).

Table 4.6: Results of the effects of temperature and LHSV on feed vaporization, H_2 dissolution, H_2 consumption and inlet and outlet H_2 pp.

LHSV (h^{-1})	Vaporized feed @ outlet (g/h)	Dissolved H_2 @ outlet (scf/bbl)	H_2 consumption (scf/bbl)	Inlet H_2 partial pressure (MPa)	Outlet H_2 partial pressure (MPa)
0.65	0.73	48	1358	8.9	8.2
1	0.84	81	1352	8.9	8.2
1.5	0.91	129	1249	8.9	8.3
2	1.00	173	1170	8.9	8.3
Temperature(°C)					
360	0.52	81	1234	8.9	8.4
370	0.67	81	1286	8.9	8.3
380	0.84	81	1352	8.9	8.2
390	1.15	77	1319	8.8	8.1
400	1.40	74	1285	8.8	8.1

Increasing LHSV leads to increases in feed vaporization and H_2 dissolution. An increase in LHSV corresponds to an increase in the feed rate (liquid flow rate). According to Raoult's Law, as the mole fraction of a component in a solution increases so does its partial pressure, and consequently its escaping tendency increases. Therefore, as more liquid feed is introduced into the reactor, more of it evaporates. Also, by increasing the liquid flowrate, there is more liquid volume for H_2 to dissolve in. Hence, increases in H_2 dissolution were observed.

H_2 consumption decreases with increasing LHSV. Increasing LHSV results in decreases in hydrotreating conversions because the residence time is reduced. A result there is a decrease in H_2 consumption. H_2 consumption passes through a maximum with respect to temperature. The reason for this is that, shown in Figure 4.20, HDA passes through a maximum as the temperature is gradually increased from 360 to 400°C. Inlet and outlet H_2 partial pressure do not vary significantly with changes in temperature or LHSV (see Table 4.6).

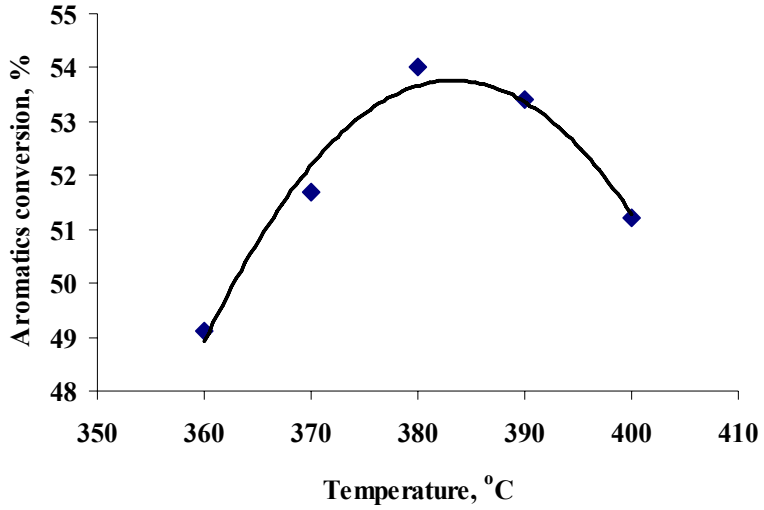

Figure 4.20: Effect of temperature on HDA. Pressure, LHSV, gas/oil ratio, and H_2 purity were 9 MPa, 1 h^{-1}, 800 mL/mL, and 100%, respectively.

4.2.3 Effect of H_2 pp on H_2 consumption dissolved H_2, and feed vaporization

It is important to look at the above factors because of their influences on H_2 pp (Speight, 1981 & 2000). Hence, an attempt was made to correlate H_2 pp and these factors. The results are shown in Figure 4.21. From Figure 4.21, it is evident that both hydrogen consumption and hydrogen dissolution increase with increasing H_2 pp. The reason for this is that increasing H_2 partial pressure generally improves hydrotreating activities, thus, increasing H_2 consumption. And as explained by Henry's Law, increases in gas' partial pressure result in increases in its dissolution. Hence, increasing H_2 pp brings about increases in H_2 dissolution. No clear correlation between H_2 pp and feed vaporization was observed.

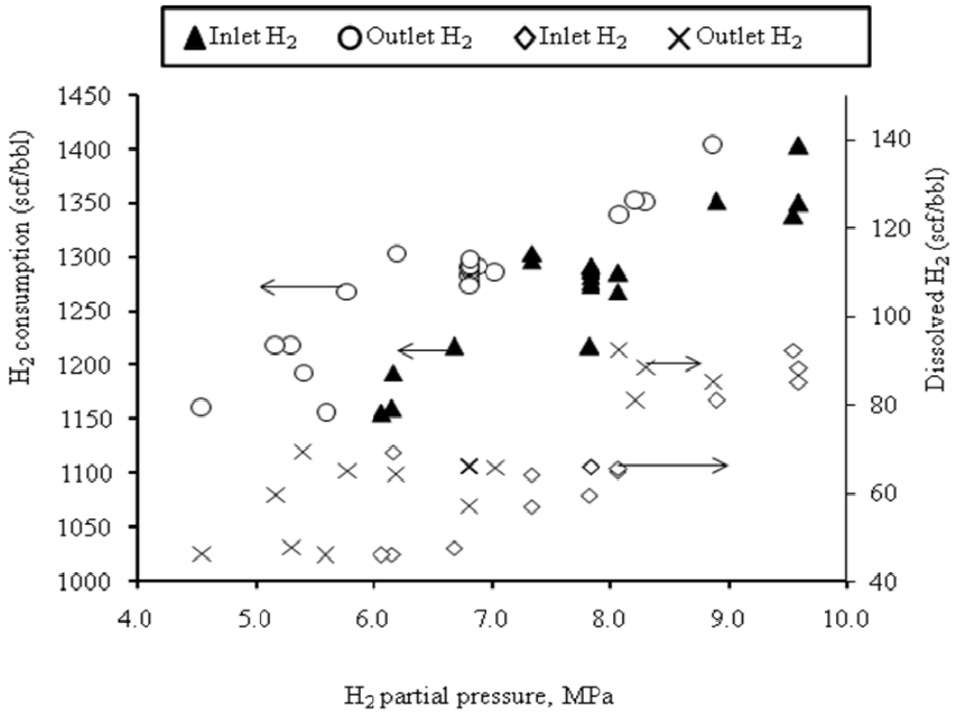

Figure 4.21: Correlations between H_2pp and H_2 consumption and H_2pp and dissolved H_2.

4.2.4 Effect of H_2 pp on hydrotreating activities

Figure 4.22 and 4.23 show that HDN and HDA were significantly more affected by H_2pp than HDS. This fact is often explained in terms of HDS mechanism versus HDN mechanism (Kabe et al., 1999; Fang, 1999). Hydrogenation of a N-containing ring occurs prior to C-N bond scission. Thus, the HDN rate can be affected by the equilibrium of N-ring hydrogenation because N-ring hydrogenation occurs before nitrogen removal (hydrogenolysis). HDS can proceed via two possible mechanisms: (i) ring hydrogenation followed by hydrogenolysis or (ii) direct hydrogenolysis. To understand the difference in HDS mechanism versus that of HDN, the bond energies of C=S, C-S, C=N, and C-N must be compared. The bond energies of C=S and C-S are the same, 536 kJ/mol, and the bond energies of C=N and C-N are 615 and 389 kJ/mol, respectively (Kabe et al., 1999). It is therefore energetically favorable to hydrogenate C=N to C-N before C-N bond scission, whereas for C=S and C-S there is no particular preference (Kabe et al., 1999). The mechanism for HDA is hydrogenation and an increase in the H_2pp results in an enhancement of hydrogenation rate. Consequently, an increase in HDA conversion is observed as H_2 pp is raised.

Simple models that relate hydrotreating conversions to inlet and outlet H_2 pp were developed and the results are given in Table 4.7. It can be seen in this table that the R^2 for HDS is very small because, within the H_2 pp range of study, HDS is not strongly affected by H_2 pp for reasons discussed in the paragraph above. To test the predictive ability of the generated models three experiments were conducted at conditions that were not part of the experimental runs used to generate the models, and their conversions were compared to those predicted by the models (see Table 4.8). In these

three experiments pressure, temperature, LHSV, gas/oil ratio were constant at 9 MPa, 380 °C, 1 h^{-1}, and 800 mL/mL, respectively, while H_2 purity was varied as follows: 50, 80, and 90 vol. % (with the rest methane). It was determined that the maxmium precentage differences for HDN and HDA using inlet H_2 pp models were 3% and 4 %, respectively. They were 4% and 7%, resepectively, when outlet H_2 pp models were used. The percentage differences for HDS were not determined because the R^2 was too small indicating that HDS developed model does not accurately represent the experimental data.

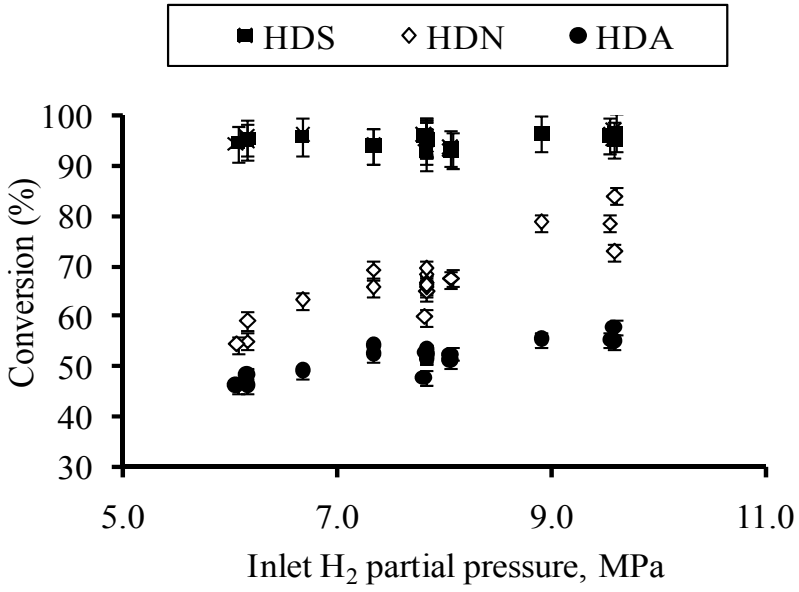

Figure 4.22: Effect of inlet H_2 partial pressure on HDS, HDN, and HDA.

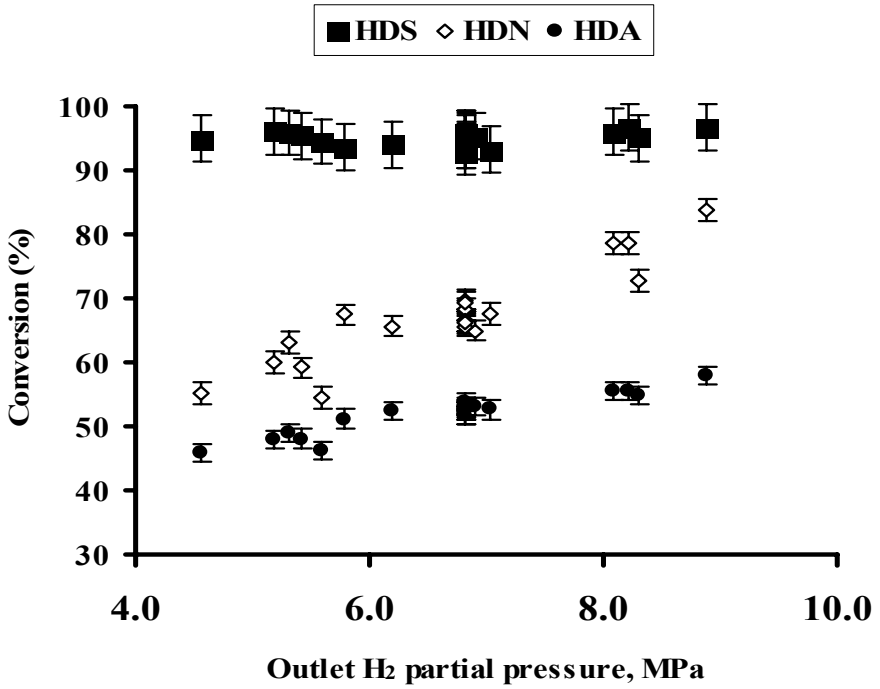

Figure 4.23: Effect of outlet H_2 partial pressure on HDS, HDN, and HDA.

Table 4.7: Correlations between H_2 partial pressure and hydrotreating conversions y: hydrotreating conversion; x: H_2 partial pressure.

Activity	*Equations*	R^2
	For Inlet H_2 partial pressure	
HDS	$y = 0.2932\ x + 92.694$	0.0773
HDN	$y = 0.231x^2 + 2.675x + 31.954$	0.8018
HDA	$y = -\ 0.2506\ x^2 + 6.5619\ x\ +\ 16.192$	0.7727
	For outlet H_2 partial pressure	
HDS	$y = 0.2417\ x + 93.374$	0.062
HDN	$y = 0.5883\ x^2 - 1.9673\ x + 53.48$	0.8414
HDA	$y = -0.1759\ x^2 + 4.9757\ x + 26.778$	0.8935

Table 4.8: Comparison between the predicted and observed values for the correlations between H_2 partial pressure and hydrotreating conversions

Purity (vol. %)	Determined experimentally (%)			Determined from the models (%)					
				Using inlet H_2 partial pressure			Using outlet H_2 partial pressure		
	HDS	HDN	HDA	HDS	HDN	HDA	HDS	HDN	HDA
50	92	38	38	94	46	41	94	52	42
80	95	64	48	95	63	50	95	62	53
90	96	71	49	95	68	53	95	69	56

4.2.5 Effect of H_2S on hydrotreating activities

H_2S is generated during hydrotreating as a product of HDS reactions. Most studies report that H_2S inhibits hydrotreating activities (Herbert et al., 2005; Girgis and Gates; 1991 Hanlon, 1987; Sie, 1999; Ancheyta et al., 1999; Bej et al. 2001), yet it is required to maintain the active chemical state of the catalyst (Bej et al., 2001). H_2S inhibition is caused when H_2S competes with organosulfur and organonitrogen for the same active sites on the catalyst. H_2S generated inside a hydrotreater can have an equilibrium value as high as 5 mol.% in the recycle gas (Gruia, 2006). This concentration of H_2S not only inhibits hydrotreating activities, it also reduces H_2 pp. Therefore, in practice, H_2S is removed in the amine unit. Unfortunately, some of H_2S remain in the recycle stream and is fed into the hydrotreater (Gruia, 2006) along with other difficult to remove impurities such as methane (Turner and Reisdorf, 2004).

In phase I, it was determined that the only effect induced by methane's presence was the decrease of H_2 pp inside the reactor, which in turn led to decreases in hydrotreating conversions. In this section an effort was made to determine what takes place when both methane and high concentrations of H_2S are present in the reactor. Due to the serious health hazards associated with direct handling of H_2S, high concentrations of H_2S were generated inside the reactor by adding different concentrations of buthanthiol to the HGO feed (Bej et al., 2001b). Buthanthiol decomposes under the chosen reaction conditions into 1-butene and H_2S (Horie et al., 1978).

Two sets of experiments were conducted. One set with no methane in the gaseous stream (100% H_2 purity) and another with 20 vol. % methane and 80 vol. % H_2.

In both sets of experiments, tests were carried out at different concentrations of butanethiol, 0, 1, and 3 wt. %, in the HGO feed. Temperature, pressure, gas/oil ratio and LHSV were kept constant at 380°C, 9 MPa, 800 mL/mL, and 1 h^{-1}, respectively. The results of the effect of H_2S on hydrotreating conversions are presented on Table 4.9. The results show that all HDS, HDN, and HDA conversions decrease as the concentration of H_2S is increased by adding butanethiol to the HGO feed. A notable point is that as the butanethiol concentration was increased from 0 to 1 wt. % there were considerable decreases in HDS, HDN, and HDA conversions. However, as the butanethiol concentration was increased from 1 wt. % to 3 wt. %, no major changes in HDS, HDN, and HDA conversions were observed. This may be interesting with regards to H_2S removal from the recycled gas. As this finding suggests there appears to be an optimal amount of H_2S that has to be removed, beyond which no significant beneficial effects on the hydrotreating conversions are realized.

Table 4.9: Effect of butanethiol added to feed on hydrotreating conversions

Conversion (%)	**100 vol. % H_2 purity**			**80 vol. % H_2 purity**		
	added butanethiol (wt.%)			**added butanethiol (wt. %)**		
	0	*1*	*3*	*0*	*1*	*3*
HDS	96.6	95.4	94.3	95.1	90.6	90.4
HDN	76.1	69.0	67.2	65.2	52.2	51.3
HDA	54.3	46.7	45.5	48.2	43.6	44.9

4.2.6 Effects of pressure, H_2 purity, and gas/oil ratio on hydrotreating activities

Often H_2 purity is not included as an operating variable in hydrotreating studies even though, along with pressure and gas/oil ratio, it has a significant effect on H_2 partial pressure. For this reason, H_2 purity, pressure, and gas/oil ratio, were used in an experimental design using a central composite design method (available in Expert design 6.0.1) in an effort to study their effects on HDS, HDN, and HDA activities. H_2 purity, pressure, and gas/oil ratio were varied within the range of 75-100 vol. % (with the rest methane), 7 – 11 MPa, and 400 – 1200 mL/mL, respectively. Temperature and LHSV were kept constant at 380°C and $1h^{-1}$, respectively. The experimental results obtained at conditions specified by the experimental design are summarized in Table 4.10. Analysis of the experimental results was carried out using DESIGN-EXPERT 6.0.1 to optimize the considered operating conditions with respect to HDS, HDN, and HDA conversions. Regression analysis of experimental data generated the following generalized regression equation (Equation 4.2), which coefficients are summarized in Table 4.11.

$$Y = e + a * Purity + b * Pressure + c * gas/oil + d * Purity^2 \quad (4.2)$$

Where: Y is HDS, HDN, or HDA (%); purity, pressure, gas/oil are in vol.%, MPa, and mL/mL, respectively. *The equations are valid within the operating conditions studied*.

Table 4.10: Experimental results at the conditions specified by the CCD experimental design.

Experimental Conditions			Response				
Pressure MPa	Gas/oil mL/mL	Purity %	HDN %	HDS %	HDA %	Inlet H_2 pp MPa	Outlet H_2 pp MPa
9.0	800	75	63.2	95.8	48.9	6.7	5.3
7.8	1038	80	59.1	95.4	48.1	6.2	5.4
10.2	562	80	67.4	93.6	51.2	8.1	5.8
7.8	562	80	55.1	94.9	46.0	6.2	4.6
10.2	1038	80	67.6	93.2	52.6	8.1	7.0
9.0	400	88	59.9	96.0	47.9	7.8	5.2
9.0	1200	88	65.0	95.3	53.0	7.8	6.9
7.0	800	88	54.4	94.5	46.1	6.1	5.6
9.0	800	88	66.7	95.5	51.8	7.8	6.8
9.0	800	88	65.7	94.0	52.4	7.8	6.8
11.0	800	88	72.8	95.0	54.9	9.6	8.3
9.0	800	88	68.2	95.6	52.4	7.8	6.8
9.0	800	88	66.6	92.9	53.1	7.8	6.8
9.0	800	88	69.6	95.8	52.6	7.8	6.8
9.0	800	88	66.3	95.0	51.8	7.8	6.8
7.8	1038	95	69.3	93.8	53.9	7.3	6.8
7.8	562	95	65.7	94.0	52.3	7.3	6.2
10.2	562	95	78.5	96.0	55.5	9.5	8.1
10.2	1038	95	83.9	96.7	58.0	9.6	8.9
9.0	800	100	78.8	96.6	55.4	8.9	8.2

Table 4.11: Summary of the coefficients of Equation 4.2.

Coefficients	HDS (%)	HDN (%)	HDA (%)
a	0.0467	-5.879	0.322
b	0.137	4.873	1.958
c	-1.777×10^{-4}	6.704×10^{-3}	4.980×10^{-3}
d	-	0.038	-
e	89.774	-	2.073

Table 4.12 and 4.13 contain the test of significance (*f*-test) and R^2 test results, respectively, of HDS, HDN and HDA models. Table 4.12 shows that the operating variables have no significant effects on HDS, i.e. *p*-value < 0.05 (Montgomery, 1997). Moreover, Table 4.13 shows that R^2 value for HDS model is very small, 0.0843, which means that HDS developed model poorly represents the experimental data. The *f*-test of HDN and HDA data shows that pressure, H_2 purity, and gas/oil ratio have significant effects on HDN and HDA activities. Moreover, it shows that these three factors do interact as they affect HDN and HDA activities, meaning that the effect of each factor is independent of the values of the other two factors. R^2 values of HDN and HDA developed models were 0.9262 and 0.9125, respectively.

Table 4.12: Results of test of the significance of factors and interactions for HDS, HDN, and HDA models

Factor or interaction	*p*-Value of factor or interaction		
	HDS	**HDN**	**HDA**
Purity	0.2916	< 0.0001	< 0.0001
Pressure	0.6136	< 0.0001	< 0.0001
Gas/oil	0.8961	0.0199	0.0005
$(Purity)^2$	-	0.0030	-
$(Pressure)^2$	-	-	-
$(Gas/oil)^2$	-	-	-
Purity x Pressure	-	-	-
Purity x Gas/oil	-	-	-
Pressure x Gas/oil	-	-	-
Model	0.6937	< 0.0001	< 0.0001

Table 4.13: *R*-Squared statistics for the developed models of HDS, HDN and HDA.

Model	R^2	Adjusted R^2	Predicted R^2
HDS	0.0843	-0.0875	-0.4553
HDN	0.9262	0.9065	0.8570
HDA	0.9125	0.8961	0.8496

Equation 4.2 does not show straightway the dependence of HDN and HDA conversions on the operating variables. Therefore, to clearly illustrate the dependence, surface response plots were developed, and are presented in Figure 4.24 and 4.25 for

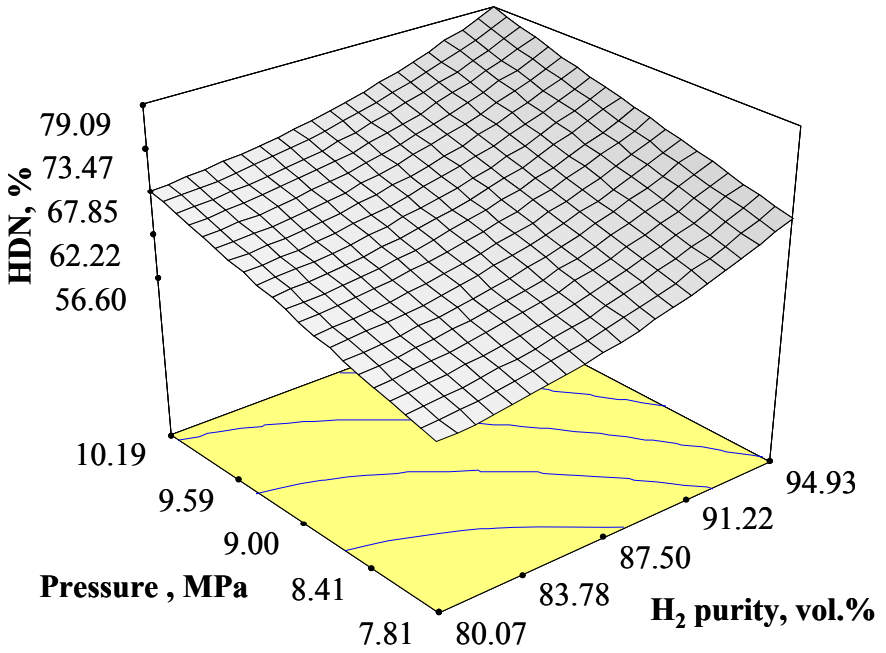

(a)

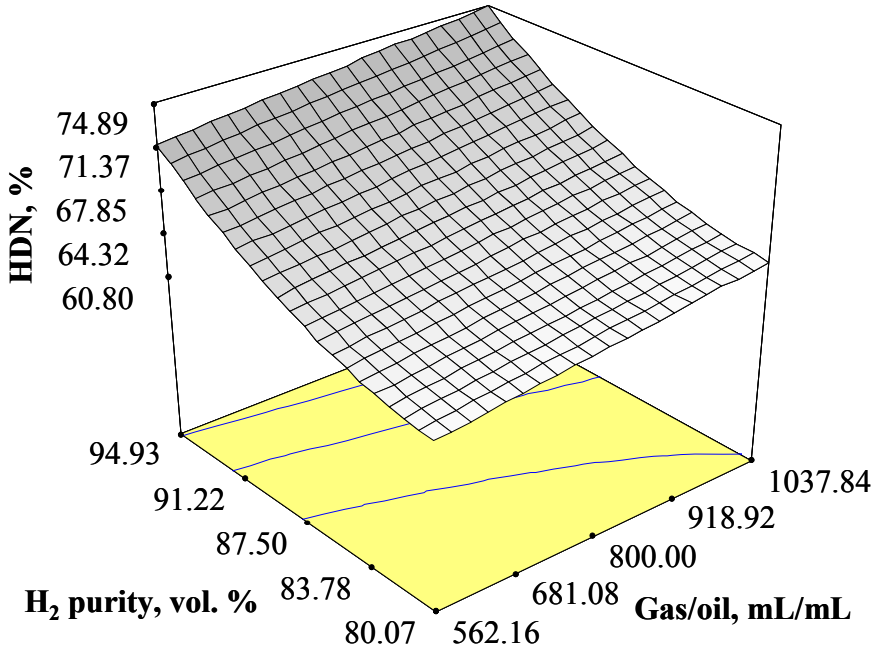

(b)

Figure 4.24: Surface response of the effects of pressure, H_2 purity, and gas/oil ratio on HDN activity.

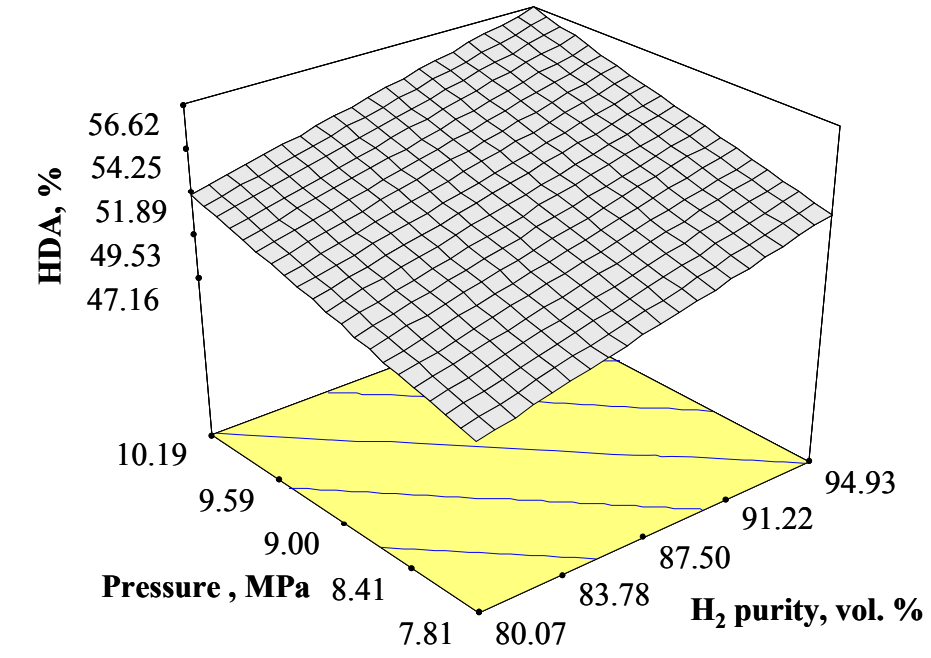

(a)

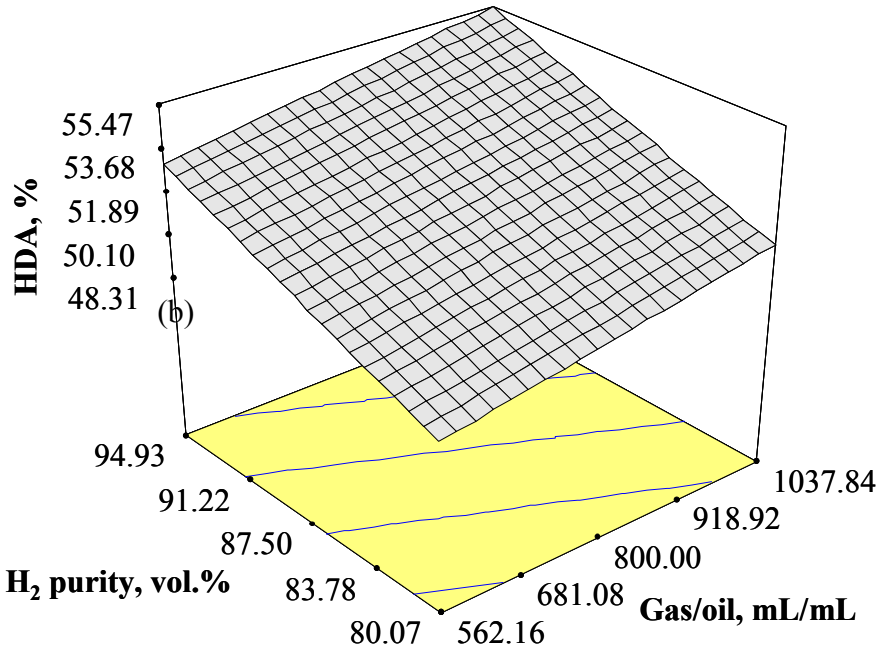

(b)

Figure 4.25: Surface response of the effects of pressure, H_2 purity, and gas/oil ratio on HDA activity.

HDN and HDA, respectively. These figures show that increasing pressure, H_2 purity, and gas oil ratio led to increases in HDN and HDA conversions. As interpreting the 3-D surface response can be difficult, the perturbation plots of the effects of the variables on HDS (no surface response of HDS is shown), HDN and HDA are provided in Figure 4.26, 4.27, and 4.28. When interpreting a perturbation plot, one needs to be cautious since it looks only at one-dimensional paths through a multifactor surface. Therefore, it is recommended that perturbation plots are used in conjunction with the 3-D surface responses. Nonetheless, it is a powerful method of comparing the relative influences of factors (Anderson; Patrick, 2005).

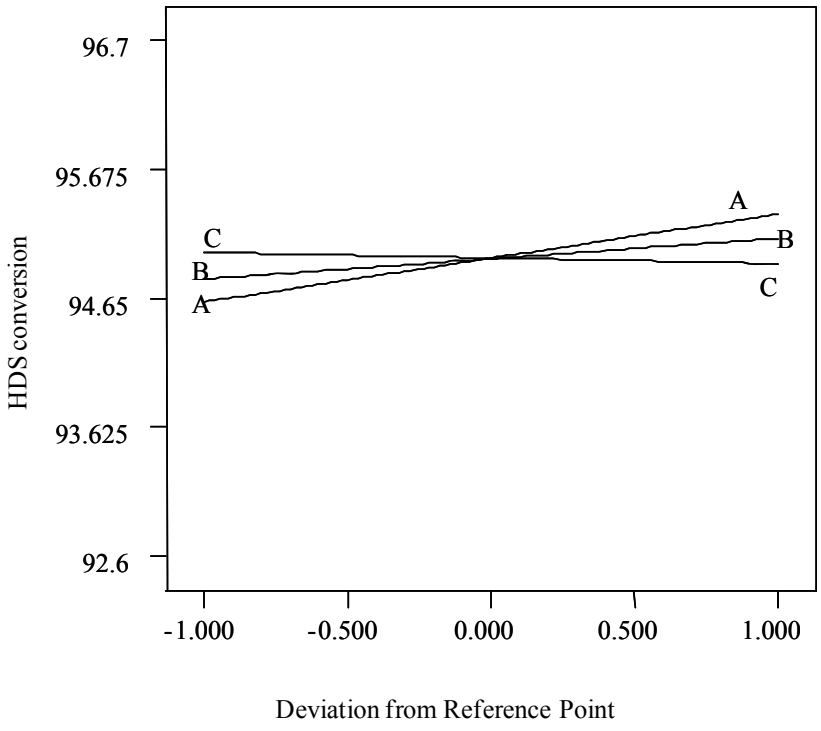

Figure 4.26: HDS perturbation plot. (A) is H_2 purity, (B) is pressure, and (C) is gas/oil ratio.

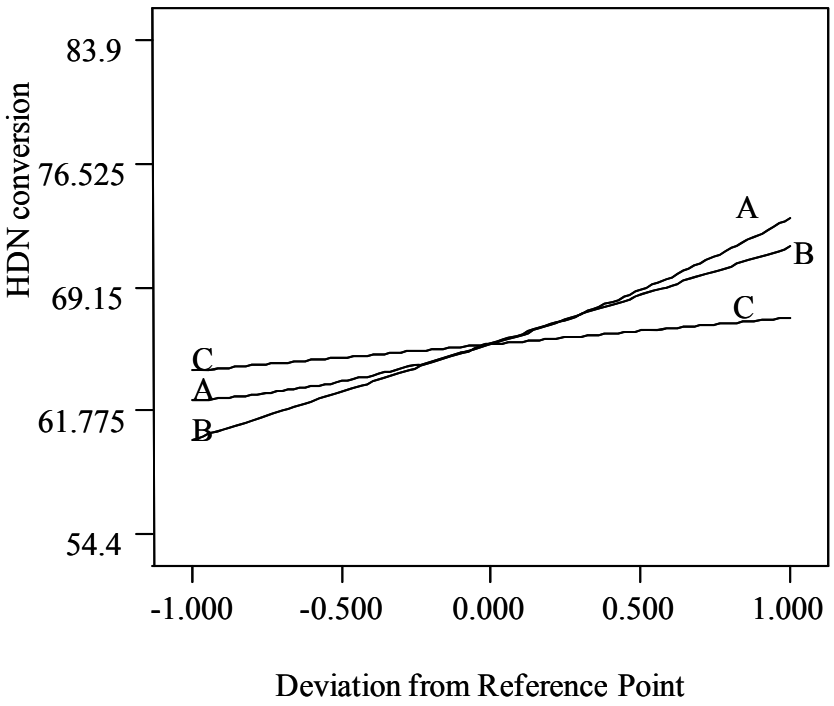

Figure 4.27: HDN perturbation plot. (A) is H_2 purity, (B) is pressure, and (C) is gas/oil ratio.

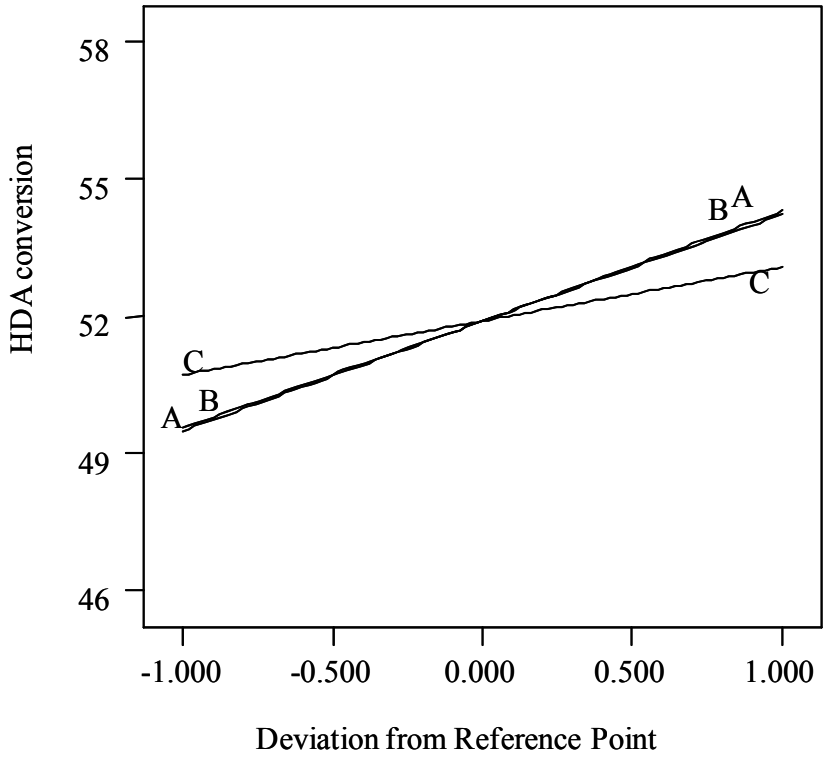

Figure 4.28: HDA perturbation plot. (A) is H_2 purity, (B) is pressure, and (C) is gas/oil ratio.

A perturbation plot shows the effect of each individual variable as the others are held constant (Anderson; Patrick, 2005). Figure 4.26 shows that effects of pressure, H_2 purity, and gas/oil ratio on HDS are not considerably significant. Nonetheless, Figure 4.26 does show that the effects of pressure and H_2 purity on HDS are slightly greater than that of the gas/oil ratio. Figure 4.27 and 4.28 show that the effects of the pressure, H_2 purity, and gas/oil ratio on HDN and HDA are noticeably significant, and that increasing these variables will lead to increases in HDN and HDA conversions. Moreover, these figures show that the effects of pressure and H_2 purity on HDN and HDA are more significant than that of the gas/oil ratio.

In Figure 4.27 and 4.28, it can also be observed that effects of the variables are greater on HDN than on HDA. This correlatively implies that the effect of H_2 pp is far greater on HDN than on HDA. However, by considering the mechanisms of HDN and HDA, one may expect the contrary. HDA reaction proceeds through hydrogenation, whereas HDN reaction proceeds through hydrogenation followed by hydrogenolysis, and hydrogenolysis is not affected by H_2 pp (Girgis and Gates, 1991). One explanation may be that at an operating temperature of 380°C HDA activity is close to optimum due to equilibrium thermodynamic limitation (Girgis and Gates, 1991; Gray , 2007). Thus, the effects of the other variables are not as significant as they would have been at lower operating temperatures. A second explanation may be the fact that the overall rate of HDN is frequently determined by the hydrogenation rate rather than by hydrogenolysis (Girgis and Gates, 1991), and hydrogenolysis is not affected by H_2 pp. Thus, pressure, H_2 purity, and gas/oil ratio can only affect hydrogenation processes in HDN and HDA reactions. Since, hydrogenation of aromatic rings with heteroatoms is easier than of

those which lack a heteroatom, HDN is more affected than HDA. A possible third explanation is that the initial concentration of aromatics is about 100 fold that of the nitrogen concentration in the feed, indicating that no fair comparison can be made by looking at HDN and HDA conversions.

Differences among the HDS, HDN, and HDA mechanism may offer an explanation as to why there are dissimilarities in the effects of the variables on HDN and HDA versus those on HDS. As previously mentioned in this section, HDN reaction takes place via hydrogenation followed by hydrogenolysis, and HDA reaction occurs via hydrogenation. Increasing H_2 purity, pressure, and gas/oil ratio result in increases in H_2 pp. This increase in H_2 pp directly affects the hydrogenation process. As a result, changes in HDA and HDN conversions were observed as H_2 purity, pressure, and gas/oil ratio were varied. On the other hand, HDS reaction can proceed via two pathways: 1) hydrogenation followed by hydrogenolysis or 2) direct hydrogenolysis (Anderson and Patrick, 2005; Knudsen et al., 1999). Consequently, HDS conversions were only very slightly affected by H_2 partial pressure since HDS reaction has the option of taking place directly via hydrogenolysis. Consequently, no significant effects of pressure, H_2 purity, and gas/oil ratio on HDS conversions were observed.

The optimal operating conditions were calculated based on constraints in which HDS, HDN, and HDA conversions were to be maximized within the ranges of the operating variables studied. The collective optimum operating conditions for HDS, HDN, and HDA were determined to be: pressure of 10.2 MPa, H_2 purity of 95 vol. %, and gas/oil ratio of 1037 mL/mL. Experiments were conducted under these conditions, and the experimental data was compared to those predicted (see Table 4.12). As shown

in Table 4.14, the percentage differences of HDS, HDN, and HDA for the experimental results versus the predicted results were 0.7%, 2.3%, and 0.2%, respectively. It may be noted that the results for HDS may not be reliable since the R^2 of the developed model was only 0.0843.

Table 4.14: Comparison between the predicted and observed values of hydrotreating at optimal conditions: pressure of 10.1 MPa, H_2 purity of 95vol. %, and gas/oil ratio of 1037 mL/mL. Temperature and LHSV were 380°C and 1h^{-1}, respectively.

Reactions	Predicted by models (%)	Observed Experimentally (%)	Percentage differences (%)
HDS	95.4	96.1	0.7
HDN	80.1	82.0	2.3
HDA	57.8	57.9	0.2

4.2.7 Effects of temperature and LHSV on hydrotreating activities

Effects of temperature and LHSV on the hydrotreating activity were also studied. Temperature and LHSV ranges were 360 to 400°C and 0.65 to 2 h^{-1}, respectively. H_2 purity, pressure and gas/oil ratio were kept constant at 100 %, 9 MPa, and 800 mL/mL, respectively. LHSV was kept constant at 1 h^{-1} when the effect of temperature was studied. Temperature was kept constant at 380°C when the effect of LHSV was studied.

LHSV, which is the inverse of residence time, is an indication of the time spent in the reactor by the reactants (Botchwey et al., 2003). It was observed that decreasing LHSV led to increases in HDS, HDN, and HDA conversions (see Figure 4.29). However, one needs to bear in mind that for HDA this observation is only true for the conditions employed in this work, especially temperature. For example, Mann et al. (1987) found that HDA is independent of LHSV (between 0.5-4 h^{-1}) at the temperature of 450°C and pressure of 6.99 MPa. The reason is that HDA maximum conversion is achieved between 370°C to 400°C (usually 375-385°C) due to the interrelation between thermodynamic equilibrium and reaction rates (Gray et al., 2007). The authors observed similar results for HDS and HDN to those found in this work. Increasing the

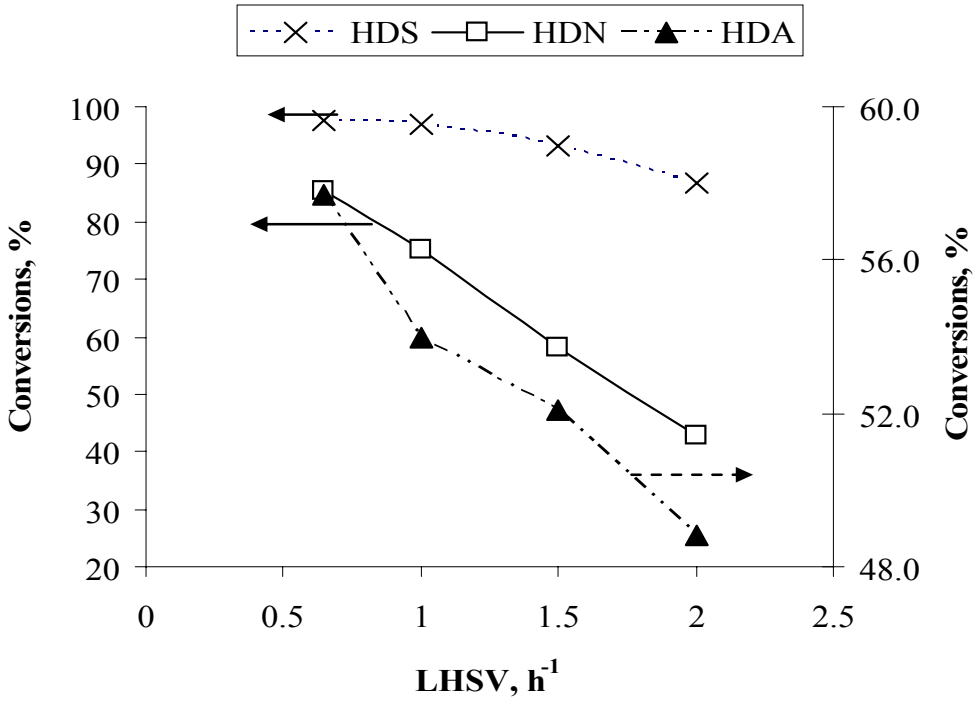

Figure 4.29: Effect of LHSV on hydrotreating conversions. Pressure, temperature, H_2 purity, and gas/oil ratio were 9MPa, 380°C, 100%, and 800 mL/mL, respectively.

temperature generally leads to increases in hydrotreating conversions. Nevertheless, excessive temperature may impose thermodynamic equilibrium limitations leading to decreases in hydrotreating conversions. In the cases of HDS and HDN, this hindering effect of temperature is observed at temperatures higher than those used in practice (i.e. > 425°C) (Girgis and Gates, 1991). In the case of HDA, the hindering effect of temperature is observed at lower temperatures than that of HDS and HDN. As mentioned earlier in this section, the maximum HDA conversion usually occurs at temperature range of 370°C to 385°C (Gray et al., 2007); this range could be little higher if the H_2 partial pressure is substantially increased.

In this work it was found that both HDS and HDN conversions increase with increasing temperature, however, HDN shows superior increases than that of HDS (see Figure 4.30). This superior effect of temperature on HDN could not be because HDN has higher reaction rate than HDS. The bond energy of C=N (147 kcal/mol) is higher than that of C=S (114-128 kcal/mol). Moreover, N (0.75Å) has smaller atomic radius than S (1.09Å), therefore is more difficult to remove N than S (Landau , 1997). Thus in theory, HDS should be more significantly affected by temperature than HDN; however, this is not the case. An explanation may be that, at the temperature range under study, the effect of temperature on HDS starts to subside, while the effect of temperature on HDN starts to become more pronounced. In a study by Mann et al. (1987) using NiMo/γ-Al_2O_3 as a catalyst and HGO as a feed, it was found that in the temperature range of 300 to 350°C, HDS and HDN percentage conversions per °C (degree Celsius) were 0.25 and 0.10 %/°C, respectively. However, in the temperature range of 350 to

400°C HDN has a higher percentage conversion per °C (0.36%/°C) than HDS (0.22%/°C). Figure 4.30 also shows that HDA conversion passes through a maximum with respect to the temperature, which is in agreement with the literature. By taking the first derivative of the equation of the empirical equation (see Equation 6), maximum HDA conversion was determined to have occurred at 385°C. From the foregoing discussion it seems that temperature is most critical of all of the variables.

$$\text{HDA conversion} = -0.0089\ \text{Temperature}^2 + 6.8447\ \text{Temperature} - 1258 \quad (4.9)$$

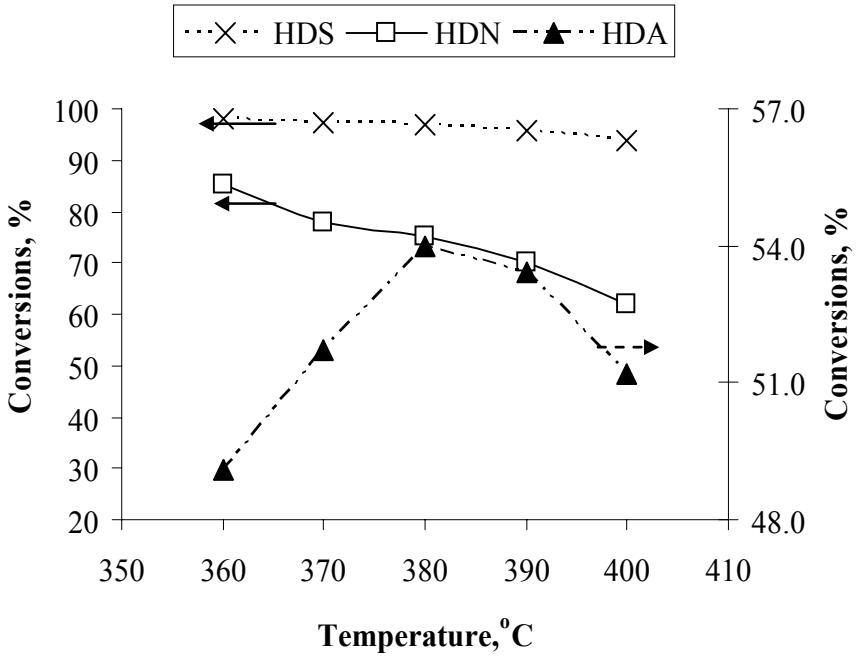

Figure 4.30: Effect of temperature on hydrotreating conversions. Pressure, LHSV, H_2 purity, and gas/oil ratio were 9MPa, 1h^{-1}, 100%, and 800 mL/mL, respectively.

4.3 Phase III: Kinetic Modeling

In this section three commonly used kinetic equations for modeling of hydrotreating of real feed were used. These kinetic equations are: Power Law model

(PL), Langmuir Hinshelwood model (L-H), and Multi-parameter model (M-P). The results obtained were compared those found in literature.

4.3.1 Power law analysis of HDS, HDN, and HDA

The Power law model has been used in many studies of kinetics modeling of HDS and HDN. However, open literature information on the kinetic studies of the HDA of real feed such as petroleum and synthetic middle distillate are very scarce; possibly due to complexity of the reactions (Owusu-Boakye, 2005). In this work, the reaction orders for the HDS, HDN, and HDA determined using the power law model and the results are summarized in Table 4.15. The values of reaction orders were determined from the best fit of experimental data. Different values of n, thus different forms of Equation 2.6 solutions (see chapter 2), were tested and the ones that yielded the highest R^2's values were considered the appropriate reaction orders (Bej et al. 2002).

Table 4.15: Results of Activation energies and reaction orders using power law, L-H, and multi-parameter kinetic models

	Activation Energy (kJ/mol)			Reaction order	
Reactions	Power Law	Langmuir-Hinshelwood*	Multi-parameter	Power Law	Multi-parameter
HDS	101	99	119	2	2.68
HDN	79	69	112	1.5	2.02
HDA (360-380 °C)	30	62	34	1.5	Pseudo-1st
HDA (380-400 °C)	-18	-9	-	1.5	-

*The assumption for L-H is that HDS, HDN, and HDA are pseudo-1st

In the experimental conditions chosen LHSV ranged between 0.65 and 2 h^{-1}, while temperature, pressure, gas/oil ratio, and H_2 purity were constant at 380 °C, 9 MPa, 800 mL/mL, and 100 %, respectively. The reaction orders of HDS, HDN, and HDA were determined to be 2, 1.5, and 1.5 respectively.

Arrhenius plots for HDS, HDN, and HDA (see Figure 4.31) were generated using experimental conditions where temperature ranged between 360 to 400°C, while LHSV, pressure, gas/oil ratio, and H_2 purity were constant at 1 h^{-1}, 9 MPa, 800 mL/mL, and 100 vol. %, respectively. R^2 for Arrhenius plots range between 0.97 and 0.99. The Arrhenius plots show that HDS and HDN reactions are irreversible under these experimental conditions used in this study. It is well known that under industry conditions (Temperature: 340-425 °C and Pressure: 55-170 atm [5.6 – 17.2 MPa]) both HDS and HDN are irreversible (Girgis and Gates). Also, the Arrhenius plot shows that HDA is a reversible process under the considered experimental conditions. HDA apparent reaction rate increases with temperature until 380 °C, after which it starts to decrease. According to the literature maximum HDA is achieved between 370-385°C (Gray et al., 2007).

The activation energies for HDS, HDN, and HDA were calculated and the results are summarized in Table 4.15. The activation energies for HDS and HDN were 79 and 101 kJ/mol, respectively. Due to reversibility of HDA two activation energies were calculated for the temperature ranges of 360-380°C and 380-400°C. In the 360-380°C range the value was 30 kJ/mol, and in the 380-400°C range the value was -18 kJ/mol. The explanation for this phenomenon is that increasing temperature has two competing effects on HDA: increased reaction rates and lower equilibrium conversions (Girgis and

Gates 1991). Thus at lower temperatures HDA is kinetically controlled, while at higher temperatures it is equilibrium controlled. Consequently in practice a balance must be struck between using lower temperatures to achieve maximum reduction of aromatic content and using higher temperatures to give high reaction rates and a minimum amount of catalyst charge per barrel of feed (Gray et al., 2007).

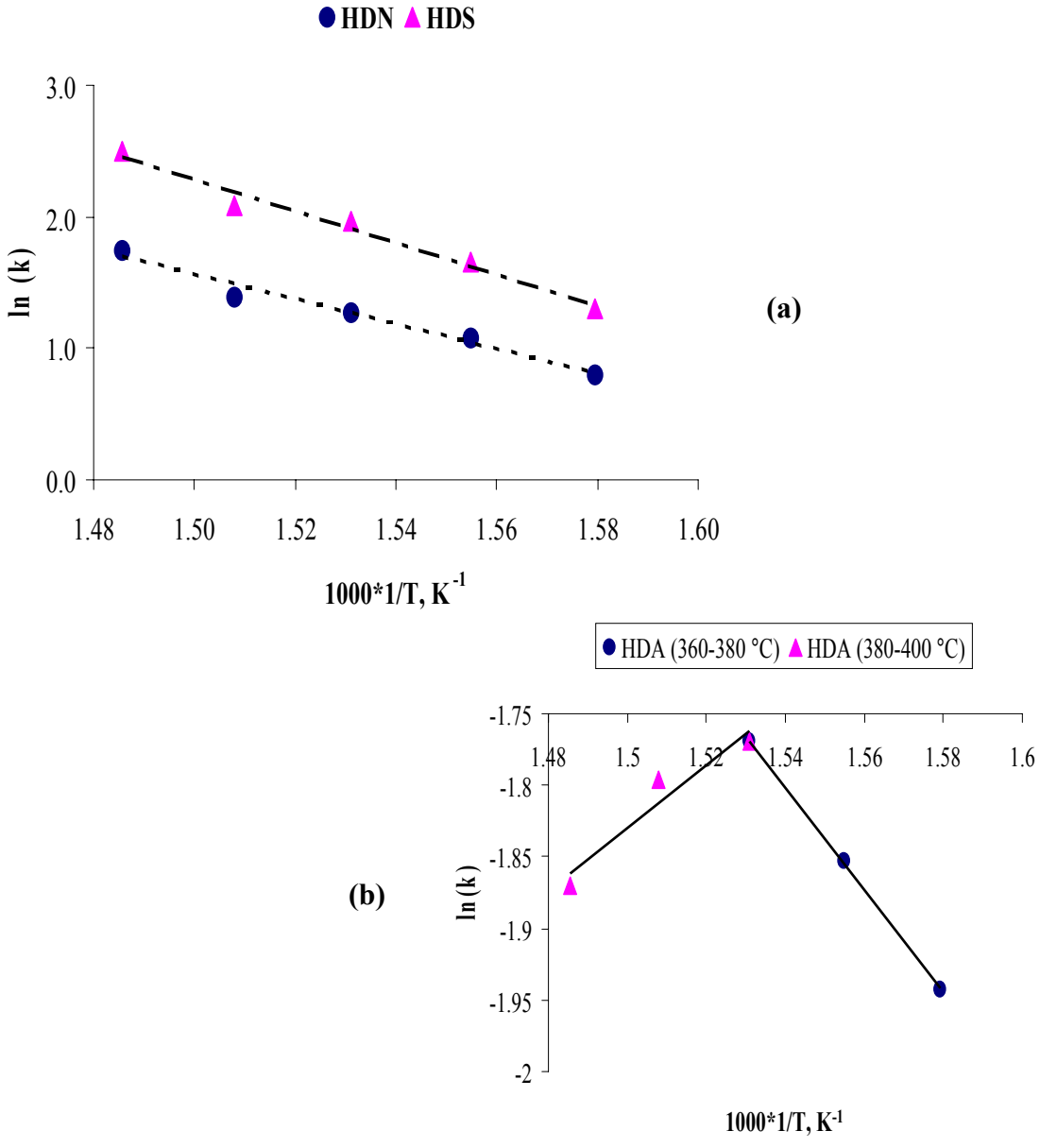

Figure 4.31: Arrhenius plot for: a) HDS, HDN, and b) HDA using power law model.

The effect of H_2pp on HDS, HDN, and HDA kinetics were also observed. In the experiments H_2 purity was varied between 50 and 100 vol. % (with the rest methane), while temperature, pressure, gas/oil ratio, and LHSV were kept constant at 380°C, 9 MPa, 800 mL/mL, and 1 h^{-1}, respectively. The data was analyzed using the power law model and the results are presented in Figure 4.32. The results show that HDN is more sensitive to H_2pp than HDS and HDA. This is explained by the differences in mechanisms of the HDS, HDN, and HDA, as discussed in section 4.2.4. Similar results were observed by Fang (1999), however, the study did not address HDA.

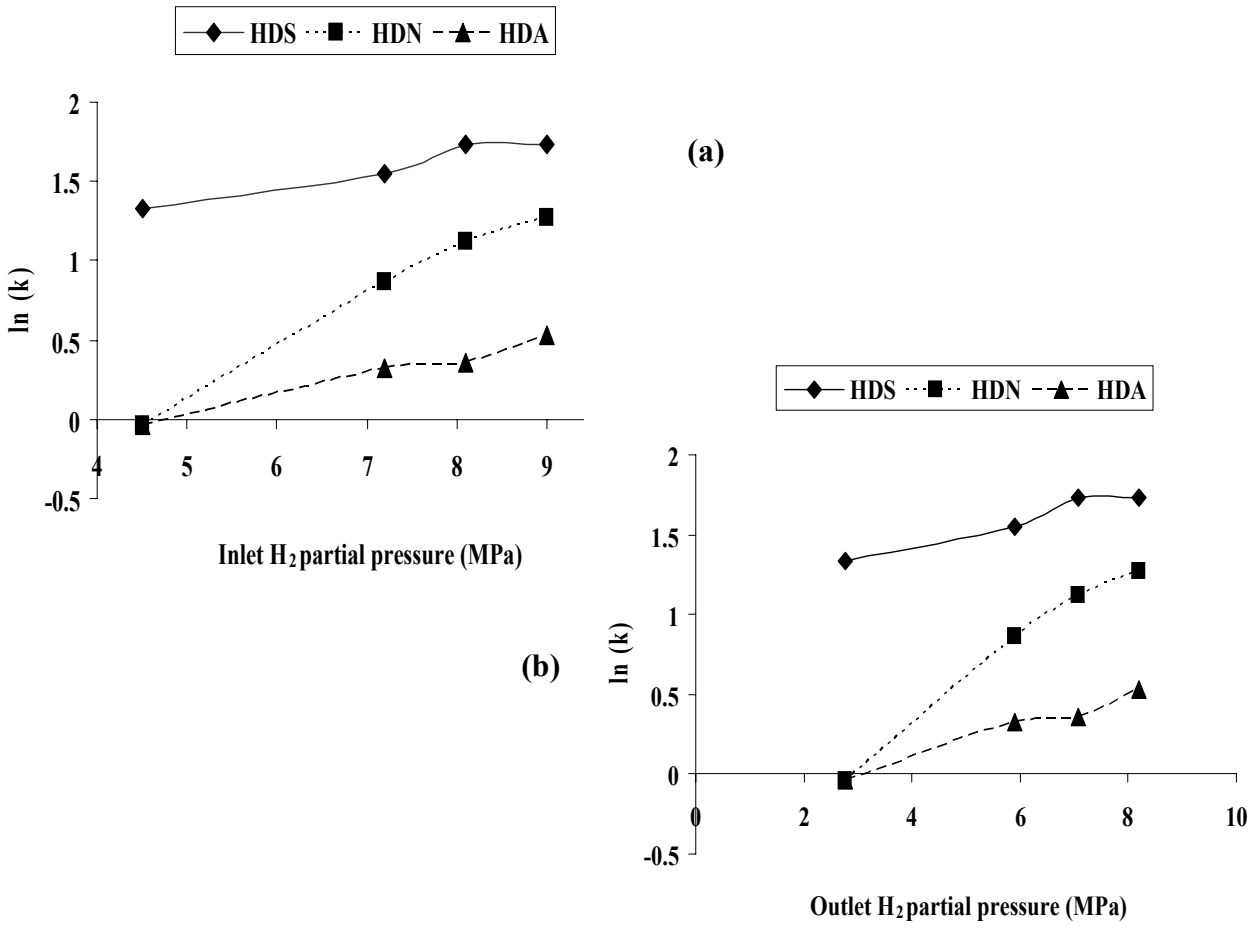

Figure 4.32: Rate constant as a function of: a) inlet H_2 partial pressure and b) outlet H_2 partial pressure

4.3.2 Langmuir-Hinshelwood analysis of HDS, HDN, and HDA

The data for this analysis was generated using experimental conditions where temperature ranged from 360 to 400 °C, while LHSV, pressure, gas/oil ratio, and H_2 purity were constant at 1 h^{-1}, 9 MPa, 800 mL/mL, and 100 vol. % , respectively. Equations 2.7.a, 2.8.a were used to determine apparent rate constants and adsorption equilibrium constants for HDS, HDN, and HDA. The apparent rate constants and adsorption equilibrium constants were determined using non-linear least squares approach. Apparent activation energies were determined from the slopes of the curve fitting by plotting the inverse of temperature against the logarithm of apparent kinetic rate constant (Owusu-Boakye, 2005). All the adsorption constants showed a decreasing trend with increasing temperature implying that HDS, HDN, and HDA are all exothermic reactions (Fogler, 1999).

The decrease of H_2S adsorption constant with temperature means that H_2S inhibition on hydrotreating decreases with increasing temperature (Ferdous et al., 2006). Results of apparent rate constants show that HDA increases with temperature at temperatures below 380 °C and decreases at temperatures above 380 °C due to HDA reversibility. Activation energies were also calculated from Arrhenius plots (see Figure 4.33). The activation energies (see Table 4.15) for HDS and HDN were 99 and 69 kJ/mol, respectively. Due to the reversibility of HDA, two activation energies were calculated within the temperature ranges of 360-380°C and 380-400°C. In the 360-380°C range, the value was 62 kJ/mol and in the 380-400°C range, the value was - 9 kJ/mol. R^2 for the Arrhenius plots ranged between 0.98 and 0.99.

Table 4.16: Summary of the rate constants and Adsorption constants determined using L-H model

	Temperature, °C				
HDS	**360**	**370**	**380**	**390**	**400**
k_S (h^{-1})	1.73	2.20	2.90	3.86	5.29
K_S (MPa)	8.93	7.30	5.74	4.26	3.18
K_{H_2} (MPa)	1.81	1.80	1.74	1.61	1.55
K_{H_2S} (MPa)	125.99	113.99	101.99	91.00	79.90
HDN					
k_n (h^{-1})	2.08	2.64	3.15	3.68	4.66
K_n(MPa)	2.15	2.09	1.97	1.78	1.67
K_{H_2} (MPa)	1.81	1.80	1.74	1.61	1.55
K_{H_2S} (MPa)	125.99	113.99	101.99	91.00	79.90
HDA					
k_a (h^{-1})	4.01	4.92	5.74	5.61	5.47
K_a (MPa)	4.50	3.79	3.16	2.91	2.65
K_{H_2} (MPa)	2.86	2.54	2.45	2.40	2.34
K_{H_2S} (MPa)	119.00	108.99	101.98	88.49	74.99

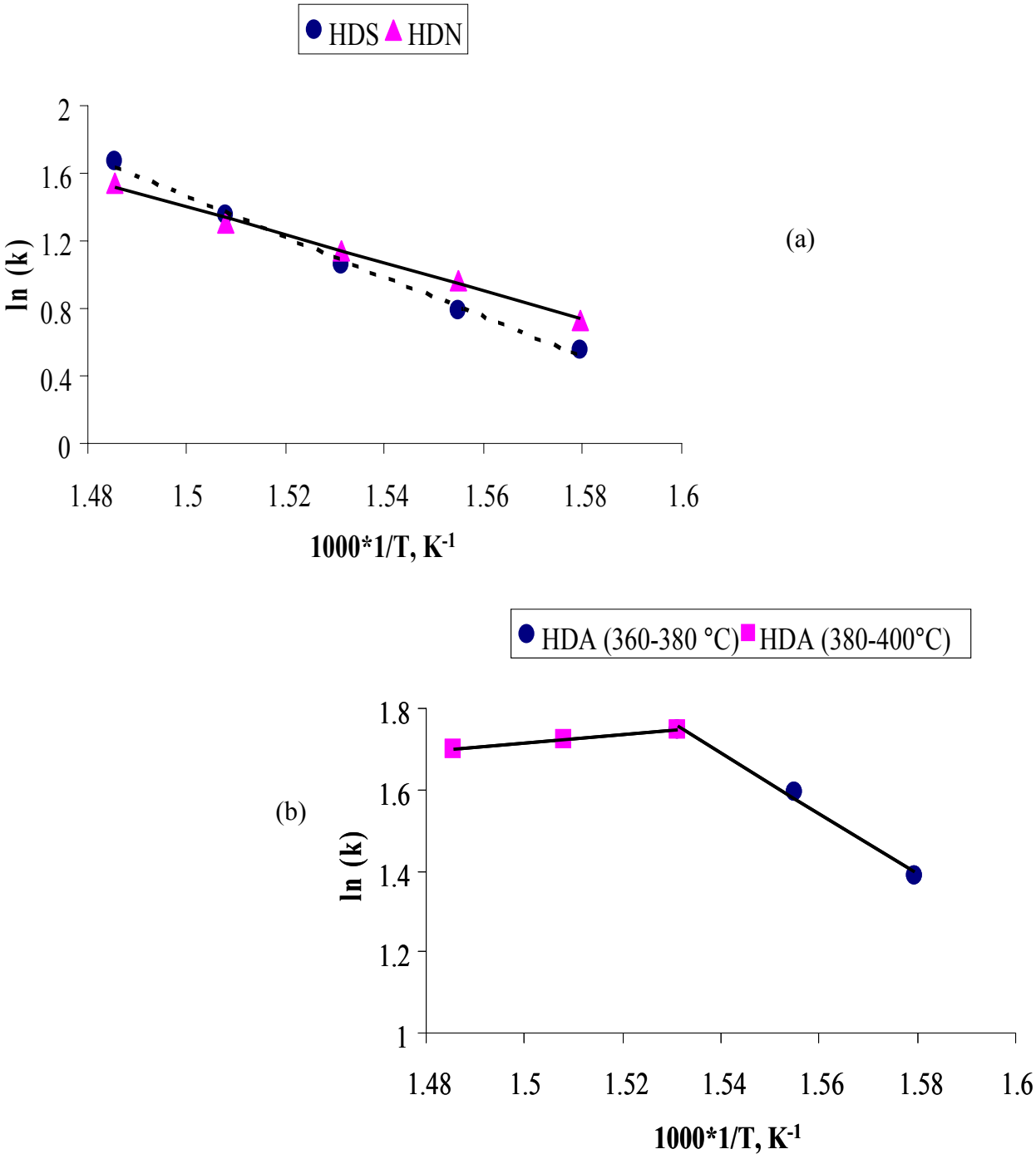

Figure 4.33: Arrhenius plot for: a) HDS, HDN, and b) HDA using L-H model

4.3.3 Multi-parameter Model analysis of HDS, HDN, and HDA

The data for this analysis was generated under experimental conditions where temperature, pressure, gas/oil ratio, LHSV and H_2 purity ranged between 360 to 400 °C, 7 to 11 MPa, 400 to 1200 mL/mL, 0.65 to 1 h^{-1}, and 75 to 100 vol. % (with the rest methane), respectively. The data was analyzed using the non-linear regression model in Polymath software. The parameters for HDS, HDN and HDA are shown in Table 4.17. The activation energies (Table 4.15) and reaction orders of HDS, HDN, and HDA were 119 kJ/mol and 2.68, 112 kJ/mol and 2.02, 34 kJ/mol and 1 (pseudo-first order), respectively. The parameters for HDA were determined for temperature below 380 °C. As the temperature went above 380 °C, the HDA conversion decreased as the hydrogenation reversed. R^2 for HDS, HDN, and HDA were 0.76, 0.92, and 0.90, respectively.

Table 4.17: Multi-parameter model parameters for HDS, HDN, and HDA.

Parameter	HDS	HDN	HDA
k_o	3.53×10^{10}	8.03×10^{8}	1.63×10^{2}
s	1.42×10^{4}	1.35×10^{4}	4.08×10^{3}
m	0.98	1.82	0.47
q	-0.31	-0.22	-0.01
c	2.72	2.04	0.24
n	2.68	2.02	Pseudo-1st

4.3.4 Comparison of the prediction power of different kinetics models

Comparison of activation energies and reaction orders obtained using different kinetics model are presented in Table 4.15. Most studies often report how well the predicted data agrees with the experimental data, which is used to generate the model(s), i.e. they report R^2. A better approach is to test the ability of the developed model (s) to predict new observations or data that are not used in generation of the model (s), i.e. to test their predicted R^2. Hence, three experiments were conducted in which pressure, temperature, LHSV, gas/oil ratio were kept constant at 9 MPa, 380 °C, 1 h^{-1}, and 800 mL/mL, respectively. Only H_2 purity was varied as follows: 50, 80, and 90 vol. % (with the rest methane). None of these conditions were used in the development of the kinetic models. Also, note that experimental condition at 50 % H_2 purity is an extrapulated condition, i.e. falls outside the range of the conditions originally used to develop the models. The power law model could not be used because of its exclusion of many of the process variables.

The comparison between the multi-parameter model and the L-H model is presented in Table 4.15. Muti-parameter model was reasonably accurate at predicting values for HDS, HDN and HDA conversions. L-H model was reasonably accurate at predicting values for HDS and HDN conversions , however, it could not predict well the extrapulated condition. Moreover, HDA predicted results using Equation 2.9.a, which is a version of L-H type model, were not logical as they suggested that HDA conversion increases with decreasing H_2 purity. Thus, the assumption that H_2 does not inhibit HDA was discarded, and Equation 2.8.a was used instead. The results of the predictions are shown in Table 4.18. With the assumption that H_2 does indeed inhibit HDA, better

agreement between the predicted and experimental data was obtained. The results of the apparant rate constant and equilibrium adsorption constants of HDA using Equation 2.8.a are given in Table 4.19. Activation energy was calculated for each of the two temperature ranges: 360-380 °C and 380-400 °C. In the 360-380 °C range the value was 58 kJ/mol, and in the 380-400 °C range the value was - 5 kJ/mol. R^2 for Arrhenius plots ranged between 0.92 and 0.99. The advantage of the multi-parameter model is that it results in better predicted values even for extrapolated conditions, while the advantage of the L-H model is that a smaller amount of experimental data is needed to determine its parameters.

A comparison between the activation energies and reaction orders determined in this work and range to those found in the literature is summarized in Table 4.20. It can be seen in this table that activation energies and reaction orders determined in this are in reasonable agreement with those reported in the literature. Discrepancies in the activation energy values can be attributed to changes in the (assumed) reaction mechanism or interference of physical phenomenon such as diffusion (Ferdous et al., 2006).

Table 4.18: Comparison on the predictive power of multi-parameter versus L-H

Purity (vol. %)	Determined experimentally (%)			Determined from the models (%)						
				Multi-parameter			L-H Model			
	HDS	HDN	HDA	HDS	HDN	HDA	HDS	HDN	HDA‡	HDA*
50	92	38	38	92	45	38	73	30	100	29
80	95	64	48	95	67	50	93	63	93	46
90	96	71	49	95	72	53	95	70	83	50

‡ Using Equation 2.9, *Using Equation 2.8.

Table 4.19: Rate constants and Adsorption constants of HDA using Equation 2.8a

	Temperature, °C				
HDA	**360**	**370**	**380**	**390**	**400**
k_a (h^{-1})	3.70	4.45	5.18	5.14	5.05
K_a (h^{-1})	0.85	0.76	0.60	0.58	0.55
K_{H_2} (MPa)	2.54	2.37	2.21	2.15	2.09
K_{H_2S} (MPa)	124.99	113.99	102.06	80.83	76.99

Table 4.20: Comparison of reaction orders and activation energies determined in this work and those found in the literature

References	Boiling range feed,°C	Kinetic model	Reaction order				Activation energy, kJ/mol			
			HDS	HDN	HDA <380°C	HDA >380°C	HDS	HDN	HDA <380°C	HDA >380°C
Yui and Dodge, 2006	286-541	P-L	1.5	1	1	-	151	132	72	-
Ai-jun *et al.,*2005	214-559	M-P	1.5	1.6	-	-	141	94	-	-
Owusu-Boakye *et al.*	170-439	L-H	Pseudo 1st	-	Pseudo 1st	-	55	-	85	-

2006										
Ferdous *et al.* 2006	185-576	L-H	1	1.5	-	-	87	74	-	-
Bej *et al.* 2001a & b	210-655	P-L	1.5	2	-	-	28	80	-	-
Mann *et al.*1987	HGO	P-L	1.5	2	-	-	87	105	-	-
Yui and Sanford,1989	196-515	P-L	1	1.5	-	-	138	92	-	-
Botchwey *et al.*,2004	210-600	L-H	Pseudo 1st	Pseudo 1st	-	-	114.2	93.5	-	-
Present work	258 - 592	P-L	2	1.5	1.5	1.5	101	79	30	-17
Present work	259 - 592	M-P	2.68	2.02	Pseudo 1st	-	119	112	34	-
Present work	260 - 592	L-H	Pseudo 1st	Pseudo 1st	Pseudo 1st	Pseudo 1st	99	69	58	-5

4.3.5 Importance of Outlet H_2 pp

McCulloch and Roeder (1976) suggested that more meaningful results are attained when outlet H_2 partial pressure is used especially from the catalyst's deactivation standpoint, however, the authors did not support this suggestion with experimental evidences. Catalyst deactivation is the most important concern in any catalytic process. In hydrotreating it is well known that increasing H_2 pp results in decreases in deactivation rate. Due to H_2 consumption, the reactor's outlet H_2 pp pressure can be considerably lower than its inlet H_2 pp, especially for heavy feedstock . Therefore the portion of the catalyst bed at and near the reactor outlet may experience higher deactivation rate as a results of lower H_2 pp environment.

Botchwey et al. (2006) and Alvarez and Ancheyta et al.(1999) experimentally showed that the largest portion of hydrotreating conversions take place in the first ~30% of the catalyst bed's length. Consequently this is also where most of the hydrogen consumption takes place, leaving a large portion of the catalyst's bed at a H_2 pp level significanlty lower than that at the inlet. Another noteworthy point that can be deduced from Botchwey et al. (2006) and Ancheyta et al. (1999) findings is that for about ~70% of the catalyst bed's length the H_2 pp level is closer in value to the outlet H_2 partial pressure than it is to the inlet H_2 pp. In other words, outlet H_2 pp level resembles that experienced by most parts of the catalyst's bed. Therefore, it is very critical that the outlet H_2 partial pressure is determined so more complete and meaningful conclusions are drawn.

To show the relationship between the catalyst deactivation and H_2 pp levels, a commerical NiMo/γ-Al_2O_3 catalyst bed was subjected to two inlet H_2 pps of 4.5 MPa and 8.1 MPa for a period of three days while carrying out hydrotreating experiments. Before the catalyst bed was subjected to either of the two H_2 pp levels a designated experiement with inlet H_2 pp of 9 MPa , named "control" , was conducted. The same "control" experiment was then repeated after the catalyst bed had been subjected to inlet H_2 pp of 4.5 MPa or 8.1 MPa. The hypothesis was that if the "before" and the "after" hydrotreating conversions of the "control' experiment were different it can be concluded that the catalyst underwent some deactivation. The temperature and LHSV were 380°C and 1 h^{-1} repectively for all experiments. The results are presented in Table 4.21.

Table 4.21 shows that for the experiment at 4.5 MPa inlet H_2 pp, the "after" HDN and HDA conversions of the "control" are lower than those of the "before" conversions , indicating that the catalyst suffered deactivation due to low H_2 pp levels. No significant differences were observed between the "after" and "before" HDN and HDA conversions in the experiment conducted at H_2 pp of 8.1 MPa. Thus, it can be seen that lower H_2 pp may cause severe catalyst deactivation in a very short time. It is therefore important that the entire catalyst bed is maintained at a high enough H_2 partial pressure (i.e. pressure and H_2 purity should not drop below the design levels (Gruia, 2006)) to avoid deactivation. One way of ensuring that the entire catalyst bed is at sufficient H_2 pp level is to ensure that the outlet H_2 pp, the reactor point with the lowest H_2 pp, is high enough to avoid untimely catalyst deactivation catalyst.

Table 4.21: Results of the catalyst deactivation testing. T = 380˚C and LHSV = 1 h^{-1}.

Activity	For H_2 pp of 8.1 MPa		For H_2pp of 4.5 MPa	
	Before	After	Before	After
HDN (%)	75	75	74	68
HDA (%)	53	54	53	50

5. Summary, Conclusions and Recommendations

5.1 Summary

(a) Phase I

(1) Methane is inert toward the hydrotreating activity of Ni-Mo/γ-alumina. Its presence in the hydrogen stream only affects the hydroprocessing conversions through the reduction of the hydrogen partial pressure of the system.

(2) Increasing system total pressure can be used to offset the use of lower hydrogen purity to attain similar hydrogen partial pressure, such as that of higher purity hydrogen at a lower total pressure. This can be performed without negatively affecting the hydroprocessing conversions.

(3) Dilution of hydrogen gas with methane gas up to 25 vol. % did not significantly change the HDS, HDN, and HDA activities of Ni-Mo/γ-alumina catalyst.

(4) Because methane was proven to be inert toward the catalyst and because reasonable conversions can be realized using less pure hydrogen, as low as 80% purity, it is not a necessity to produce ultra-pure hydrogen to be used in hydrotreating purposes. Thus, cheaper hydrogen recovery units featuring moderate product purities may be used to purify hydrotreater effluent gases. For PSA, better recoveries can be attained when hydrogen purity criteria are relaxed; thus, lower hydrogen losses and optimal economics are attained.

(b) Phase II

(1) Increasing reactor pressure and H_2 purity lead to increases in inlet H_2 pp, whereas, increasing gas/oil ratio does not have significant effect on inlet H_2 pp

(2) Increasing pressure, gas/oil ratio, and H_2 purity lead to increases in outlet H_2 pp. The effects of pressure and H_2 purity are more significant than that of gas/oil ratio on outlet H_2 pp.

(3) Temperature and LHSV do not have significant effects on inlet or outlet H_2 pp.

(4) HDS, HDN, and HDA increase with increasing H_2 pp. Within the range of the conditions studied HDN is more affected by H_2 pp than HDS and HDA .

(5) Correlations between outlet H_2 pp and hydrotreating conversions had higher R^2 than those of inlet H_2 pp. This may suggest that it is better to use outlet H_2 pp for design applications.

(6) Increasing H_2 pp results in increases in hydrogen consumption and dissolution, however, no clear correlation was obtained with regard to feed vaporization.

(7) Increasing pressure, H_2 purity, and gas/oil ratio led to increases in HDN and HDA activities. Effects of these variables on HDS activity are not considerably significant.

(8) The positive effects of H_2 purity on HDN and HDA activities were greater than those of gas/oil ratio and comparable to those of reactor pressure.

(9) The optimal conditions for HDS, HDN, and HDA are: pressure of 10.1 MPa, H_2 purity of 95vol. %, and gas/oil ratio of 1037 mL/mL. This is achieved at temperature and LHSV of 380°C and 1 h^{-1}, respectively.

(10) Decreasing LHSV led to increases in HDS, HDN, and HDA activities, while increasing temperature led to increases in HDS and HDN. HDA passed through a maximum of 380°C as the temperature was varied.

(c) Phase III

(1) Multi-parameter model gave better hydrotreating conversions' predictions than L-H.

(2) A low H_2 pp environment can accelerate the catalyst's deactivation

(3) Information on H_2 pp effects on hydrotreating activities can be equally satisfactorily obtained using either inlet or outlet H_2 partial pressure. However, from the catalyst deactivation standpoint it is vital to use outlet H_2 pp, since it is the point in the reactor point with the lowest H_2 pp.

5.2 Hypothesis Evaluation

In Chapter 1 three hypotheses were made, and are evaluated below:

- Within the experimental limits, it was confirmed that methane does not inhibit the NiMo/γ-Al_2O_3 catalyst. However, its presence resulted in decreases in HT activities due to reduction in H_2 pp.
- Increasing pressure and H_2 purity let to increases in inlet and outlet H_2 pp's; this finding was in accordance with the hypothesis. However, increasing gas/oil only increased outlet H_2 pp, and had no effect on the inlet H_2 pp.
- The Multi-parameter kinetic model yielded better prediction than L-H. Thus, hypothesizing that L-H would yield the best predictions amongst the three considered models (L-H, P-L, and M-P) was false.

5.3 Conclusion and Recommendations

The main objective of this thesis was to study the effect of hydrogen partial pressure on hydrotreating of heavy gas oil over a commercial NiMo/γ-Al_2O_3 in a micro-trickle bed reactor. It was concluded that increasing hydrogen partial pressure resulted in increases on HDS, HDN, and HDA conversions; HDN and HDA were significantly influenced by hydrogen partial pressure in comparison to HDS. From the catalyst deactivation standpoint it is a better approach to use the outlet H_2 partial pressure, not the inlet H_2 partial pressure, to correlate the hydrotreating conversions to H_2 partial pressure, since the reactor's outlet is the point with the lowest H_2 partial pressure in the system.

5.4 Future Work

A single feed, HGO, was used in the current study. The observations and conclusions made here can not be generalized for the rest of the petroleum fractions. Light feeds such as naphtha may give totally different results, since feed vaporization can be as high as 100%. Thus it is recommended that future studies should be carried out using different feedstocks.

REFERENCES

Abdel-Aal, H. K.; Bakr,Bakr A.; Al-Sahlawi, M. A. Petroleum economics and engineering, Mercal Dekker, NY, 1992.

Ai-jun, Duan; Chun-ming, XU; Shi-xing, LIN; Keng H, Chung."Hydrodesulfurization and Hydrodenitrogenation Kinetics of a Heavy Gas Oil over NiMo/Al_2O_3", *Journal of Chemical Engineering of Chinese Universities*, 2005, 19 (5), 762.

Al-Dahhan, Muthanna H.; Larachi, Faical; Dudukovic, Milorad P.; Laurent, Andre, "High-Pressure Trickle-Bed Reactors: A Review", *Ind. Eng. Chem. Res.* 1997, 36, 3292-3314.

Ancheyta, J.; M. J. Angeles; J. M. Macias; G. Marroquin; R. Morales, "Changes in Apparent Reaction Order and Activation Energy in the Hydrodesulfurization of RealFeedstocks", *Energy and Fuels*, 16, 189-193, (2002).

Ancheyta, Jorge and Speight, James G., Hydroprocessing of Heavy Oils and Residua, CRC press, p.114, 2007.

Andari, Mounif K.; Abu-Seedo, Fatima; Stanislaus, Anthony; Qabazard, Hassan M. "Kinetics of individual sulfur compounds in deep hydrodesulfurization of Kuwait diesel oil", *Fuel*, 1996, *Vol. 75*, *Issue 14*, 1664-1670.

Anderson, Mark J.; Whitcomb, Patrick J. RSM Simplified: Optimizing Processes Using Response Surface Methods for Design of Experiments, Productivity Press: New York, NY, 2005.

Anton Alvarez; Jorge Ancheyta, "Modeling residue Hydroprocessing in a multi-fixed-bed reactor system", *Applied Catalysis A: General, 351(2)* (2008) 148.

Bej, S. K.; Dalai, A. K.; Adjaye, J. "Kinetics of Hydrodesulfurization of Heavy Gas Oil Derived from Oil-Sands Bitumen", *Petroleum Science and Technology*, 20(7&8), 895-905, (2002).

Bej, S. K.; Dalai, A. K.; Adjaye, J. "Comparison of Hydrodenitrogenation of Basic and Nonbasic Nitrogen compounds Present in Oil Sands Derived Heavy Gas Oil", *Energy and Fuels*, 15, 375-383, (2001).

Bob R.; G. Leliveld; Jos A. J. van Dillen; John W. Geus; Diek C. Koningsberger "Structure and Nature of the Active Sites in CoMo Hydrotreating Catalysts. An EXAFS Study of the Reaction with Selenophene", *J. Phys. Chem. B* 1997, *101,* 11160-11171.

Botchwey, Christian, "TWO-STAGE HYDROTREATING OF HEAVY GAS OIL WITH INTER-STAGE HYDROGEN SULFIDE REMOVAL", Master Thesis, University of Saskatchewan, 2003.

Botchwey, Christian; Dalai, Ajay; Adjaye, John. "Product Distribution during Hydrotreating and Mild Hydrocracking of Bitumen-Derived Gas Oil", *Energy & Fuels*, 2003, *17*, 1372.

Botchwey, Christian; Dalai, Ajay; Adjaye, John; "Two-Stage Hydrotreating of Athabasca Heavy Gas Oil with Interstage Hydrogen Sulfide Removal: Effect of Process Conditions and Kinetic Analyses", *Ind. Eng. Chem. Res.*, 43 (18) (2004), 5854.

Botchwey, Christian; Dalai, Ajay; Adjaye, John' " Simulation of a Two-Stage Micro Trickle-Bed Hydrotreating Reactor using Athabasca Bitumen-Derived Heavy Gas Oil over Commercial NiMo/Al_2O_3 Catalyst: Effect of H_2S on Hydrodesulfurization and Hydrodenitrogenation", *International Journal of Chemical Reactor Engineering*, 4 (2006) A20.

Ferdous, D.; Dalai, A. K.; Adjaye, "Hydrodenitrogenation and Hydrodesulfurization of Heavy Gas Oil Using $NiMo/Al_2O_3$ Catalyst Containing Boron: Experimental and Kinetic Studies", J. *Ind. Eng. Chem. Res.,* 2006, *45,* 544.

Fogler, H. Scott. Elements of Chemical Reaction Engineering, 3rd, Prentice Hall PTR: Lebanon, Indiana, U.S.A., 1999.

Frye, C. G., "Equilibrium Hydrogenation of Polycyclic Aromatics". *J. Chem. Eng*. Data 1962, 7, 592-595.

Frye, C. G.; Weitkamp, A. W. "Equilibrium Hydrogenation of Multi-Ring Aromatics", *J. Chem. Eng*. Data 1969, 14, 372-376.

Gary, H. James; Handwerk, Glenn E.; Kaiser, Mark J. Petroleum Refining: Technology and Economics; 5th ed., CRC Press: N.Y., 2007.

Girgis, Michael J.; Gates, Bruce C. "Reactivities, Reaction Networks, and Kinetics in High-pressure Catalytic Hydroprocessing", *Ind. Eng. Chem. Res.*, 30 (1991) 2021.

Gruia, Adrian; in David S. J. Jones; Peter R. Pujadó (eds.), Handbook of Petroleum Processing, Springer Netherlands: 2006, Ch8.

Hanlon, Robert T. "Effects of P_{H2S}, P_{H2}, and P_{H2S}/P_{H2} on the hydrodenitrogenation of pyridine", *Energy and Fuels*, 1987, 1, 424.

Heinemann, Heinz; Somorjai, Gabor A. Catalysis and surface science: developments in chemicals from methanol, hydrotreating of hydrocarbons, catalyst preparation, monomers and polymers, photocatalysis and photovoltaics, CRC Press, 1985.

Herbert, Javier; Santes, Vı´ctor; Cortez, Maria Teresa; Za´rate, Rene´; Dı´az, Leonardo. *Catalysis Today*, 2005, 107–*108*, 559.

Hisamitsu, Tashiaki; Shite, Yasuo; Maruyama, Fumio; Yamane, Mamoru; Satomi, Yashihito; Ozaki, Hiromi. "Studies on Hydrodesulfurization of Heavy Distillates: Hydrogen Consumption and Reaction Kinetics", *Bulletin of the Japan Petroleum Institute*, 1976, 18(2), 146.

Huang, Qinglin; Malekian, Amir; Mladen, Eic," Optimization of PSA process for producing enriched hydrogen from plasma reactor gas", *Separation and Purification Technology*, 2008, 62, 22.

Jiang, Xudong; Goodman, D. Wayne. "The effect of sulfur on the dissociative adsorption of methane on nickel", Catalysis Letters*, 1990,* 4*, 173.*

Kabe T.; Ishihara A.; Qian W. Hydrodesulfurization and Hydrodenitrogenation ,Kodanacha Ltd., Tokyo, (1999).

Knudsen, K. G. B.; Cooper, H.; Topsoe, H. "Catalyst and Process Technologies for Ultra Low Sulfur Diesel". *Appl. Catal*. *189* (1999) 205.

Lal, D.; Otto, F.D.; Mather, A.E., "Solubility of hydrogen in Athabasca bitumen" *Fuel* 78 (1999) 1437–144.

Leffler, William, Petroleum refining in nontechnical language, 3rd ed., PennWell Corporation, 2000.

Landau, M. V. "Deep desulfurization of diesel fuels: kinetic modeling of model compounds in trickle-bed", *Catal. Today 36* (1997) 393.

Lee , Sunggyu. Methanol Synthesis Technology, Published by CRC Press, 1990.

Luis F. Ramírez; José Escobar; Ernesto Galván; Heriberto Vaca; Florentino R. Murrieta; María R. S. Luna, "Evaluation of Diluted and Undiluted Trickle-Bed Hydrotreating Reactor with Different Catalyst Volume", *Petroleum Science and Technology* (22) (2004) 157-175.

M. Machida; Y. Sakao; S. Ono, "Influence of hydrogen partial pressure on hydrodenitrogenation of pyridine, aniline and quinoline", *Applied Catalysis A: General*, 187, Issue 1, 1999, Pages L73-L78.

Mann, Ranveer S.; Sambi, Inderjit S.; Khulbe, Kailash C, "Hydrofining of Heavy Gas Oil on Zeolite-Alumina Supported Nickel-Molybdenum Catalyst", *Ind. En. Chem. Res*. 1988, *27*, 1788-1792.

Mann, Ranveer S.; Sambi, Inderjit S.; Khulbe, Kailash C. "Catalytic Hydrofining of Heavy Gas Oil", *Ind. En. Chem. Res.* 1987, 26, 410.

Mapiour, M.; Sundaramurthy, V.; Dalai, A. K.; Adjaye, J. "Effect of Hydrogen Purity on Hydroprocessing of Heavy Gas Oil Derived from Oil-Sands Bitumen", *Energy and Fuels*, *Energy Fuels*, *23* (4) **(**2009) 2129–2135.

Maples, Robert. Petroleum Refinery Economics, 2nd ed., PennWell Books: Tulsa, OK, U.S.A., 2000.

Mark A. Keane; Patricia M. Patterson, "The Role of Hydrogen Partial Pressure in the Gas-Phase Hydrogenation of Aromatics over Supported Nickel", *Ind. Eng. Chem. Res.*, 1999, *38* (4), pp 1295–1305.

Masataka Makabe; Hironori Itoh ; Koji Ouchi, "Effect of temperature and hydrogen partial pressure on the hydrogenolysis reaction of model compounds", *Fuel*, 69 (5), 575-579, 1990.

Matar, Sami; Hatch, Lewis Frederic, Chemistry of petrochemical processes, ed. 2nd, Gulf Professional Publishing, 2001.

McCulloch, Donald C.; Roeder, R. A. “Find hydrogen partial pressure”, *Hydrocarbon Processing*, February (1976) 81.

Mochida, Isao; Choi, Ki-Hyouk, “An Overview of Hydrodesulfurization and Hydrodenitrogenation”, *Journal of the Japan Petroleum Institute*, 47 (3), 145-163 (2004).

McKetta J. J., Petroleum Processing Handbook, Marcel Dekker Inc.: New York, 108-633, (1992).

Montgomery, D.C. Design and Analysis of Experiments, (4th ed.), John Wiley & Sons: USA, 1997.

Mounif K. Andari, Fatima Abu-Seedo, Anthony Stanislaus, Hassan M. Qabazard, “Kinetics of individual sulfur compounds in deep hydrodesulfurization of Kuwait diesel oil”, *Fuel*, *Vol. 75 Issue 14* (1996) 1664-1670.

Mun˜oz , Jose´ A.D.; Elizalde , Ignacio; Ancheyta , Jorge, “Scale-up of experimental data from an isothermal bench-scale hydrotreatment plant to adiabatic reactors”, *Fuel* 86 (2007) 1270–1277.

Nagy ,Gábor; Pölczmann, György; Kalló, Dénes; Hancsók, Jeno″ “Investigation of hydrodearomatization of gas oils on noble metal/support catalysts”, *Chemical Engineering Journal* , online (2009).

Owusu-Boakye, Abena. *Two-Stage Aromatics Hydrogenation of Bitumen-Derived Light Gas Oil*, Master Thesis, University of Saskatchewan, 2005.

Owusu-Boakye, Abena; Dalai, Ajay; Ferdous, Deena; Adjaye, John. “Experimental and Kinetics Studies of Aromatic Hydrogenation in a Two-Stage Hydrotreating Process using NiMo/Al_2O_3 and NiW/Al_2O_3 Catalysts”, *The Canadian Journal of Chemical Engineering*, 2006, *84*, 572.

P. Dufresne, P.H. Bigeard and A. Billon , "New developments in hydrocracking: low pressure high-conversion hydrocracking", *Cata. Today*, 1:367 (1987).

Paal, Zoltan; Menon, P.G. Hydrogen Effects in Catalysis: Fundamentals and Practical Applications, CRC Press, 1987.669

Peramanu, S.; Cox, B. G.; Pruden, B.B. "Economics of hydrogen recovery processes for the purification of hydroprocessor purge and off gases", *Internal Journal of Hydrogen Energy*, 24 (1999) 405.

Ruthven, D.M.; Farooq, S.; Knaebel, K.S. Pressure Swing Adsorption , VCH Publisher (1994).

Sidhpuria, Kalpesh B.; Parikh, Parimal A.; Bahadur, Pratap; Jasra, Raksh V. "Rhodium Supported Hβ Zeolite for the Hydrogenation of Toluene" , *Ind. Eng. Chem. Res*. 2008, 47, 4034–4042.

Sie, S.T. "Reaction order and role of hydrogen sulfide in deep hydrodesulfurization of gas oils: consequences for industrial reactor configuration" *Fuel Process. Technol*. 1999, 61, 149.

Sinnott, R. K.; Coulson, John Metcalfe; Richardson, John Francis. Coulson & Richardson's Chemical Engineering; ed. 4th, Butterworth-Heinemann: UK, 2005.

Slavcheva, E.; Shone B.; Turnbull, A. "Review of naphthenic acid corrosion in oil refining", *Br. Corros. J*. 34 (1999), pp. 125–131.

Speight, J. G. The Desulfurization of Heavy Oils and Residua, Marcel Dekker Inc.: New York, 1981.

Speight, J. G. The Desulfurization of Heavy Oils and Residua; Marcel Dekker Inc: New York, 2000.

Speight; J. G. The Chemistry of Petroleum, 3rd ed. Marcel Dekker, NY, 1999

Srinlvasan Ramanujam, Stuart Lelpzlger, Sanford A. Well, "Computation of Vapor-Liquid Equilibria Behavior of Coal Gasification Systems", *Ind. Eng. Chem. Process Des. Dev.* 1985, 24, 658-665.

Sun, Mingyong; Nelson, Alan E.; Adjaye, John, "Adsorption and hydrogenation of pyridine and pyrrole on NiMoS: an ab initio density-functional theory study", *Journal of Catalysis*, 231 (2005) 223–231.

Swarbrick, James; Boylan, James C. Encyclopedia of pharmaceutical technology, 2nd ed. , Marcel Dekker, New York, 2002.

T.L.Cottrell, The strength of Chemical Bonds, 2nd.Ed, Butterworth, London, 1958.

Topsøe, H., B. Clausen, R. Claudia, C. Wivel and S. Morup, "In Situ Mossbauer Emission Spectroscopy Studies of Unsupported and Supported Sulfided Co-Mo Hydrodesulfurization Catalysts: Evidence for and Nature of a Co-Mo-S Phase", *Journal of Catalysis*, 68, 433-452, (1981).

Topsøe, Henrik, "The role of Co–Mo–S type structures in hydrotreating catalysts", Applied Catalysis A: General 322 (2007) 3–8

Topsøe,H.; Clausen, B.S.; Masoth, F.E. in J.R. Anderson; M. Boudart, eds.: "Catalysis Science and Technology", Vol.11, Speinger-Verlag, NY (1996)

Turner, J.; Reisdorf, M. "Consider revamping hydrotreaters to handle higher H_2 partial pressures", *Hydrocarbon Processing*, March (2004), 61-70.

Wauquier, Jean-Pierre; Trambouze, Pierre; Favennec, Jean-Pierre., Petroleum refining, Editions Technip: Paris, France, 1995.

Whitehurst, D. D., I, Takaaki and I Mochida, "Present State of the Art and Future Challenges in the Hydrodesulfurization of Polyaromatic Sulfur Compounds", *Advances in Catalysis*, 42, 344-368, (1998).

Wilson, Grant M.; Johnston, Robert H.; Hwang, Shuen-Cheng; Tsonopoulos, Constantine "Volatility of Coal Liquids at High Temperatures and Pressures", *Ind. Eng. Chem. Process Des. Dev*. 1981, 20, 94-104.

Yang, Hong; Fairbridge, Craig; Hill, Josephine; Ring; Zbigniew. "Comparison of hydrogenation and mild hydrocracking activities of Pt-supported catalysts", *Catalysis Today*, 2004, *93-95*, 457-465.

Yang, Hong; Wilson, Michael; Fairbridge, Graig; Ring, Zbigniew. "Mild Hydrocracking of Synthetic Crude Gas Oil over Pt Supported on Pillared and Delaminated Clays", *Energy & Fuels*, 2002, *16*, 855.

Yang, S.H.; Satterfield, C.N. "Catalytic hydrodenitrogenation of quinoline in a trickle-bed reactor. Effect of hydrogen sulfide", *Ind. Eng. Chem. Process. Des. Dev.,* 1984, 23,20

Yépez, O. "Influence of different sulfur compounds on the corrosion due to naphthenic acid", *Fuel* 84 (2005) (1), pp. 97–104.

Yongloi, Wenzhao Li ; Hengyong, Xu. "A new explanation for the carbon deposition and elimination over supported Ni, Ni-Ce and Ni-Co catalysts for CO_2-reforming of methane", React. Kinet. Catal. Lett*., 2002, 77, 155.*

Zeinalov, E. B.; Abbasov, V. M. ; Alieva, L. I. "Petroleum Acids and Corrosion", *Petroleum Chemistry,* 2009, Vol. 49, No. 3, pp. 185–192.

APPENDICE

Appendix A: Experimental calibration

A.1 Mass flow meter calibration

Two mass flow meters were calibrated one for hydrogen and another for methane using bubble flow meter attached at the exit of the backpressure regulator (see Figure 3.1, Chapter 3). The calibration was done at experimental conditions and the measurements were standardized to atmospheric conditions using Equation A.1. Figures A.1, A.2, A.3 show the calibration curves of hydrogen, helium, and methane flow controllers, respectivley.

$$V^\circ = \left(\frac{P}{P^\circ}\right)\left(\frac{T}{T^\circ}\right)V \qquad (A.1)$$

Where: V°, T°, P° = volume, temperature, and pressure, respectively, at STP; V, T, P = volume, temperature, and pressure at normal operating conditions

A.2 Reactor temperature calibration

The reactor was loaded following the loading method highlighted in Figure 3.2 (Chapter 3). Two thermocouples were used to calibrate the temperature. One thermocouple was attached to centre of the catalyst bed to measure the corresponding temperature while the other was moved axially at the centre of the reactor at 1 cm intervals and temperature was recorded at each point. The results of the calibration are presented in figures A.4 & A.5. Figure A.4 shows the axial temperature profile while Figure A.5 shows the temperature controller calibration curve.

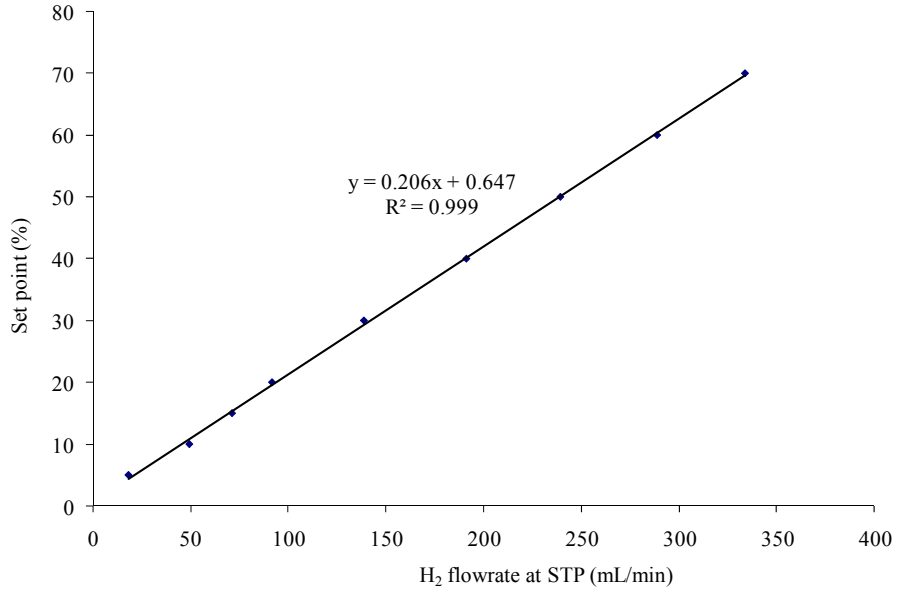

Figure A.1: Calibration curve for H_2 mass flow meter

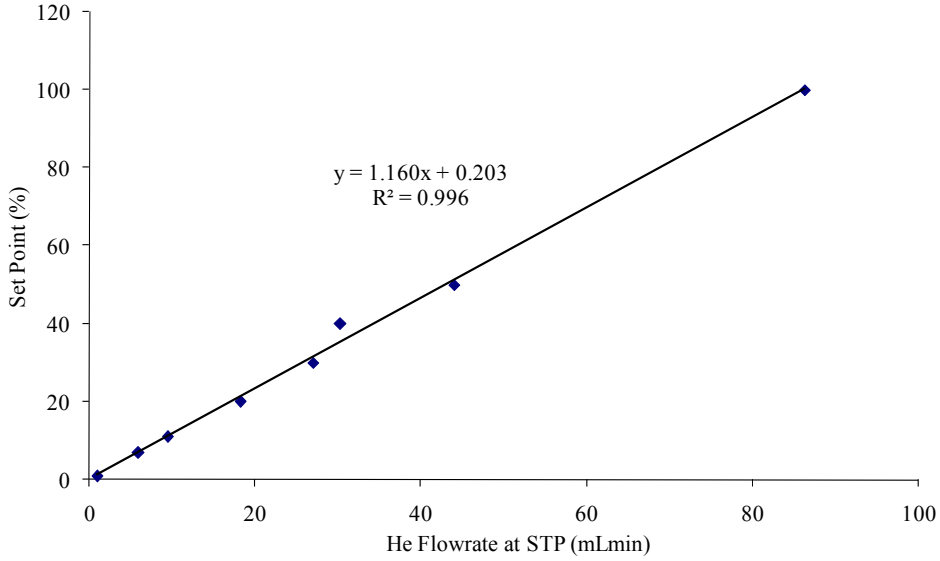

Figure A.2: Calibration curve for He mass flow meter

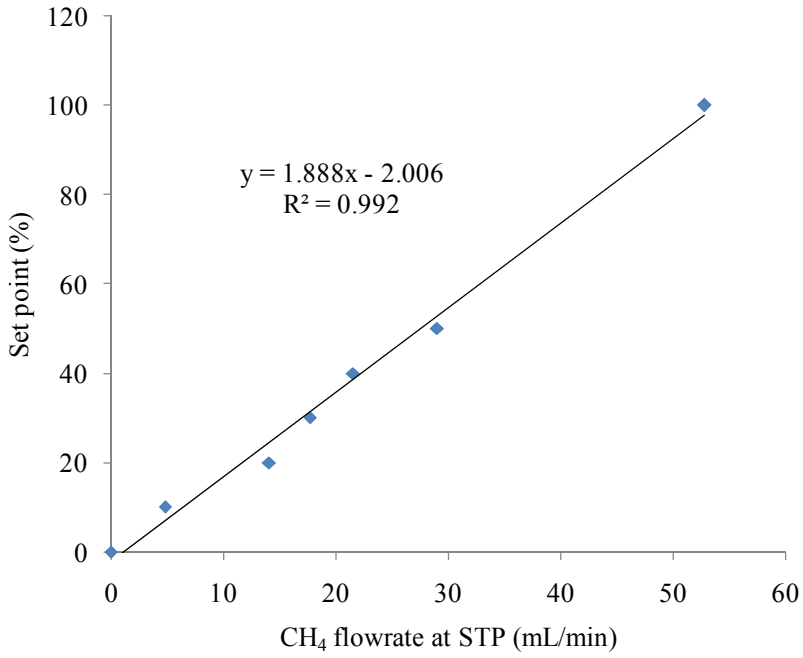

Figure A.3: Calibration curve for CH_4 mass flow meter.

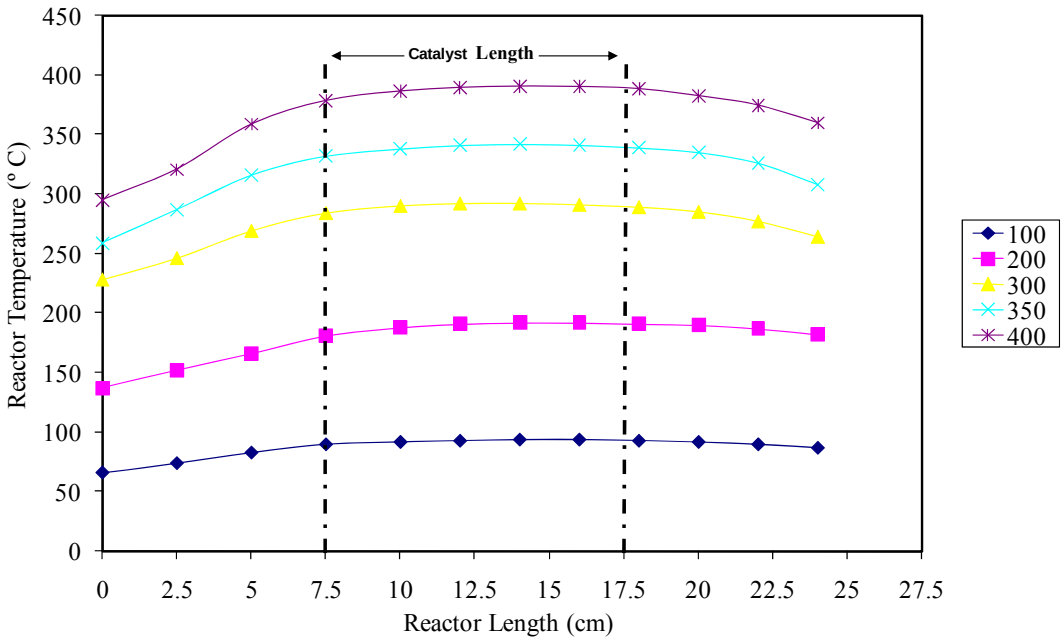

Figure A.4: Axial temperature profile.

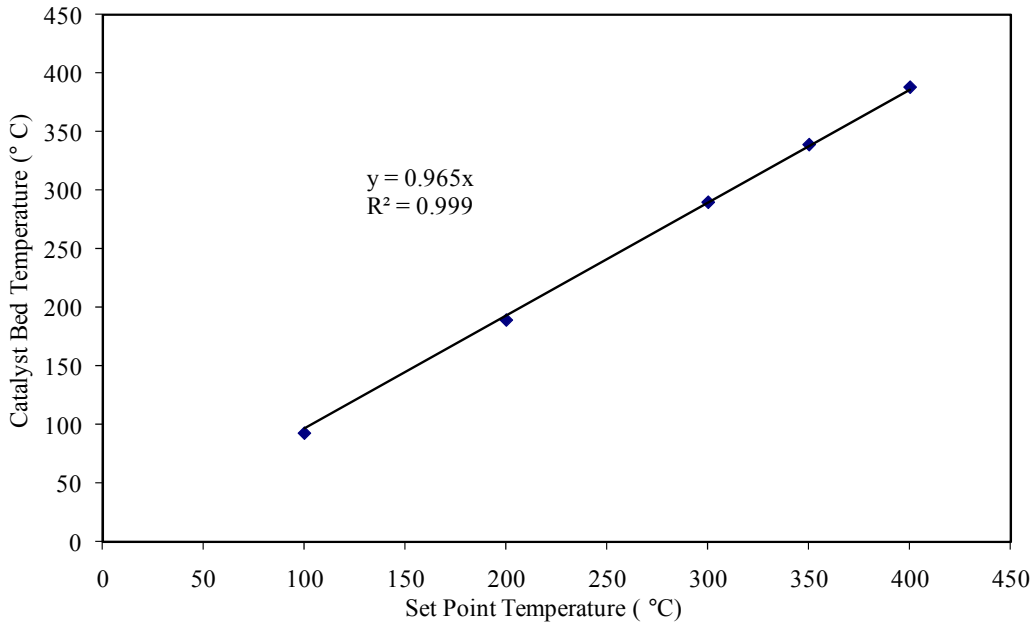

Figure A.5: Temperature calibration curve.

Appendix B: Experimental calculations and mass balance closure

The H_2 mass balance closure was measured using Equation B.1. This steady-state equation assumed that the summation amount of H_2 in the liquid feed and the inlet gas stream is equal to that of amount of H_2 in the liquid products and outlet gas stream. The H_2 contents of the liquid feed and the liquid products were measured using CHNS analyzer (model: VARIO ELIII, Elementar Americas, USA), while the H_2 contents of the inlet and outlet gas streams were measured using a GC (model: 6890N, Agilent, USA). The overall material balance was 96%.

$$\mathrm{Feed}_{H_2} + \mathrm{IG}_{H_2} = \mathrm{Pr\,oduct}_{H_2} + \mathrm{OG}_{H_2} \qquad \text{(B.1)}$$

Where: Feed $_{H2}$, IG_{H2}, Product $_{H2}$, and OG $_{H2}$ are the H2 contents of feed, inlet gas, liquid product, and outlet gas, respectively.

Appendix C: Experimental data

Table C.1: Experimental data for the effect of hydrogen purity study. Temperature and LHSV were kept constant at 380ºC and 1 h^{-1}, respectively.

Pressure MPa	Gas/oil mL/mL	H_2 purity vol.%	Gas mixture	HDN %	HDS %	HDA %
9	800	0	H_2	1.0	1.0	1.0
9	800	50	H_2/CH_4	38.1	94.1	38.0
9	800	80	H_2/CH_4	64.1	95.2	48.0
9	800	90	H_2/CH_4	71.0	96.0	49.0
9	800	100	H_2/CH_4	75.0	96.0	54.0
7.2	800	100	H_2	61.1	95.0	48.0
9	800	80	H_2/CH_4	64.1	95.2	48.0
9	800	80	H_2/He	64.8	95.0	49.0
9	800	50	H_2/CH_4	38.1	94.1	37.3
9	800	50	H_2/He	36.6	91.8	35.9
9	400	100	H_2	67.8	95.6	49.2
9	800	50	H_2/CH_4	38.0	92.2	37.1
10.1	800	50	H_2/CH_4	49.1	93.8	46.3
9	1,270	50	H_2/CH_4	38.2	92.8	38.1
9	800	90	H_2/CH_4	71.2	96.0	49.1
9	800	80	H_2/CH_4	66.8	95.5	46.9
10.1	800	80	H_2/CH_4	73.1	96.8	55.0

Table C.2: Experimental data for phase II; temperature and LHSV were kept constant at 380°C, and 1 h^{-1}, respectively

Experimental Conditions			Response							
Pressure (MPa)	Gas/oil (mL/mL)	Purity (%)	HDN (%)	HDS (%)	HDA (%)	Inlet H_2 pp (MPa)	Outlet H_2 pp (MPa)	H_2 consumption (scf/bbl)	Vaporized feed (g/h)	H_2 consumption (scf/bbl)
9.0	800	75	63.2	95.8	48.9	6.7	5.3	47.4	1.00	1217.4
7.8	1038	80	59.1	95.4	48.1	6.2	5.4	69.2	1.37	1193.3
10.2	562	80	67.4	93.6	51.2	8.1	5.8	64.9	0.59	1268.5
7.8	562	80	55.1	94.9	46.0	6.2	4.6	46.0	0.77	1160.7
10.2	1038	80	67.6	93.2	52.6	8.1	7.0	65.5	0.60	1285.4
9.0	400	88	59.9	96.0	47.9	7.8	5.2	59.5	0.33	1217.6
9.0	1200	88	65.0	95.3	53.0	7.8	6.9	103.0	1.46	1292.4
7.0	800	88	54.4	94.5	46.1	6.1	5.6	45.9	0.89	1155.8
9.0	800	88	66.7	95.5	51.8	7.8	6.8	65.8	0.92	1277.4
9.0	800	88	65.7	94.0	52.4	7.8	6.8	65.9	0.92	1282.4
11.0	800	88	72.8	95.0	54.9	9.6	8.3	88.2	0.75	1350.9
9.0	800	88	68.2	95.6	52.4	7.8	6.8	65.8	0.92	1287.7
9.0	800	88	66.6	92.9	53.1	7.8	6.8	65.9	0.92	1290.4
9.0	800	88	69.6	95.8	52.6	7.8	6.8	65.8	0.92	1292.2
9.0	800	88	66.3	95.0	51.8	7.8	6.8	65.9	0.92	1274.8
7.8	1038	95	69.3	93.8	53.9	7.3	6.8	56.9	1.25	1297.2
7.8	562	95	65.7	94.0	52.3	7.3	6.2	64.0	0.67	1304.2
10.2	562	95	78.5	96.0	55.5	9.5	8.1	92.3	0.51	1339.1
10.2	1038	95	83.9	96.7	58.0	9.6	8.9	85.1	0.99	1404.2
9.0	800	100	78.8	96.6	55.4	8.9	8.2	80.9	0.84	1352.5

Table C.3: Experimental data for the effects of temperature and LHSV on hydrotreating conversions. Pressure, gas/oil ratio, and H_2 purity were kept constant at 9MPa, 800 mL/mL, and 100%, respectively.

	LHSV = 1 h^{-1}		
Temperature, °C	HDS (%)	HDN (%)	HDA (%)
360	93.92	62.09	49.1
370	95.67	70	51.7
380	96.79	75.17	54
390	97.14	77.96	53.4
400	98.09	85.41	51.2
LHSV, h^{-1}	T= 380ºC		
0.65	97.51	85.3	57.7
1	96.79	75.17	54.0
1.5	93.22	58.05	52.1
2	86.73	42.73	48.8

D. A Simple Approach for the Determination of Outlet H_2 pp

D.1 Background

H_2 partial pressure is a principal variable in hydrotreating applications (Gray et al., 2007). Due to the considerable hydrogen consumption during the process of hydrotreatment, outlet H_2 partial pressure varies significantly from that at the inlet. Outlet H_2 partial pressure is of great importance in that: (i) Outlet conditions reflect the catalyst's last opportunity to hydrotreat the feedstock, and (ii) the outlet conditions, to a large extent, more nearly approximates the average conditions throughout the catalyst bed" (McCulloch and Reader, 1976).

Determination of the outlet H_2 partial pressure can be facilitated with the use of vapor-liquid equilibrium (VLE) data offered by engineering software such as HYSYS (ASPEN). HYSYS presents functionalities like Peng-Robinson equation (P-R), Soave-Redlich-Kwong equation (SRK), and Grayson-Streed equation (G-S), which are suitable models for hydrotreating applications (Lal et al. 1999). These models can also give information on the solubility of H_2 in petroleum products. Such information can be valuable in the design of up-grading processes for such materials (Lal et al. 1999).

However, it is worth noting that the use of HYSYS to determine outlet H_2 partial pressure for hydrotreating application can be quite a lengthy process. Thus, an attempt was made to develop a shortcut estimation method which can determine the outlet H_2 partial pressure to a reasonable degree of accuracy. This aim therefore was the objective of this work.

D.2 Results and Discussion

H_2 partial pressure is not a dependent variable. It is a function of pressure, H_2 purity, gas/oil ratio, temperature, and LHSV (McCulloch and Reader, 1976). However, the effects of pressure, H_2 purity, and gas/oil ratio on H_2 partial pressure are much more significant than that of temperature and LHSV (Antes and Aitani, 2004). Hence, experiments were carried out at constant temperature and LHSV, while pressure, H_2 purity, and gas/oil ratio were varied in the range of 7-11 MPa, 75-100 vol.% (with the rest methane), and 400-1200 mL/mL, respectively. In our previous work methane was found to be inert toward commercial NiMo/γ-Al_2O_3 catalyst (Mapiour et al., 2009). Expert Design 6.0.1 was used in experimental design.

D.2.1 Determination of Total H_2 consumption. Unlike the determination of inlet H_2 partial pressure, the determination of outlet H_2 partial pressure requires the knowledge of H_2 consumption. Total H_2 consumption is a summation of the chemical H_2 consumption and dissolved H_2, assuming that any mechanical H_2 loss and hydrocracking are negligible ((McCulloch and Reader, 1976). An equation that may aid in total H_2 consumption calculation is (McCulloch and Reader, 1976; Hisamitsu et al. 1976):

Total H_2 consumption = chemical H_2 consumption + dissolved H_2 (scf/bbl) (D.1)

where:

Dissolved H_2 can be determined from vapor/liquid equilibrium

$$\text{Chemical } H_2 \text{ consumption} = \frac{[(C_A)_f - (C_A)_p] \times \text{density}_{feed}}{100 \times 2 \times 12} \times 379 + H'_{H_2S} + H'_{NH_3} + H_{H_2S} + H_{NH_3} \quad \text{(D.1a)}$$

$$H'_{H_2S} \approx H_{H_2S} = \frac{[(S)_f - (S)_p] \times \text{density}_{feed}}{100 \times 32} \times 379 \quad \text{(D.1b)}$$

$$H'_{NH_3} \approx H_{NH_3} = \frac{[(N)_f - (N)_p] \times \text{density}_{feed}}{100 \times 14} \times 379 \quad \text{(D.1c)}$$

where:

C_A, S, and N = aromatic carbon, sulfur, and nitrogen contents (wt.%), respectively, and subscripts "f" and "p" = feed and products, respectively; H'_{H_2S} and H'_{NH_3} = amount of H_2 necessary to form hydrocarbon during HDS and HDN (scf/bbl), respectively; H_{H_2S} and H_{NH_3} = H_2 content of H_2S and NH_3 in the product gas (scf/bbl) , respectively; 379 = number of standard cubic feet in a mole of an ideal gas (scf/mole); density_{feed} = 346 lb/bbl. The units for H_2 consumption is scf/bbl.

D.2.2 Vapor/liquid equlibrium. The Peng-Robinson, Soave-Redlich-Kwong, and Grayson-Streed equations available in HYSYS 2006 were used to perform the VLE analysis from the following input data: temperature, pressure, treat gas rate and composition, and feed rate and properties. Boiling range distributions of the feed and the liquid products were determined using GC – simulated distillation (model: CP3800, Varian, Palo Alto, CA, USA) following standard procedure ASTM D2887. To determine the inlet hydrogen partial pressure, feed's boiling range data was fed into HYSYS along with the gaseous compositions and flowrates information. To determine the outlet hydrogen partial pressure the product's boiling range data was fed into HYSYS along

with the gaseous compositions and flowrates information. It is note worthy that at the outlet conditions the gaseous compositions account for the produced H_2S and NH_3, and also the decrease in H_2 amount due to H_2 consumptions. H_2S and NH_3 are produced as a result of HDS and HDN, respectively. HYSYS was set such that it reported vapor/liquid equilibrium as mole fractions. Inlet or outlet H_2 partial pressure was then calculated by multiplying the H_2 mole fraction by the system's pressure. Results of the outlet H_2 partial pressure using the Peng-Robinson's equation, Soave-Redlich-Kwong equation, and Grayson-Streed equation are presented in Table D.1.

D.2.3 Estimation of outlet H_2 partial pressure: It is always desirable in general engineering practice to develop approaches that can estimate quantities to a certain degree of accuracy. As mentioned in the introduction, the use of tools such as HYSYS demands extended time since it requires additional analysis of the liquid products beside analysis for sulfur, nitrogen, and aromatics contents. Our approach only requires sulfur, nitrogen, and aromatics contents analysis of the liquid products. The derivation of this approach is shown below as adopted from (Fogler, 1999).

Consider the following hydrotreating reaction equation:

$$CH_{4(g)} + 2.5H_{2(g)} + unsaturated_{(l)} \rightarrow saturated_{(l)} + NH_{3(g)} + H_2S_{(g)} + CH_{4(g)} \quad \text{(D.2)}$$

Assume isothermal and isobaric, then H_2 gas phase is:

$$C_H = C_{H_o}\left(\frac{1-x}{1+\varepsilon\, x}\right) \quad \text{(D.3)}$$

where:

Table D.1: Results of the outlet H_2 partial pressure using SRK, G-S, and P-R equation, and the estimation method.

Experimental Conditions			Outlet H_2 partial pressure (MPa)			
Pressure (MPa)	**Gas/oil (ml/ml)**	**Purity (%)**	**SRK**	**G-S**	**P-R**	**Estimation**
9.0	800.0	75.0	5.32	5.32	5.32	5.44
7.8	1037.8	80.1	5.41	5.41	5.41	5.43
10.2	562.2	80.1	5.81	5.79	5.82	5.81
7.8	562.2	80.1	4.57	4.56	4.58	4.61
10.2	1037.8	80.1	7.03	7.04	7.03	7.01
9.0	400.0	87.5	5.16	5.18	5.18	4.93
9.0	1200.0	87.5	7.19	6.89	7.19	7.06
7.0	800.0	87.5	5.33	5.60	5.33	5.22
9.0	800.0	87.5	6.80	6.81	6.81	6.58
9.0	800.0	87.5	6.80	6.82	6.81	6.57
11.0	800.0	87.5	8.30	8.31	8.30	7.96
9.0	800.0	87.5	6.80	6.81	6.81	6.57
9.0	800.0	87.5	6.80	6.82	6.81	6.98
9.0	800.0	87.5	6.80	6.81	6.81	6.97
9.0	800.0	87.5	6.80	6.82	6.81	6.98
7.8	1037.8	94.9	6.80	6.81	6.80	6.80
7.8	562.2	94.9	6.20	6.20	6.21	6.21
10.2	562.2	94.9	8.04	8.08	8.04	8.01
10.2	1037.8	94.9	8.86	8.88	8.85	8.81
9.0	800.0	100.0	8.19	8.22	8.19	8.02

$$\varepsilon = y_{H_o} * \delta = y_{H_o}(1+0+1+1-0-2.5-1) = -0.5 \quad \text{(D.4)}$$

$$C_{H_\circ} = y_{H_o} * \left(\frac{P_o}{RT_o}\right) \text{(D.5)}$$

$$C_H = y_H * \left(\frac{P}{RT}\right) \text{(D.6)}$$

but: $T = T_o$ and $P = P_o$

thus:

$$P_{H_{out}} = P_H = P_{H_{in}} * \left(\frac{1-x}{1-0.5x}\right) \text{(D.7)}$$

where: $x = \dfrac{F_{A_O} - F_A}{F_{A_O}} = \dfrac{H_2\ consumption}{F_{A_o}}$ (D.8)

Hence:

$$P_{H_{out}} = P_{H_{in}}\left(\frac{F_{A_O} - H_2\ consumption}{F_{A_O} - 0.5 * H_2\ consumption}\right) \text{(D.9)}$$

where:

C_{Ho} and C_H = initial and final concentration of H_2, respectively; x = conversion of H_2; P_o and P = inlet and outlet pressure, respectively; T_o and T = inlet and outlet temperature, respectively; y_{Ho} and y_H = inlet and outlet H_2 mole fractions, respectively; $P_{H\ in}$ and $P_{H\ out}$ = inlet and outlet H_2 partial pressure, respectively; F_{Ao} and F_A H_2 inlet and outlet molar flowrate, respectively; ε = the change in the number of moles per mole of H_2 fed; δ = the change in the number of moles per mole of H_2 reacted.

H_2 consumption can be determined using Equation D.1. However, there is no means of determining the amount of the dissolved H_2. Thus the amount of dissolved H_2 is assumed negligible in the approach, and Equation D.1.a can be used instead for approximating the amount of H_2 consumption. This is a reasonable assumption since chemical H_2 consumption is a lot larger than the amount of the dissolved H_2. The results of the calculation of the outlet H_2 partial pressure using this estimation approach are presented in Table D.1. Inlet Hydrogen partial pressure can simply be estimated by multiplying pressure by H_2 purity (or H_2 mole fraction in the gaseous phase).

D.2.4 Comparison between the results of the estimation approach and that of HYSYS. Figure D.1, D.2, and D.3 show the agreements between outlet H_2 partial pressures using the estimation approach and those using Soave-Redlich-Kwong equation, Grayson-Streed equation, and Peng -Robinson equation, respectively. The R^2 for these plots were found to be 0.9737, 0.9596, and 0.9733, respectively. These high R^2 values suggest that the estimation approach gives a reasonable means for quick determination of outlet H_2 partial pressure for industrial hydrotreating applications. Moreover, these R^2 values show that the estimation approach is in sound agreement with SRK and P-R than with G-S. This fact adds to the credibility of this estimation approach, since, the SRK and P-R present a better approach for hydrotreating applications (Lal et al., 1999) (further discussion in section D.2.5). Figure D.4 shows that H_2 partial pressure determined using SRK and P-R are in nearly prefect agreement with R^2 of 1. Also shown in the same figure, the R^2 for the agreement between H_2 partial pressure determined using P-R and G-S is 0.9933. A source of discrepancy between the outlet H_2 partial pressure

determined using the estimation approach and those using HYSYS is that in the estimation approach, H_2 consumed due to the dissolution is not accounted for.

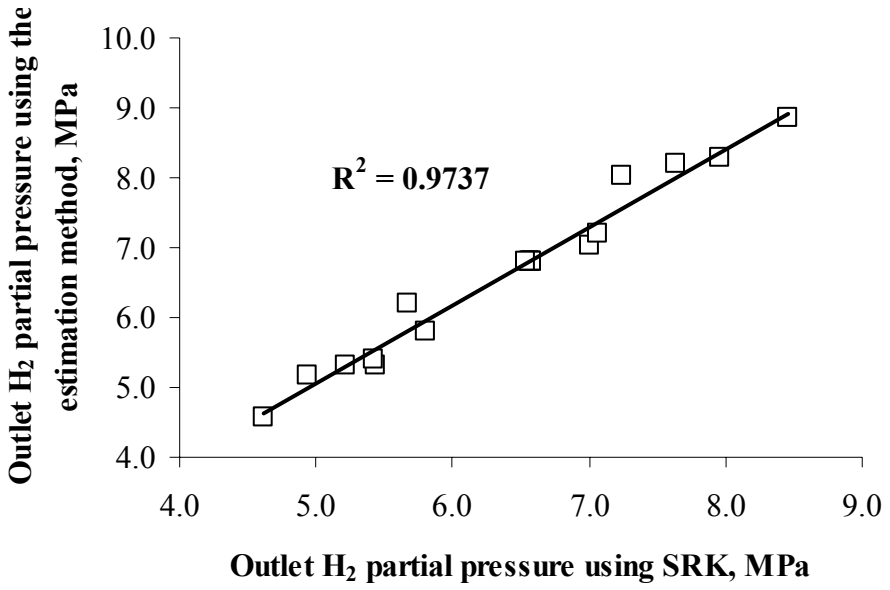

Figure D.1: Correlations of the outlet H_2 partial pressure using the estimation approach and SRK equation

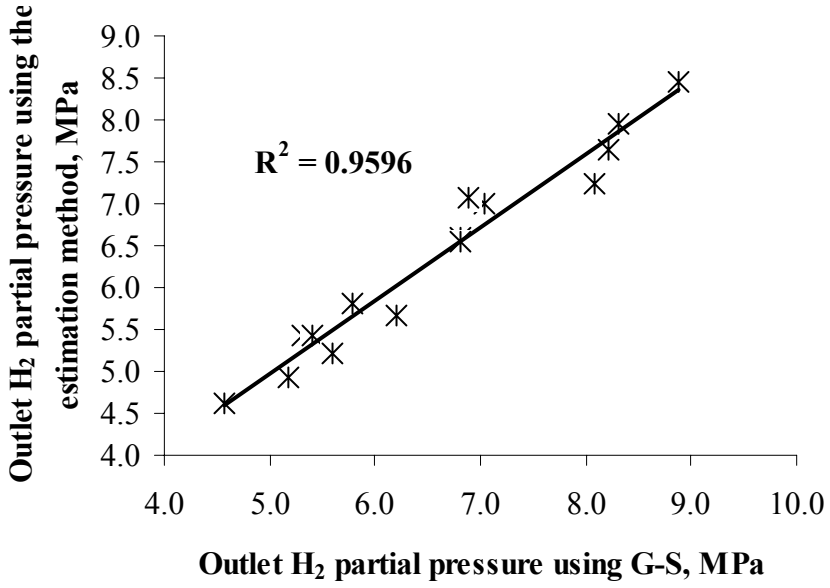

Figure D.2: Correlations of the outlet H_2 partial pressure using the estimation approach and G-S equation

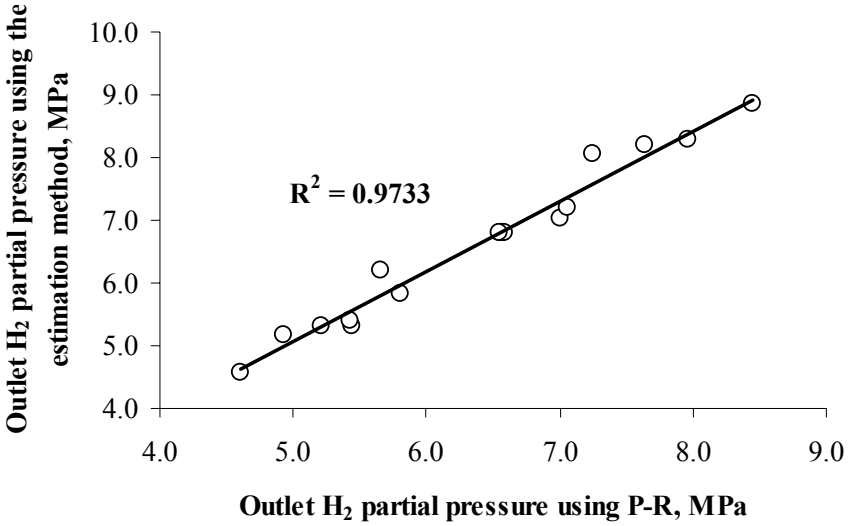

Figure D.3: Correlations of the outlet H_2 partial pressure using the estimation approach and P-R equation.

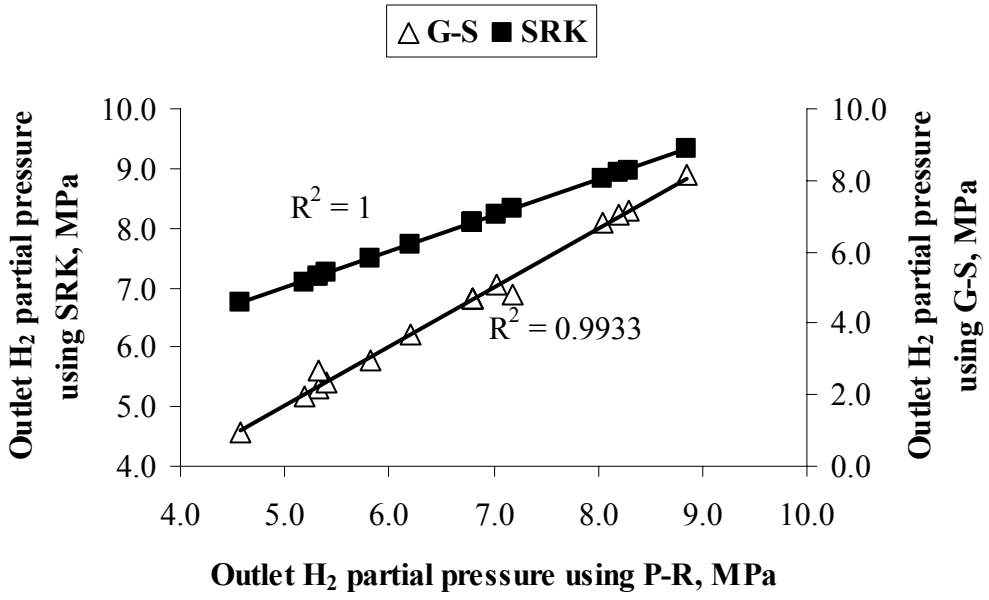

Figure D.4: Correlations of the outlet H_2 partial pressure using P-R, SRK, and G-S equations

D.2.5 H_2 dissolution. The knowledge of the amount of the dissolved H_2 is required for more accurate determination of H_2 consumption and consequently outlet H_2 partial pressure. The amounts of the dissolved H_2 were determined using SRK, P-R, and G-S equations. The agreements among these three equations in the determination of the amount of H_2 dissolved are presented in Figure D.5. The R^2 values obtained for the SRK versus the P-R method is 0.9984, whereas that for the G-S versus P-R method was 0.9586. Similar results were observed by Lal *et al* .(1999). Moreover, the authors reported that results of H_2 dissolution obtained from SRK and P-R equations were more in agreement with the experimental data than were those obtained from the G-S equation. For more accurate VLE for hydrotreating applications, the use of either SRK or P-R for the determination of dissolved H_2 is recommended in comparison to that of the G-S approach.

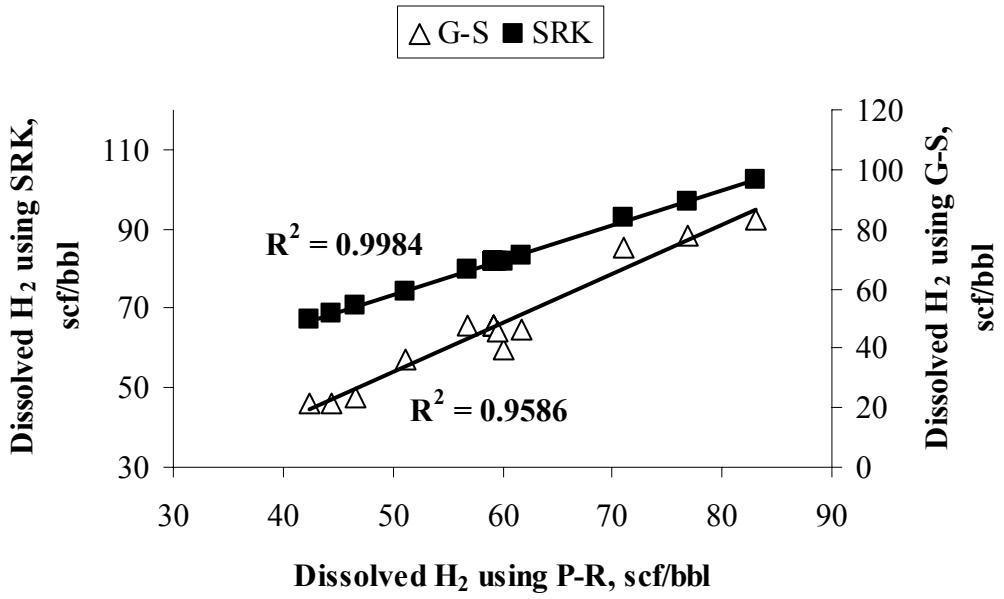

Figure D.5: Correlations of the dissolved H_2 using P-R, SRK, and G-S equations

D.3 Application

Frequently refiners draw their process conclusions from the reactor inlet H_2 partial pressure. McCulloch and Roeder argued that from a catalyst deactivation standpoint, it more important to look at outlet H_2 partial pressure especially in cases where H_2 consumption is high such as in hydrotreating of heavier feedstock with high concentrations of sulfur and nitrogen. This equation can be used as a quick way to determined outlet H_2 partial pressure, which then can be used to draw more appropriate conclusions.

D.4 Limitation

For lighter petroleum products such as naphthas, this estimation may yield less accurate results as compared to heavier petroleum products. The reason is that this estimation assumes that feed vaporization is negligible.

D.5 Final Comments

A simple approach for the determination of the outlet H_2 partial pressure was developed. The H_2 partial pressures determined using this estimation match well those determined using Peng-Robinson equation, Soave-Redlich-Kwong equation, and Grayson-Streed equation. Hence, it was concluded that this approach may be used for a quick and reasonable determination of outlet H_2 partial pressure for industrial hydrotreating applications.

E. Reproducibility study:

The reactor was loaded and experiments were conducted as design. Specific experimental conditions were repeated several times to observed the reproducibility of the results. Subsequently, the reactor was reloaded with a fresh batch of catalyst and the experiments and repetition were carried out. This was carried out to observe whether the reproducibility was affected by the packing step (see Table E.1). The errors were determined using the student's t-test method. For column 1, in Table E.1, *unequal sample sizes-equal variance* t-test was used, and for columns 2 and 3 *independent one sample* t-test was used. The reason for using two different t-tests is the variation on sample sizes

Table E.1: The results of reproducibility Studies. The experiments below were carried out at temperature, pressure, gas/oil, and LHSV of 380 °C, 9 MPa, 800 ml/ml, and 1 hr^{-1}, respectively.

Exp #	**1**	**2**	**3**
Conditions	Purity = 100%	Purity = 80%	Purity = 50%,
		Trial 1	
# of Repetition	4	1	1
HDN	75, 75, 74, 73	64	38
HDS	96, 96, 95, 93	95	94
HDA	54,53,53,52	48	38
Fresh catalyst loaded		**Trial 2**	
# of Repetition	2	1	1
HDN	75, 74	67	38
HDS	97,96	95	92
HDA	53,52	47	37
		% Error	
HDN	0.3	2.0	0.0
HDS	1.4	0.0	2.1
HDA	0.7	2.1	2.6

F. Rights and Permissions

1. Permissions to use Figure 2.11

License Number	2242090480300
License date	Aug 04, 2009
Licensed content publisher	Elsevier
Licensed content publication	Fuel
Licensed content title	Solubility of hydrogen in Athabasca bitumen
Licensed content author	D. Lal, F. D. Otto and A. E. Mather
Licensed content date	October 1999
Volume number	
Issue number	
Pages	0
Type of Use	Thesis / Dissertation
Portion	Figures/table/illustration/abstracts
Portion Quantity	1
Format	Print
You are the author of this Elsevier article	No
Are you translating?	No
Order Reference Number	
Expected publication date	Oct 2009
Elsevier VAT number	GB 494 6272 12
Billing type	Invoice
Company	Majak L Mapiour
Billing address	57 campus drive
	Saskatoon, SK s7n 5a9
	Canada
Customer reference info	
Permissions price	0.00 USD
Value added tax 0.0%	0.00 USD
Total	0.00 USD

2. Permissions to use Figure 2.3

License Number	2242091379535
License date	Aug 04, 2009
Licensed content publisher	American Chemical Society
Licensed content publication	The Journal of Physical Chemistry B
Licensed content title	Structure and Nature of the Active Sites in CoMo Hydrotreating Catalysts. An EXAFS Study of the Reaction with Selenophene
Licensed content author	Bob R. G. Leliveld et al.
Licensed content date	Dec 1, 1997
Volume number	101
Issue number	51
Type of Use	Thesis/Dissertation
Are you the Author of original article?	No
Format	Print
Portion	Table/Figure/Chart
Number of tables/figures/charts	11
Order reference number	
Title of the thesis / dissertation	Effect of hydrogen partial pressure on hydroprocessing of Heavy gas oil
Expected completion date	Oct 2009
Estimated size(pages)	182
Billing type	Invoice
Billing address	57 campus drive
	Saskatoon, SK s7n 5a9
	Canada
Customer reference info	
Permissions price	0.0 SD

3. Permission to use my own published work

License Number	2242100039003
License date	Aug 04, 2009
Licensed content publisher	American Chemical Society
Licensed content publication	Energy & Fuels
Licensed content title	Effect of Hydrogen Purity on Hydroprocessing of Heavy Gas Oil Derived from Oil-Sands Bitumen
Licensed content author	M. Mapiour et al.
Licensed content date	Apr 1, 2009
Volume number	23
Issue number	4
Type of Use	Thesis/Dissertation
Are you the Author of original article?	Yes
Format	Print
Portion	Full article
Order reference number	
Title of the thesis / dissertation	Effect of hydrogen partial pressure on hydroprocessing of Heavy gas oil
Expected completion date	Oct 2009
Estimated size(pages)	182
Billing type	Invoice
Billing address	57 campus drive
	Saskatoon, SK s7n 5a9
	Canada
Customer reference info	
Permissions price	0.00 USD